ON THE FEASIBILITY OF APPLICATION OF FIBER-OPTICS IN PROFILE MEASUREMENT

By

LT. PRAVIN DIXIT [IN]

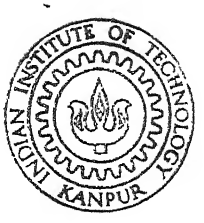

DEPARTMENT OF MECHANICAL ENGINEERING

INDIAN INSTITUTE OF TECHNOLOGY KANPUR

FEBRUARY 1992

ON THE FEASIBILITY OF APPLICATION OF FIBER-OPTICS IN PROFILE MEASUREMENT

A Thesis Submitted
in Partial Fulfilment of the Requirements
for the Degree of
MASTER OF TECHNOLOGY

By

LT. PRAVIN DIXIT [IN]

to the

DEPARTMENT OF MECHANICAL ENGINEERING

INDIAN INSTITUTE OF TECHNOLOGY KANPUR

FEBRUARY 1992

CERTIFICATE

It is certified that the work contained in the thesis entitled "**ON THE FEASIBILITY OF APPLICATION OF FIBER-OPTICS IN PROFILE MEASUREMENT**", by Lt. Pravin Dixit, has been carried out under my/our supervision and that this work has not been submitted elsewhere for a degree.

(V. K. Jain)
Assitant Professor
Mechanical Engineering
Indian Institute of Technology
Kanpur 208016

(S. K. Choudhary)
Assistant Professor
Mechanical Engineering
Indian Institute of Technology
Kanpur 208016

February, 1992

ME-1992-M-DIX-FEA

ABSTRACT

Measurement of profile of a machined component and determination of position and orientation f burrs is one of the most important subjects of investigation in the field of metrology. The surface and its quality generated by the machining processes is important not only from aesthetic point of view but also from the point of view of study of functional behaviour of parts and safety in some cases.

The mechanical profilometer which uses a diamond stylus is very sensitive and widely used but measurement is very slow and microscratches may be made on soft surfaces with sharp diamond stylus, secondly it cannot be used for the measurement in case of inaccessible areas viz., tapered hole, blind hole of small diameter etc.

Due to the growth of highly automated manufacturing processes, the demand is greately increasing for in process sensors for profile measurement for accurate evaluation of generated surfaces during the machining process. Such demand can be met in a better way by non-contact sensors like optical fibres rather than conventional stylus type sensors.

The non-contact optical sensor utilizes fibres through which laser light is passed to fall on the workpiece surface and also the intensity of the reflected light is detected by sensor (photodiode). The magnitude of the reflected light varied by varying the gap between the probe (fibres) and workpiece, the surface finish of the workpiece, the type of material of the workpiece, the medium between the workpiece and probe like air, water and Nacl solution and the inclination of the workpiece.

This non-contact optical sensor is successfully applied for the measurement of the profile and to detect the presence of burrs and measurement of burr dimensions. The sensor developed is basically an in-process non-contact sensor for the measurement of interelectrode gap and profile during unconventional machining processes like ECM, EDM, ECDe, ECBo etc.

ACKNOWLEDGEMENTS

I would like to express my deep gratitude and sincere thanks to my thesis supervisors, Dr. V. K. Jain and Dr. S. K. Choudhary, for their expert guidance and valuable suggestions and useful criticisms. I am grateful to them for their constant encouragement throughout the course of my thesis.

I am very thankful to Dr. P. K. Chatterjee for allowing me to work in Fiber-optics lab. and guiding me in the fiber-optics field. Under his guidance, I was helped by Ph.D students Mr. Abhay Karandikar and Mr. Sandeep Agarwal for initial's development of sensing and amplification circuits.

I am very thankful to Mr. Raghuram who has given very useful suggestions from time to time. Sincere thanks to Mr. R. M. Jha, Mr. O. P. Bajaj, Mr. Sharma and Mr. Gupta for providing the manufacturing Science Laboratory facility and helping me in devleoping models.

I thank Miss Sushma, Mrs. Kulkarni and Miss. Sandhya for helping me in installing and guiding in grapher package. My sincere thanks to my colleagues Lt. Ravindranath, lt. A. Dhar and lt. Pannigrahi for maintaining friendly atmosphere.

Finally I thank my parents and wife who were the constant source of encouragement and inspiration for thesis work.

(Lt. Pravin Dixit)

February, 1992

CONTENTS

LIST OF FIGURES

List of Tables

Nomenclature

AD	Angular Distribution
λ	Wavelength of He-Ne Laser = 6328.193 Å
Ra	Centre Line Average Value of Roughness
Δ	Amplification gain of the Circuit
R	Reflectance
X_i	Horizontal Probe Discplacement (mm)
Y_i	Vertical Gap between Probe and Specimen by Optical-fibers (mm)
Y_i'	Vertical Gap between Probe and Specimen by Dial-guage (mm)

4 μ.in = 100 microns
8 μ.in = 200 microns
32 μ.in = 800 microns
63 μ.in = 1575 microns
125 μ.in = 3125 microns
250 μ.in = 6250 microns

CHAPTER I

INTRODUCTION AND LITERATURE SURVEY

1.1 INTRODUCTION

"Measurement" is defined as a set of experimental operations having the object of determining the value of a quantity. It is the physical phenomenon, e.g. thermoelectric effect applied in the measurement of temperature. There are various methods of measurement but method of non contact measurement without contact is the most recent and advanced. In this method of measurement, the sensor is not placed in contact with the object whose characteristics are being measured [1].

The contactless measurement is fast, leads to no micro scratches on soft surfaces and can be used in inaccessible areas viz. tapered hole, blind holes of small diameter etc. The optical technique for non-contact measurement is the best solution. But this technique cannot be utilized in blind holes and inaccessible areas where lots of bends and small diameter of the workpiece will hamper the light to fall on required place and hence the profile cannot be measured. To overcome above limitations optical-fibers, which are dielectric wave guides and which are designed to guide

light waves along their length and unaffected by electromagnetic radiation, can be successfully used as they can be easily bent and can carry the incident and reflected light from the source and to the detector respectively and thus profile can be measured. Some profiles where contact less measurement can be applied by optical-fibers are shown in Fig. 1.1.

The reasons for recommending optical-fiber methods for the measurement of profile, surface roughness, burr height are very apparent. Optical fiber methods are simple, can be fast acting, highly sensitive, can sample a large area giving more complete and accurate information, can operate with a long working distance and usable in adverse environmental conditions [2].

The situations under which the contactless measurement by optical-fibers are feasible are as follows:

(i) Reflectivity of the workpiece surface should be high; otherwise there will be no voltage or intensity change as the gap between the probe and workpieces is varied.

(ii) The medium between the probe and the workpiece should be homogeneous during experiment; otherwise the swarf or dirt in between, will absorb or scatter the reflected light and thus actual voltage measured will be less. Hence error will come in profile measurement.

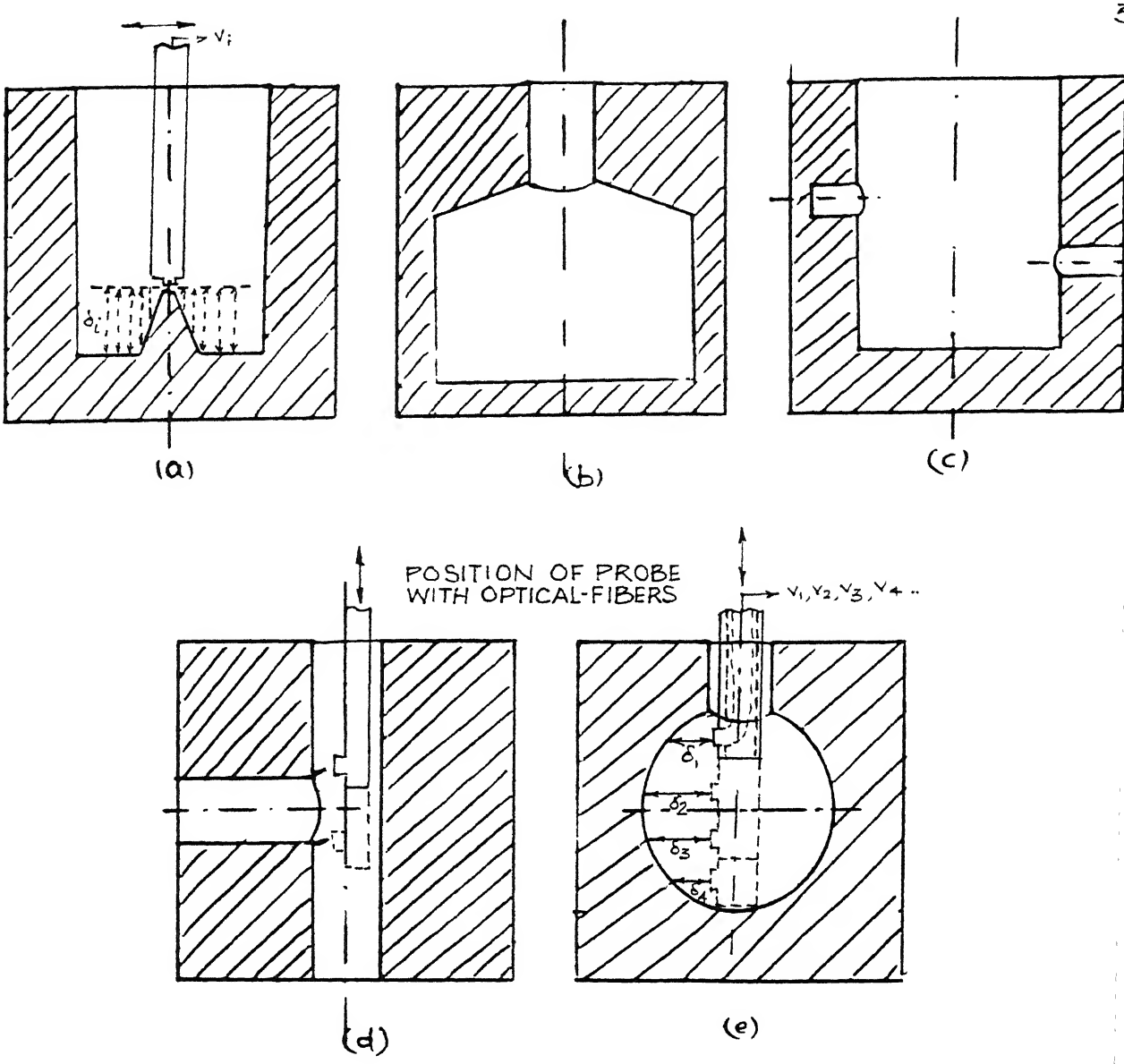

δ_i = Gap between probe and specimen in mm

V_i = Output voltage in Volts

FIG. 1.1 PROFILES OF COMPONENTS FOR WHICH CONTACTLESS MEASUREMENT CAN BE APPLIED

(iii) The light source (He-Ne laser) should be of constant intensity and power during experiments.

(iv) The light source should be of high power, so that the light reflected by the workpiece can be sensed by detector.

(v) The fibers bunched and polished together should be of lesser diameter than the minimum hole of workpiece to be measured.

(vi) Proper arrangement for holding fibers in the tool and for holding the workpiece should be made. Relative motion between them is measurable by screw gauge.

(vii) Stabilised power supply is required for all electrical equipments in the measurement method.

1.2 LITERATURE SURVEY

Historically the idea of using light waves for signalling was tested by Alexander Graham Bell as early as 1880. The invention did not yield commercial success for two reasons: (i) the medium for light wave transmission was air which is very lossy and (ii) sun light is an incoherent light source [2].

During World War-II, efforts were diverted in developing microwave and millimeter wave in millitary applications. A metallic waveguide, 5cm. in diameter was built for a 50 GHz. wave and reported loss between repeater (15-30km) was about 2dB/km. Cost was far too expensive [3].

Most researchers viewed a fiber as light wave pipe in which electromagnetic energy propagates by multi reflections from walls of pipe. After the inventions of lasers in 1960, the first discovery of low-loss glass fiber for supporting the light wave transmission was done by Kao Hockman and Co-workers in Britain (1966). They have proposed that silica based fibers could be made to transmit light waves with losses less than 20 dB/Km. Corning glass works succeeded in fabricating such low-loss fibers in 1970. The second demarcation was the invention of continuous wave (cw) room temperature diode lasers (1970) which provides coherent light sources. After this lots of improvements took place in today's fibers having a loss of 0.15 dB/Km at 1.55 μm [3,4].

There are many methods of measuring surface roughness, profiles of workpiece detection and burr shape and size. One way of classifying the methods of measurement are as follows [5]:

1.2.1 Profiling Technique

In which the topographic information is derived from a point-by-point scan of surface height Z as a function of distance X along a straight line on the surface. The resulting profile is analyzed by either analog or digital methods to derive various parameters for measurement [6]. Interferometry and stylus methods come under this technique.

1.2.1.1 Stylus Method

It is the oldest method of measuring surface profiles. The stylus instrument is generally known as "Profilometer". Fine diamond stylus is traced along the surface. It varies the output voltage which gives values either in arithmetic Average roughness of surface or height h of surface etc. The serious drawbacks in these are that it is basically laboratory instrument, hard stylus end erodes fine surface and higher setting up time is required.

1.2.1.2 Interferrometry

It is usually used for measurement by studying the fringe pattern produced. This fringe pattern is produced when the light wave interact with each other the wave effect is visible and thus made useful for measuring purposes. The phenomenon of interaction is called interference. The measuring devices which use this phenomenon of interference are known as interferrometers.

1.2.2 Parameteric Technique

The technique directly measured a parameter that represents some property of the surface topography averaged over illuminated area. Methods like measurement of light reflected in *specular direction, total intensity of scattered light, the diffuseness of the angular scattering pattern, the speckle contrast and the

---

* Specular direction is the direction at an angle of reflectance equal to angle of incidence.

polarization to study the surface topography come under this category.

1.2.2.1 Specular Reflectance

It is the method in which the light intensity scattered in specular direction is related to Roughness average values of the surface or gap between probe and workpiece in mm [7].

1.2.2.2 Diffuseness of scattered light

It employs the ratio of intensities in specular direction to some off specular direction and empirical relations to measure surface roughness and gap between probe and surface for that particular surface only [8].

1.2.2.3 Speckle Contrast

The surface illuminated by partially coherent light, reflects the beam which consists of parts of random bright and dark regions known as speckle. This is used to study surface micro topography.

1.2.2.4 Ellipsometery

It employs the measurement of change in polarization of incident polarized light, which depends upon the composition of surface, surface structure, temperature, strain and surface roughness etc.

1.2.2.5 Angular distribution (AD)

By measuring the distribution of scattered light in space around the scattering region various parameters related to surface roughness and profile of workpiece etc. is calculated [5].

1.2.3 Existing Theories

Spurgeon [3] and Lin, Shea and Hoang [10] used a fiber-optic transducer for measurement of surface roughness. They used bifurcated optical-fibers one end of which was used to carry the incident light to the surface while the other end detected the reflected light which could be measured using a photodetector. In both the works a good correlation has been shown to exist between the average roughness of the object surface and the measured reflected light. This procedure is of limited utility for two principal reasons:

(a) The roughness measurement was made in a non-normalized manner. Hence the measurement could be affected by variations in the incident light intensity and surface reflectivity, etc.

(b) The measurement lacks sensitivity limiting the roughness measurement to smooth surface up to 20 μ.in Ra.

K. Mitsui [11] proposed the potential non-contact optical method for in-process surface roughness measurement including reflected light position, focus error detection, using fibre-optics. This method was proposed for real time measurement of surface roughness change during cylindrical grinding. In this

light from a white light source was applied to the object surface through the emitting fibre and the receiving fibres transmitted the light scattered from the surface asperities to a photodiode (Fig. 1.2). The light that reaches the photodiode depends on the micro-topography of the object surface, corresponding to the surface roughness of the value. The method proposed had following limitations:

(a) The scattered light that has an incident angle greater than the critical transfer incident angle of the fibre cannot be transmitted to photodiode.

(b) The grinding fluid and swarf hamper the accuracy.

(c) Workpiece speed affects the surface roughness value.

W. P. T. North and A. K. Agrawal [12] carried out experimental investigation of a technique for the measurement of surface roughness of "ground" surfaces using fibre-optics. A pair of fibre-optic bundles of similar specifications are used to carry both the incident light to and the reflected from the object surface at different angles of incidence. It has been shown that the ratio of reflected intensities is found to vary inversely as the cube of the average surface roughness. The schematic diagram of the experimental set up is shown in Fig. 1.3. Because the measurement is electro-optical, it is many orders of magnitude

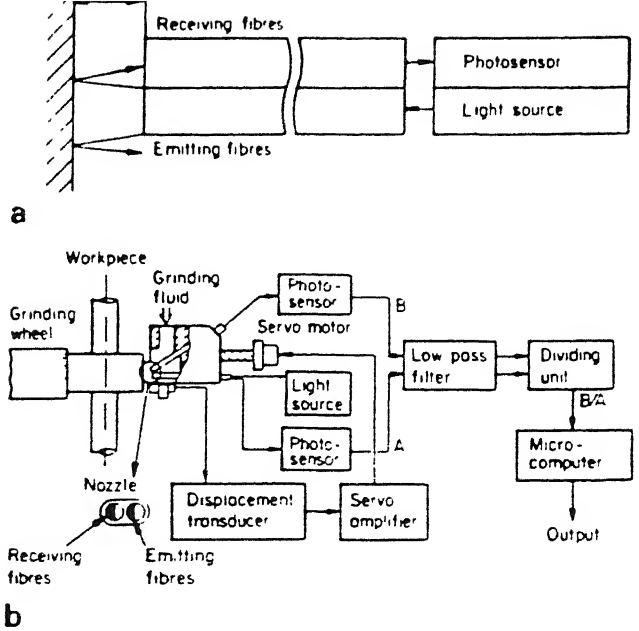

FIG.1.2 FIBER OPTIC SENSOR [11]
(a) PRINCIPLE OF DETECTION
(b) POSITION WITHIN PROCESS APPARATUS DESCRIBED BY K.MITSUI

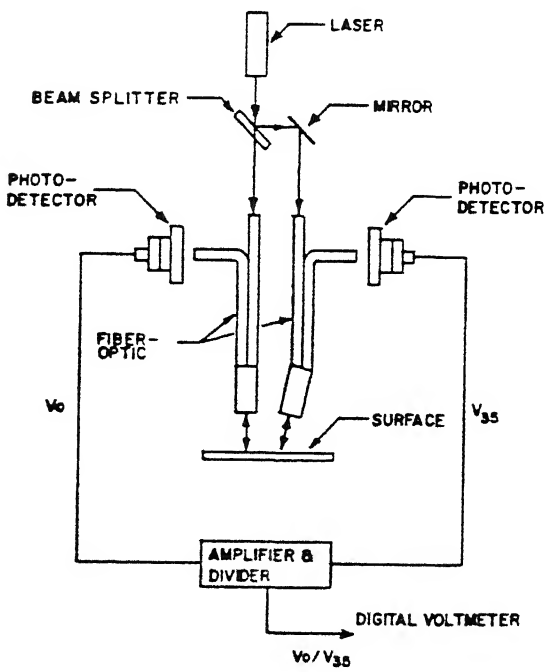

FIG.1.3 SCHEMATIC OF THE EXPERIMENTAL SET-UP [12] IN THE WORK OF NORTH W.P.T and AGARWAL A.K.

faster than the stylus profilometer. This makes the technique capable of "on line" and 100 percent roughness measurement in high volume production industries. The limitation of this technique is as follows:

(a) The sensitivity above, 40 μ.in Ra reduces significantly.

(b) The method is suitable for "ground" surface for roughness measurement.

(c) As the foot print of illumination is approx. 0.15 in. long, then Vo/V_{95} single measurement will essentially indicate the roughness as it averages over this length.

(d) The method is not valid for curved surfaces.

A. Novok, B. Colding [13] have presented an electro-optical method by using He-Ne laser for non-contact dimensional measurement the sensitivity of the device is 5mV/.001 mm, repeatability as 0.002 to 0.003 mm and accuracy as 0.01 mm. The maximum diameter of the workpiece on lathe has been limited to 280 mm. Again the basic problem in this method is to position the photodetector at an angle which gives the maximum output. Vibrations in the machine are found to change the angle of photodetector which will affect the accuracy of the measurement.

N. Ikawa, S. Shimada and H. Morooka [14] have described a photoelectronic displacement sensor consisting of a 50 W light source, optical fibre bundles for transmission of the illuminating

and the reflected light and photo-diode set up. A high resolution of 0.05 nm and a stability of 1 nm in 20 seconds has been achieved. The frequency has been limited to 1.6 KHz. As seen in graph (Fig.1.4) the best linearity is when the distance between the fibres and the reflecting surface is between 7 μm and 20 μm (around 5% linearity).

It has not been mentioned as to where the photodiode detects maximum intensity of power. The calibration curve has been stopped at 60 μm. The nature of the curve beyond 60 μm have not been shown. So close a distance as 30 μm might damage the probe surface, if the workpiece surface has a poor surface finish. The probe has been calibrated only for flat surfaces.

Kiyoshi Yanagi, Takashi Miyoshi and Katsumasa Saito [15] have developed the displacement sensor by fiber-optics which can estimate the roughness of a metal surface, form error of a machined surface and clearances between a fiber end and a free formed metal surface by detecting changes in intensity of the reflected light. The experiment were carried out for flat, concave and convex specimens of stainless material and relationship between the measuring distance d and the received luminous flux ϕ is established for all cases. In all the cases, it is found that the curve has three phases; ϕ increases linearly in the first phase, holds constant approximately in the second phases, and decreases linearly in the third phase. The limitations of these experiments are as follows:

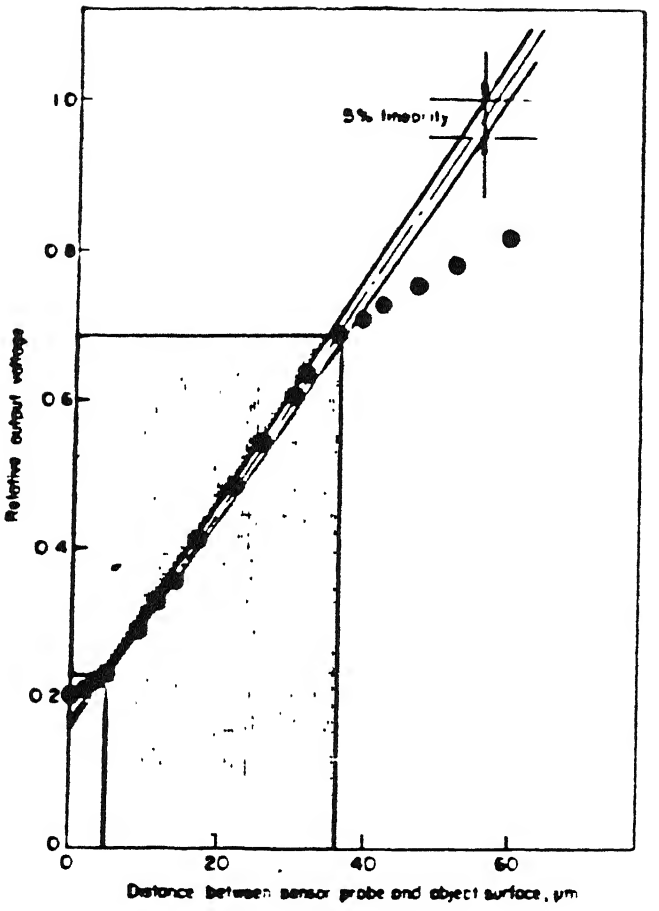

FIG. 1.4 BEST LINEARITY RANGE [9]

(a) As LED source is used, the reflected light from specimen will be very weak hence very sensitive photodetector and sensing circuit is required.

(b) The error obtained in the measurement of displacement is of the order of 13 μm.

(c) Curved specimens are approximately treated as flat ones for $R_c \geq 30$ mm.

Sigeru Ueno [16] have developed new method for detecting surface texture on turning by fiber-optics. The results of this experiments are that when the reflected light from a metal surface is obtained by the transducer under the same condition, its output can be said to be proportional to the amount in existence of the slope distribution upto $\pm 6^{\circ}$ of the surface. Chattering during turning was also detected as the amount in existence of the slope in the distribution near 0° increases when any chatter occurs while turning. The limitations in these experiments were are follows:

(a) As there are limited number of samples for correlation computation, the values are not so much exact.

(b) The reflected light from the slope ranging upto approximately $\pm 6^{\circ}$ including errors enters the fiber bundle to affect the output.

The work done in the field of contactless measurement by fiber-optics is mainly for surface roughness measurements as clear from above literature survey. Very less work has been done in the field of profile measurement i.e. using displacement transducers. Literature survey reveals that researchers use bifurcated fibres for transmitting the incident light & receiving reflected light. This reflected light from the workpiece through fibres on photodetector detects the intensity in Volts. This change in intensity i.e. in volts is studied as a function of gap between the probe and workpiece and surface roughness.

The same principle discussed above can be as well applied to measurement of gap between probe and workpeice, profile measurement, burr profile measurement, study of inclination of workpiece on output voltage, study of effect of medium between probe and workpiece on output voltage etc.

The problem mentioned above has been chosen for our research work and the same is proved experimentally and theoretically in succeeding chapters.

CHAPTER - II

THEORETICAL ANALYSIS

The relationship between scattering and surface topography is complicated and according to our survey no exact theory is available. However, full vector electromagnetic theories are available in two opposite extremes [17] namely when vertical scale of roughness is much less than the wavelength of the incident light and secondly when the roughness amplitude is much greater than the wavelength of the incident light.

2.1 DETERMINATION OF MAXIMUM OUTPUT VOLTAGE FOR PARTICULAR GAP BETWEEN PROBE AND WORKPIECE (ALUMINIUM SPECIMEN)

2.1.1 Amplification Gain of Sensing Circuit

In the sensing circuit as discussed in next chapter and shown in Fig. 3.8 the amplification of signal in volts is done in two stages by two operational amplifiers viz. AD 540J FET input op-amp and SMC741 general purpose op-amp. The total amplification gain A, of an op-amp is given by

$$A = \frac{V_o}{V_i} \cong - \frac{R_f}{R_i}$$

where V_o and V_i are output and input voltages, & R_f and R_i are resistances of op-amp.

2.1.1.1 Amplification gain (A_1) for AD-540J FET input op-amp

The circuit diagram for this op-amp is shown in Fig 2.1. The internal resistance of the photodiode (C-30808 RCA silicon photodiode) is calculated as follows:

$$R = \frac{V}{I}, \text{ where } V = +12 \text{ V}, \quad I = \cdot 3\text{mA} = \cdot 3 \times 10^{-3} \text{ Amp.}$$

Thus,

$$R = \text{internal resistance of photodiode}$$

$$= \frac{12}{\cdot 3 \times 10^{-3}} = 40 \times 10^{-3} \text{ ohm}$$

or $= 40$ K ohm.

The equivalent circuit diagram of the FET input op-amp is shown in Fig. 2.2.

Hence A_1 (Amplification Gain) $= \frac{V_o}{V_i} \cong - \frac{R_f}{R_i}$

here $R_f = 510$ K ohm

and $R_i = \frac{100 \times 40}{100 + 40} \quad \left[\frac{1}{R_i} = \frac{1}{40} + \frac{1}{100} \right]$

$$R_i = \frac{200}{7} \text{ K ohm}$$

Hence $A_1 = - \frac{510}{200} \times 7 = - \frac{357}{20}$

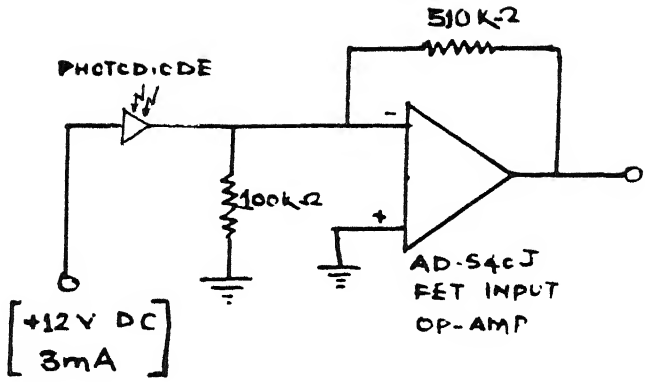

FIG. 2.1 CIRCUIT DIAGRAM FOR PREAMPLIFICATION

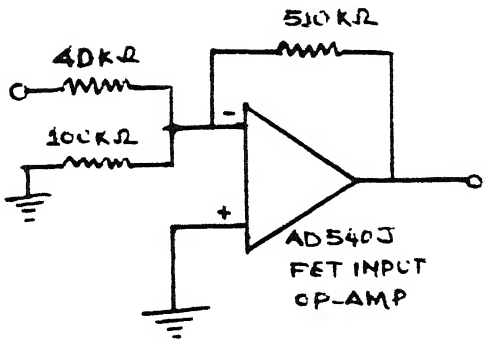

FIG. 2.2 EQUIVALENT CIRCUIT DIAGRAM FOR PREAMPLIFICATION

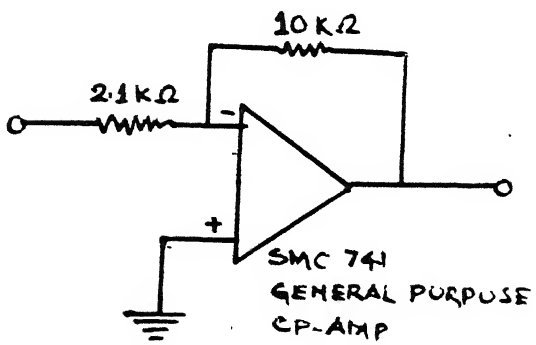

FIG. 2.3 CIRCUIT DIAGRAM FOR AMPLIFICATION

2.1.1.2 Amplification gain (A_2) for SMC-741 general purpose op-amp

The circuit diagram of sensing circuit for SMC 741 is shown in Fig. 2.3.

Here R_f = 10 K ohm

R_i = 2.1 K ohm

and A_2 (Amplification gain) $= -\frac{R_f}{R_i} = -\frac{10}{2.1} = -\frac{100}{21}$

2.1.1.3 Amplification Gain (A)

Total Amplification Gain (A) of the sensing circuit is the product of the amplification gain (A_1) by FET op-amp and amplification gain (A_2) by the general purpose op-amp, i.e.

$$A = A_1 \times A_2$$

$$= \frac{-357}{20} \times \frac{-100}{21}$$

$$= 85$$

This means the signal by photodiode is amplified 85 times by the sensing circuit.

2.1.2 Reflectance R of Aliminium Specimen

The reflectance R is defined as the ratio of the reflected energy and incident energy. Since the energy is equal to the product of the complex amplitudes for reflected and incident waves are given by Fresnel Equations [4].

For Aluminium η and K are the real and complex parts respectively, the index of reflection = 1.15 and 3.2 respectively.

From Fresnel equations for normal incidence,

$$A_2 = A_i \frac{\hat{n} - 1}{\hat{n} + 1} \qquad (1)$$

where A_2 and A_1 are complex camplitudes of reflected and incident waves. $\hat{n}$ (i.e. circumflex over η) indicates that the index of reflection is complex, i.e. $\hat{\eta} = n - jk$, $(j = \sqrt{-1})$.

Then

$$R = \frac{A_r A_r^*}{A_i^2} = \frac{\hat{n} - 1}{\hat{n} + 1} \cdot \frac{\hat{n}^* - 1}{\hat{n}^* + 1} \qquad (2)$$

where * denotes a complex conjugate.

Then from equation (2), $\hat{\eta} = n - jk$ and $\hat{\eta}^* = n + jk$ and substituting these expressions into preceeding equation gives

$$R = \frac{[(n-1)-jk]\,[(n-1)+jk]}{[(n+1)-jk]\,[(n+1)+jk]} = \frac{(n-1)^2 + K^2}{(n+1)^2 + K^2} \qquad (3)$$

Substituting given values yields

$$R = \frac{(1.15-1)^2 + (3.2)^2}{(1.15+1)^2 + (3.2)^2} = 0.69 \qquad (4)$$

2.1.3 Calculation of Output Voltage

Theoretically the maximum output voltage is calculated for particular gap (Z_{max}) between probe and workpiece (Aluminium

specimen). The gap (Z_{max}) is taken directly from the experimental results where the peak voltage in air medium between probe and specimen for aluminium specimen by buffing operation is considered. The Z_{max} from graph (Appendix-E) we get 3.1mm where the peak voltage experimentally obtained is 4.9 volts.

The schematic diagram of fibers with the angle subtended by the reflected light by receiving fibers is shown in Fig. 2.4 and its exploded half view is shown in Fig. 2.5.

Let $\phi = \theta_1 - \theta_2$ from ΔABD,

$$\tan \theta_1 = \frac{CD}{AD} = \frac{2.3}{3.1} = 0.742$$

or $$\theta_1 = \tan^{-1} (0.742) = 36.57^\circ$$

Similarly, from ΔACD, we get

$$\tan \theta_2 = \frac{BD}{AD} = \frac{1.9}{3.1} = 0.613$$

or $$\theta_2 = \tan^{-1} (0.613) = 31.51^\circ$$

Therefore, $\angle BAC = \phi = \theta_1 - \theta_2 = 36.57^\circ - 31.51^\circ = 5.06^\circ$

Therefore, total angle of reflected light incident on receiving fibers is 2ϕ i.e. $2 \times 5.06^\circ = 10.12^\circ$.

Maximum Area of fibers receiving reflected light

$$= \pi \left[\left[\frac{4.6}{2} \right]^2 - \left[\frac{2.8}{2} \right]^2 \right] = 10.46 \text{ mm}^2$$

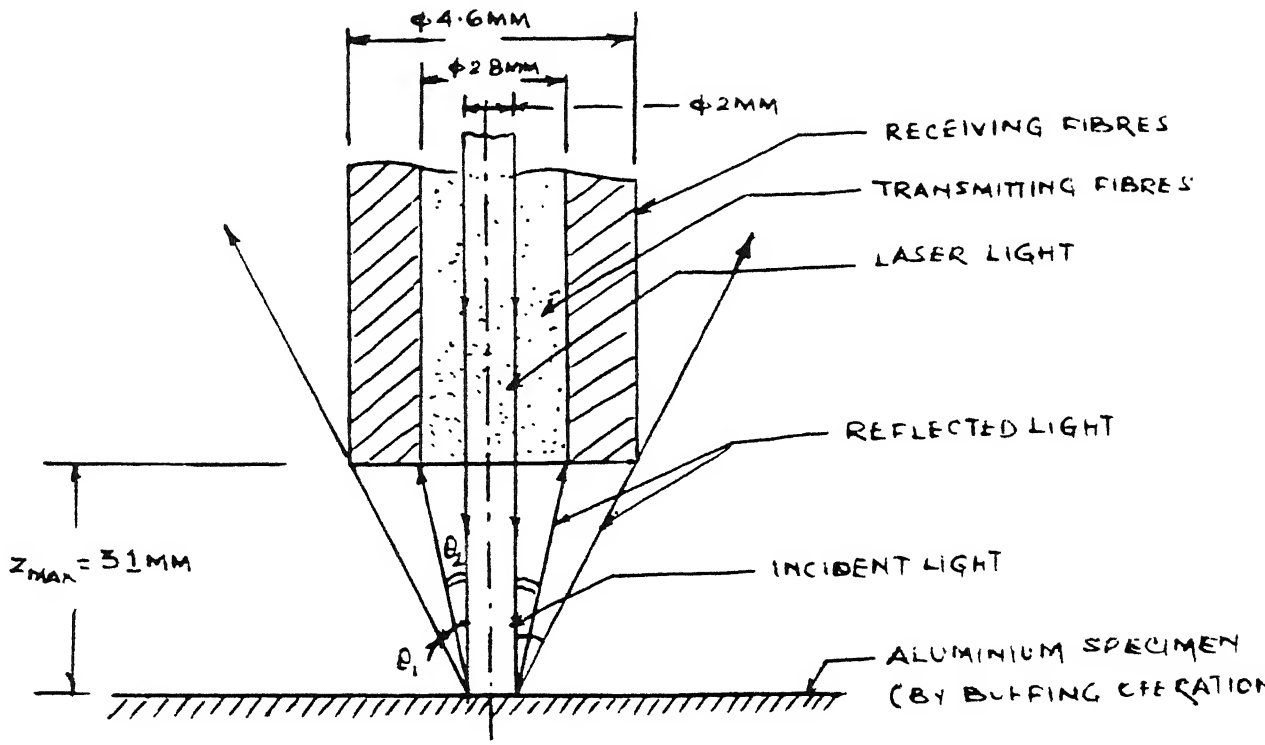

Fig. 2.4 Schematic Diagram Of Optical-Fibers With Incident And Reflected Light

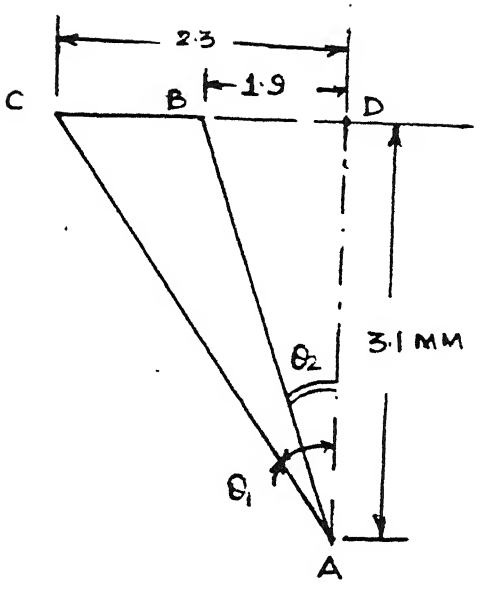

FIG. 2.5 EXPLODED HALF-VIEW OF REFLECTED LIGHT

because Area of receiving fibers $= \pi(r_2^2 - r_1^2)$

Power density of Laser Source (He-Ne) through incident fibers (considering no losses in fibers) on aluminium specimen is ratio of power and area of beam of specimen

$$\text{Power density} = \frac{\text{Power of Laser Source (He-Ne)}}{\text{Area of beam}}$$

Power of He-Ne Laser Source = 4 milliwatts

$= 4 \times 10^{-3}$ watts

Area = π (beam spot radius)^2

$= \pi\ (1)^2 = \pi$

Hence,

$$\text{Power density of incident light} = \frac{4 \times 10^{-3}}{\pi}$$

$= 1.27 \times 10^{-3}$ watts/mm^2

$$\text{Power density of reflected light} = \text{Reflectance (R)} \times \text{Power density of incident light}$$

$= 0.69 \times 1.27 \times 10^{-3}$

$= 0.8763 \times 10^{-3}$

$= 0.8763$ milliwatts/mm^2

Assuming that the power density of reflected light is scattered equally in all directions i.e. 180°.

Then the power at Z_{max} (3.1mm) i.e. gap between probe and aluminium specimen at the receiving fibers inlet (2ϕ) is

$$= \frac{\text{Power density of reflected light}}{180^{\circ}} \times 2\phi \times \text{Maximum area of receiving fibers}$$

$$= \frac{0.8763}{180^{\circ}} \times 10.12 \times 10.46, \quad \frac{mW}{mm^2} \cdot \frac{1}{Deg} \cdot Deg \cdot mm^2$$

$$= 0.515 \text{ milliwatts}$$

Assuming no losses in receiving fibers, then voltage output from the photodiode is ratio of power density and current density.

For photodiode (C-30808),

photocurrent = 5 milliAmp.

Area of diode = 5 mm^2 (Appendix-B)

Area of receiving fibers = 10.46 mm^2.

$$\text{Output Voltage from photodiode} = \frac{0.515/10.46}{5/5}, \quad \frac{mW}{mm^2} \cdot \frac{mm^2}{mA}$$

$$= 0.049 \text{ Volts.}$$

Now, the amplification gain of the sensing circuit as discussed in Sec. 2.1.1.3 is 85.

Hence output voltage at the output end = 0.049 x 85

= 4.165 Volts

≅ 4.2 Volts

2.1.4 Calculation of Output Voltage for Inclined Specimen

The principle used here for calculation of output voltage is that, when the specimen is inclined at an angle θ degrees, the reflected light is shifted or tilted by angle 2θ degrees [18]. This is shown in Fig. 2.6.

The value of Z_{max} i.e. the gap between the probe and specimen is taken directly from the experimental results. Here for $\theta = 8^{\circ}$, $Z_{max} = 28.0 \times \tan(8^{\circ}) = 3.9$ mm (Appendix-E).

Refer to Sec. 2.1.3, i.e. for the flat specimen at 0° inclination. It is proved theoretically that the angle subtended by the receiving fibers for reflected light is $2\phi = 10.12^{\circ}$ i.e. the full surface area of the receiving fibers is receiving uniform reflected light from the specimen.

But when the specimen is inclined at $\theta = 8^{\circ}$, then the reflected light from specimen is shifted by $2\theta = 16^{\circ}$. As the probe with fibers is stationary and perpendicular to base line and it is placed at $Z_{max} = 3.9$ mm from the specimen. The maximum reflected light falls only on the part of the surface area of receiving fibers which gives corresponding maximum output voltage. Hence the total angle subtended by the receiving fibers for inclination $\theta = 8^{\circ}$ is $16^{\circ} - 10.12^{\circ} = 5.88^{\circ}$. Hence at $2\phi^{\circ} = 5.88^{\circ}$, actually only the part of surface area of the receiving fibers is covered by part of reflected light.

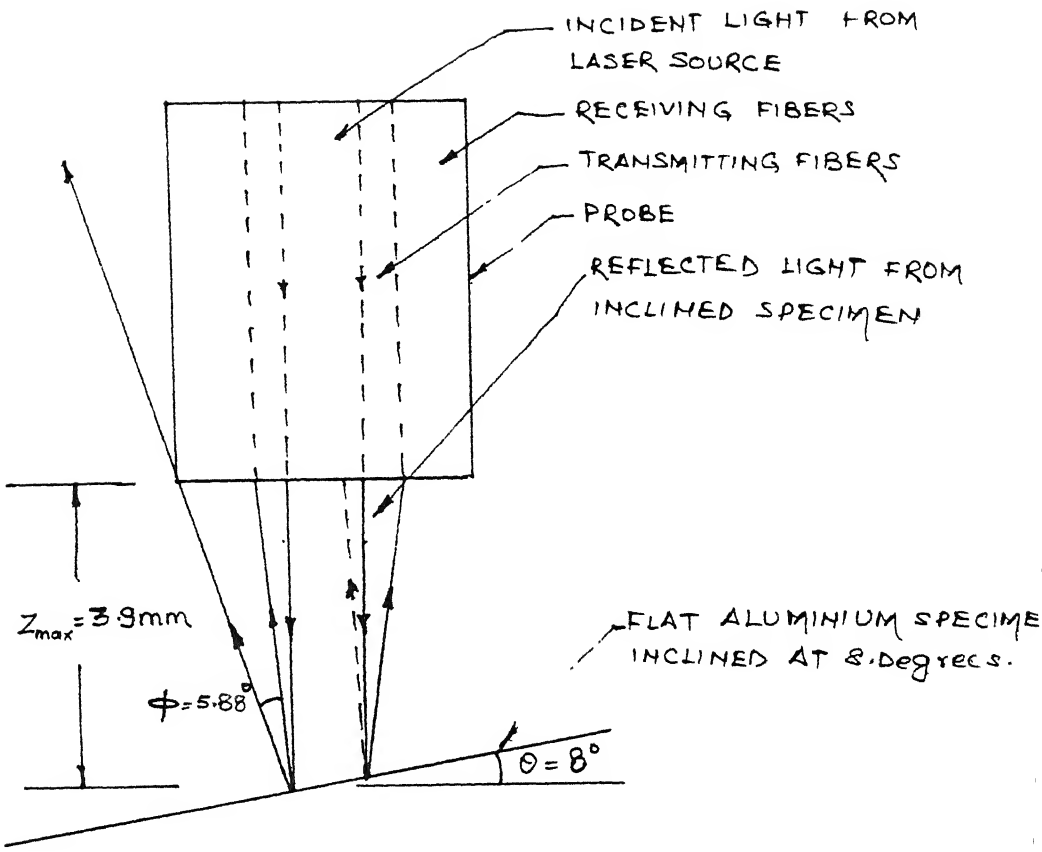

FIG 2.6 SCHEMATIC DIAGRAM OF REFLECTED LIGHT ON INCLINED SPECIMEN

Assuming that the full area of fibers is uniformaly receiving the reflected light at 5.88°.

The power density of the incident light = 1.27×10^{-9} W/mm^2

and power density of reflected light = 0.8763 milliwatts/mm^2 (calculated earlier in Sec. 2.1.3)

Hence the power obtained at Z_{max} (3.9mm) at the receiving fiber

$$= \frac{0.8763}{180^\circ} \times 5.88 \times 10.46, \quad \frac{mW}{mm^2} \cdot \frac{1}{Deg} \cdot Deg \cdot mm^2$$

$$= 0.299 \text{ milliwatts.}$$

Assuming no losses in receiving fibers, then the voltage output form the phodotiode = $\frac{0.299/10.46}{5/5}, \quad \frac{mW}{mm^2} \cdot \frac{mm^2}{mA} = 0.0286$ Volts.

Hence the output voltage obtained for Z_{max} = 3.9 mm gap after amplification is = 0.0286 x 85 = 2.431 Volts.

CHAPTER - III

EXPERIMENTAL SET-UP AND PROCEDURE

The principle of change in the intensity of the reflected light from the workpiece surface with the change in the gap between the fiber-optics probe end and the workpiece is used in the present work to detect the profile of the workpiece. The schematic diagram of the fiber bundles used is shown in Fig. 3.1. The centre part is the incident fibers of 2.8 mm diameter and the surrounding part is the receiving fibers of 4.6 mm diameter. These are called as Y-Guide Bifurcated Optical Fibers. Fig. 3.2 shows the experimental set-up. He-Ne laser source of 4 milliwatts power and 635.89 nanometres wavelength, is used as a light source. The light guided by the incident fibers bundles illuminates a specimen surface. The reflected light is detected by the receiving fiber bundles and this light is made to fall on photodiode (RCA silicon PIN photodiode, C-30808), which converts it into voltage and then through the amplified circuit (sensing circuit) the voltage is amplified which is recorded by omini-scribe recorder and viewed in oscilloscope and millimeter.

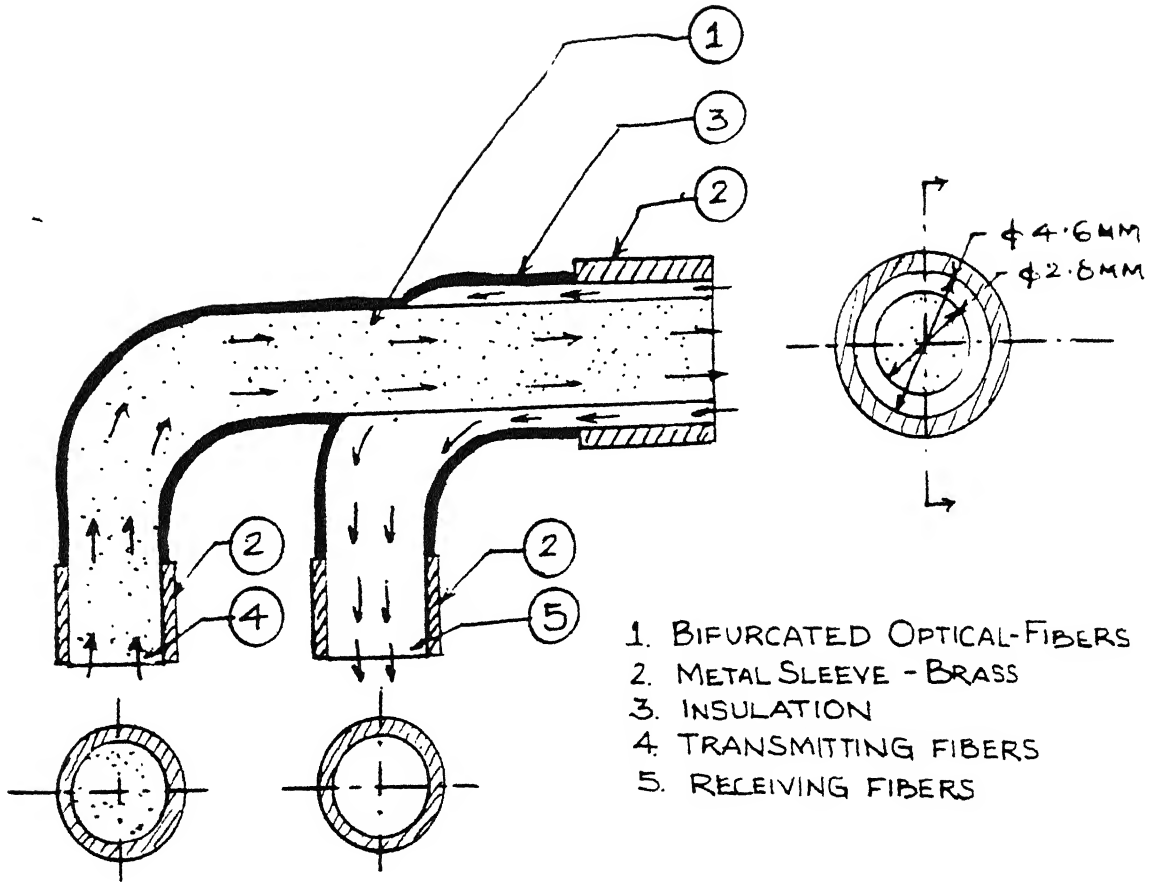

FIG. 3.1 SCHEMATIC DIAGRAM OF BIFURCATED OPTICAL-FIBERS

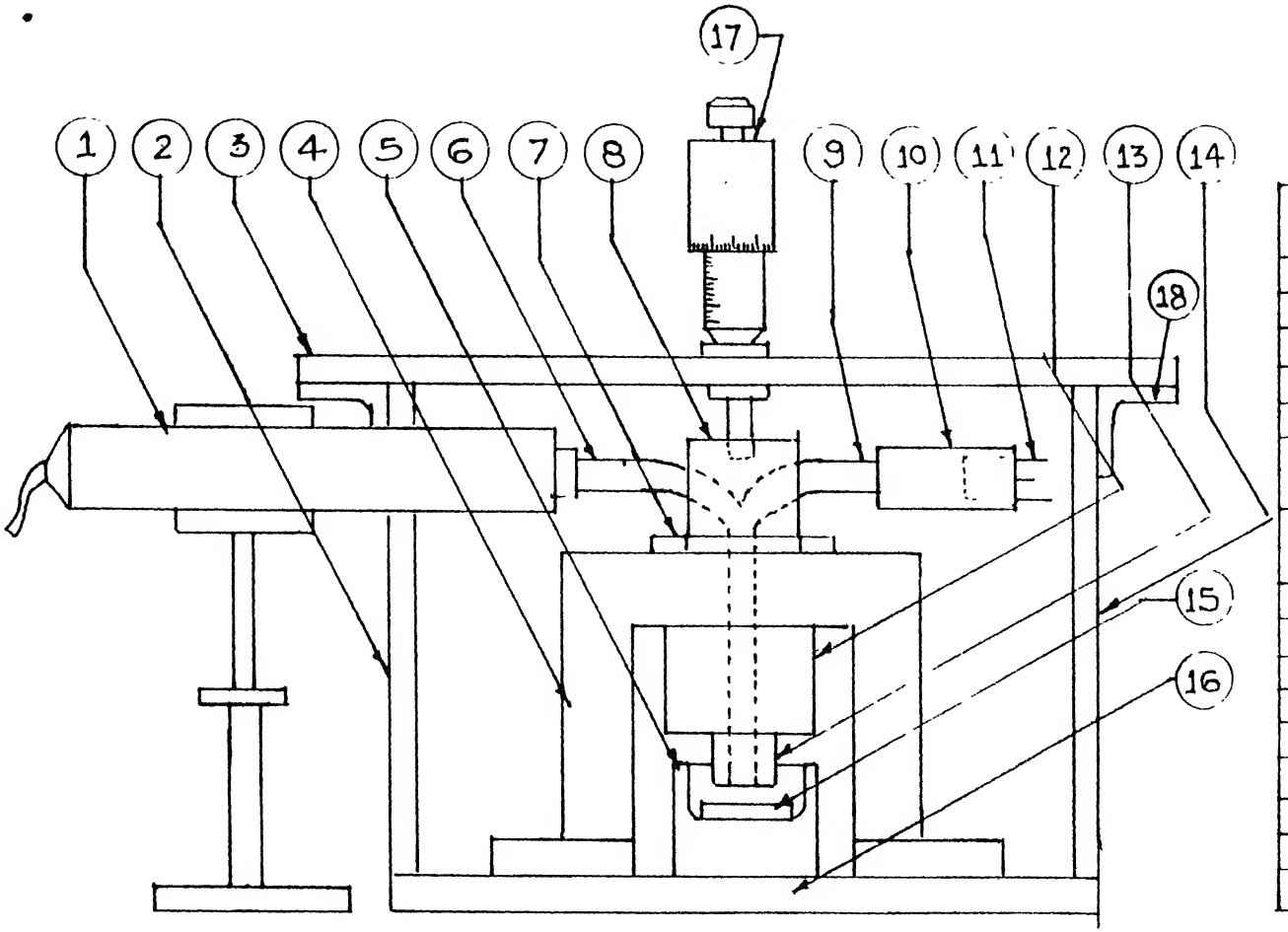

S.No	DESCRIPTION
1	HELIUM-NEON LASER SOURCE
2	LEFT SIDE PLATE - PERSPEX
3	TOP PLATE - ALUMINIUM
4	HOUSING - PERSPEX
5	WORKPIECE HOLDER - PERSPEX
6	TRANSMITTING FIBERS
7	COLLAR - BRASS
8	HOUSING - ALUMINIUM
9	RECEIVING FIBERS
10	DETECTOR HOUSING - ALUMINIUM
11	C-30808 PHOTO DIODE
12	CYLINDER - BRASS
13	TOOL HOLDER - BRASS
14	RIGHT SIDE PLATE - PERSPEX
15	WORKPIECE OR SPECIMEN
16	BOTTOM PLATE - PERSPEX
17	SCREW-GAUGE
18	ELBOW PLATE - PERSPEX

FIG 3.2. EXPERIMENTAL SET-UP WITH BIFURCATED OPTICAL-FIBERS

The nature of experiments carried out is shown in block diagram in Fig. 3.3 These experiments were carried out in two stages.

(a) In the first stage the experiments were carried out on the static model (made of perspex sheets, brass guides & tool holder for fibers, aluminium material plate for holding screw gauge etc). The study of effect of various surface roughness plates and effect of medium like Air, Water and Nacl solution between probe and workpiece, on the output voltage is carried out.

In this model the fibers are press fitted to the centre of the tool and the vertical up and down motion of tool with fibers is provided by the screw-gauge of 0.01 mm least count which is fitted on top of the tool. The tool is guided in the brass housing with the spring opposing the force exerted by screw-gauge. The output voltage is recorded by i) varying gap between probe and workpiece for various specimens (ii) varying the medium between probe and workpiece (iii) varying the surface roughness and type of material for workpiece.

(b) In the second stage the experiments were carried out using the feed mechanism of an EDM machine. The translatory motion in x and y direction is provided to the table manually which is of 0.005 mm least count. The vertical up and down

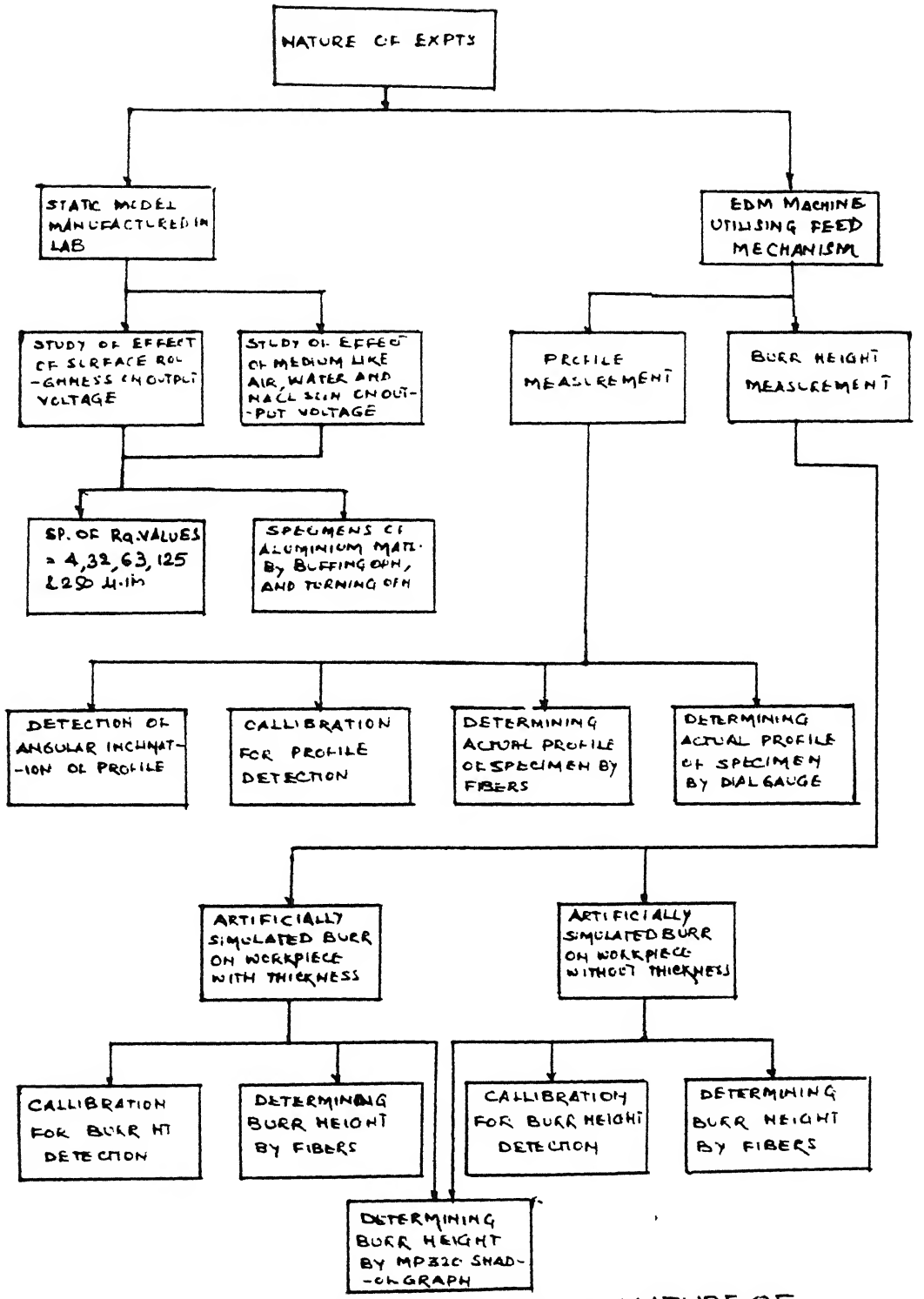

FIG. 3.3 BLOCK DIAGRAM OF NATURE OF EXPERIMENTS

motion in z direction is provided by servo motor to the spindle head and this motion can be measured by the dial-gauge fitted on spindle head of 0.01 mm least count.

On this machine, two applications of fiber-optics for contactless precision measurement are carried out. They are i) profile measurement and ii) height measurement of burrs created artificially on the specimen.

3.1 EXPERIMENTAL SET-UP

Following steps are taken before setting up the experiment:

3.1.1 Selection of Laser

Scattering of light from a rough or inclined surface depends upon the angle of incidence and the wavelength of the light source. Further, more light is scattered in all directions in which only part of it is directed on photodiode through fibers, hence intense source of light is desirable for the purpose. Laser source is highly monochromatic and intensity of light is high. Combined with its direction/ability, it is therefore found to be the ideal light source for the present experiment. A 4 milliwatts 'Melles-Griot' He-Ne laser polarised in the plane of incidence, of wavelength, λ = 6328.193 Å, is used in the experiment. Since He-Ne laser is commercially available and the

wavelength lies in the visible range, its use in the present work

is justified.

3.1.2 Selection of Photodiode

C-30808 single element, general purpose P-1-N Photodiode, RCA Solid State detector shown in Fig. 3.4 which is sensitive to He-Ne laser wavelength is selected for experimentation. Its specifications are given in Appendix-B. The detector housing as shown in Fig. 3.5 is designed in such a way that receiving fiber end and detector are press fitted in this housing very close to each other so that all the reflected light falls on the detector. This is shown in Fig. 3.6.

3.1.3 Selection of Fibers

Initially two fibers of 12 microns each were taken, one of the fiber for transmitting laser light by He-Ne laser source and another fiber to sense and receive the reflected light and then to direct it on the photodiode. But the intensity of reflected light received by fiber was so weak that it could not be sensed by photodiode.

Then several combinations of fibers of 12 microns were bunched together and by placing the receiving and the incident fibers in random and then in organised manner, experiments carried

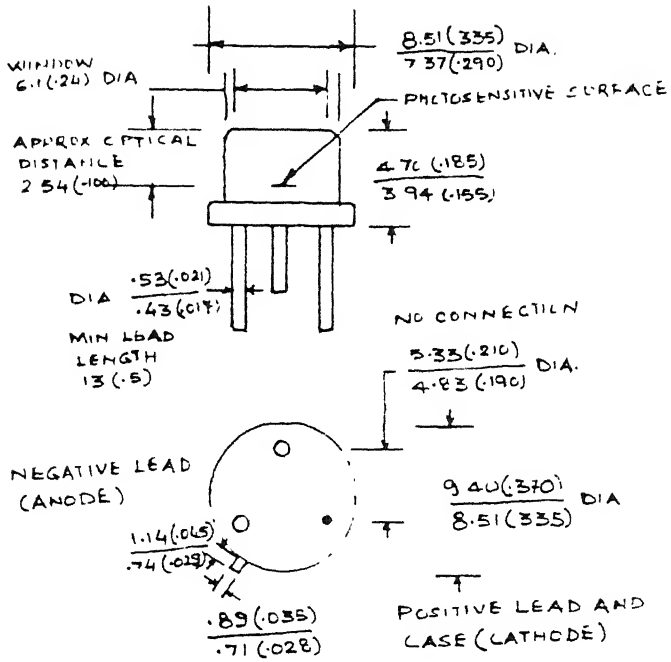

DIMENSIONS IN MILLIMETERS. DIMENSIONS IN PARENTHESES ARE IN INCHES

FIG 3.4 C-30808 PHOTOTRANSISTOR

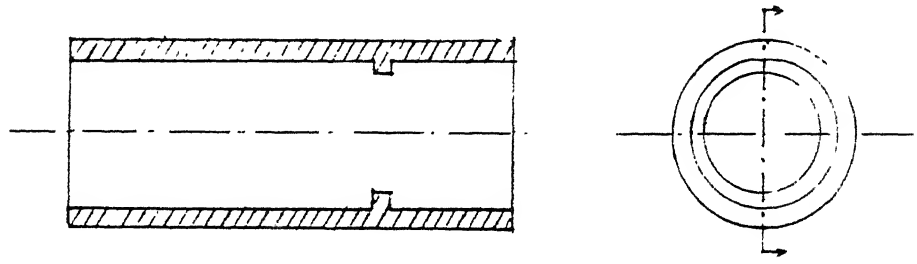

FIG. 3.5 SCHEMATIC DIAGRAM OF DETECTOR HOUSING MATERIAL - ALUMINIUM

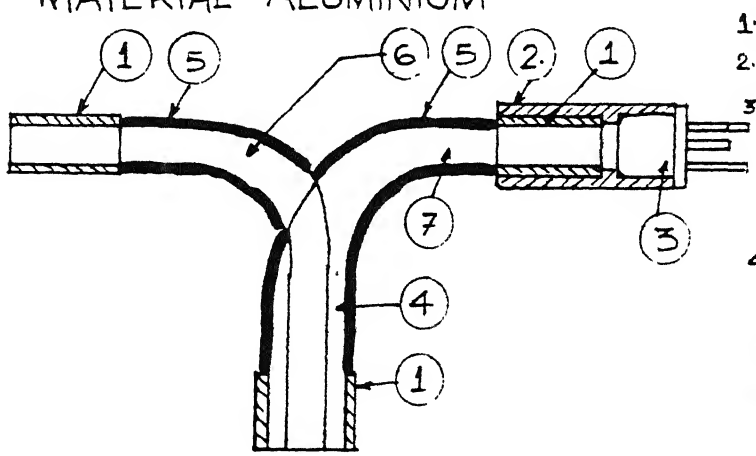

1. METAL SLEEVE
2. DETECTOR HOUSING
3. C-30808 PHOTODIODE
4. BIFURCATED OPTICAL-FIBERS
5. INSULATION
6. TRANSMITTING FIBERS
7. RECEIVING FIBERS

FIG. 3.6 ARRANGEMENT OF PHOTODIODE AND FIBER END IN DETECTOR HOUSING

ıt but still the losses of reflected right were high and signal ɔuld not be sensed by the detector.

Hence commercially available bifurcated optical fiber bunch s used in the present work with the dimensions as shown in Fig. .1.

.1.4 Design of Sensor and Amplification Circuit

The sensor should be capable of producing signals ɔroportional to the distance between the probe and the workpiece. In addition, the sensor should be reliable and accurate and sense gap in real time. Sensors based on various principle such as capacitive principle, pneumatic principle, cutting resistance and optical principle etc. have been used in the past. The one which has been widely accepted to have the best sensitivity, accuracy and reliability and are used more often [11,12,13,14,18,19,20] is the sensor based on optical principle. The photoelectronic displacement sensor consists of He-Ne laser source of 4 milliwatts power, bifurcated optical fiber bundles for transmission of illuminating and receiving the reflected light, photodiode (C-30808) and Amplifier circuit, which has very high resolution. This sensor set up is very economical and its block diagram is shown in Fig. 3.7.

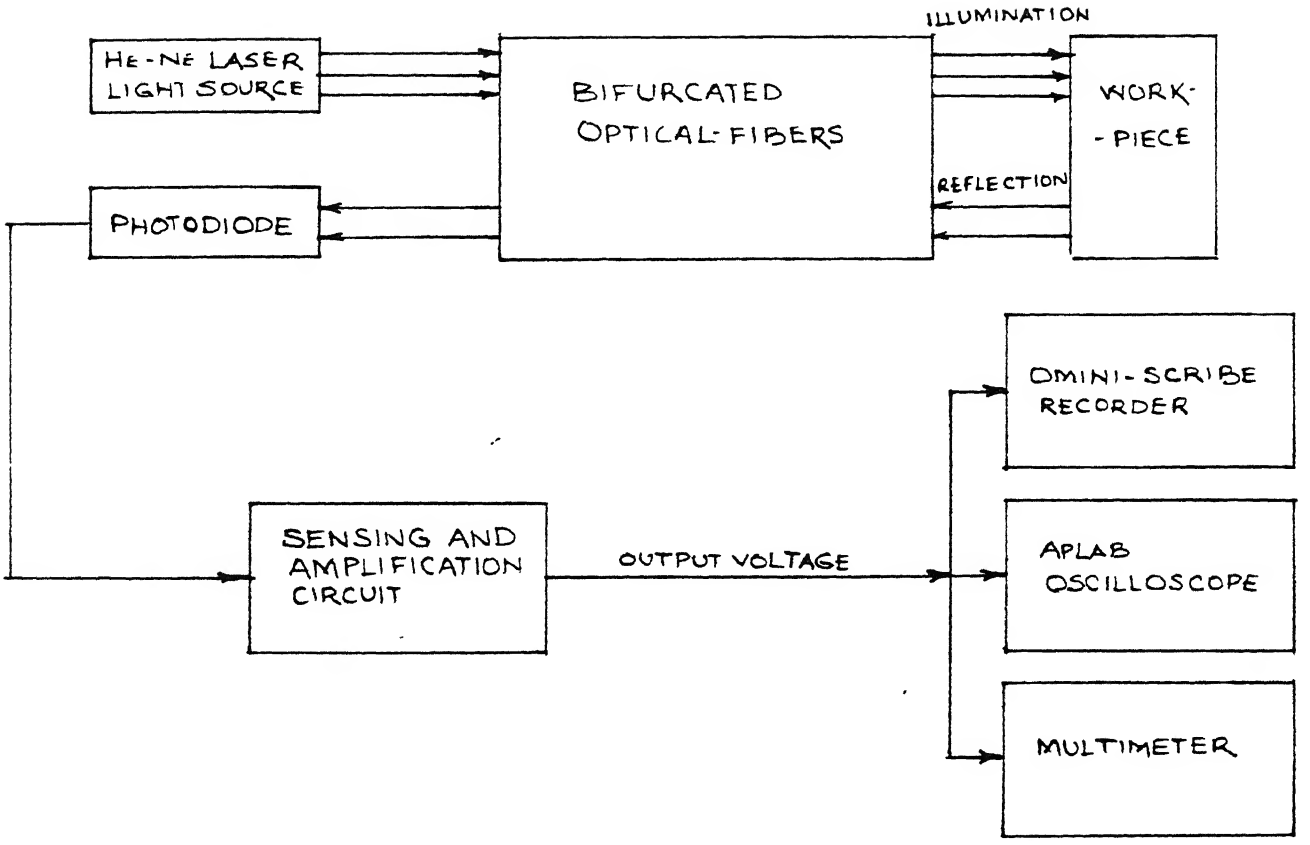

FIG.3.7 BLOCK DIAGRAM OF EXPERIMENTAL SET-UP

As the light intensity from the He-Ne laser source through he optical-fibers is constant, the variation in the light ntensity at the receiving fibers is only due to the variation of he gap between the probe and the workpiece surface, keeping all ther parameters constant like type of material of the workpiece, a. values of the specimen, medium between probe and workpiece, ngular inclination of specimen etc.

The laser light from the He-Ne laser source through the bifurcated optical-fiber illuminates the workpiece. The reflected light through the optical fibers falls on photodetector which converts the light intensity signal to the electrical signal. The photodiode C-30808 is very sensitive to the optical signals and it can measure signals of very high frequencies. But the output electrical signal from photodiode is usually very low, hence the amplifier circuit with suitable operational amplifier (op-amp) is used to amplify the electrical signal which can be measured and recorded by oscilloscope, multimeter and recorder.

The weak electrical signal from photodiode is amplified in 1st stage by FET input op-Amp (AD 540 J) whose specifications are given in Appendix-C . However it is very difficult to detect small displacement signal with this system, because the variation in intensity of the reflected light for very small displacement (gap between probe and workpiece) is very small. Therefore for better and accurate measurement of this weak signal a DC voltage

of 2 volts is introduced to pin number 3 by a variable multiturn potentiometer (2K POT of 10 turns). With this set up the initial voltage level can be set to within ± 1 millivolts. The variation from this set level will be proportional to the change in the relative displacement between probe and the workpiece surface. The sensing and amplification circuit is shown in Fig. 3.8. The op-amp AD 540 J is used as differential amplifier hence there is need of inverting amplifier which is done by another op-amp SMC 741.

The second stage amplification is carried out by general purpose 741 op-amp. By the use of SMC 741 op-amp the signal to noise ratio increases. In order to filter the high frequency noises a capacitor of capacitance 1000 microfarads is connected across the output voltage and GND (ground connection). High frequency noises are liminated with this R.C. filter.

This sensing and amplification circuit is soldered on the PC board so that no loose connection exists and conditions remains same during the course of experiments.

3.1.5 Design of Set-up

This experiment requires He-Ne laser source, bifurcated optical fibers, photodiode, sensing and amplification circuit, DC power source of ± 12 V, + 5V and GND connections, oscilloscope,

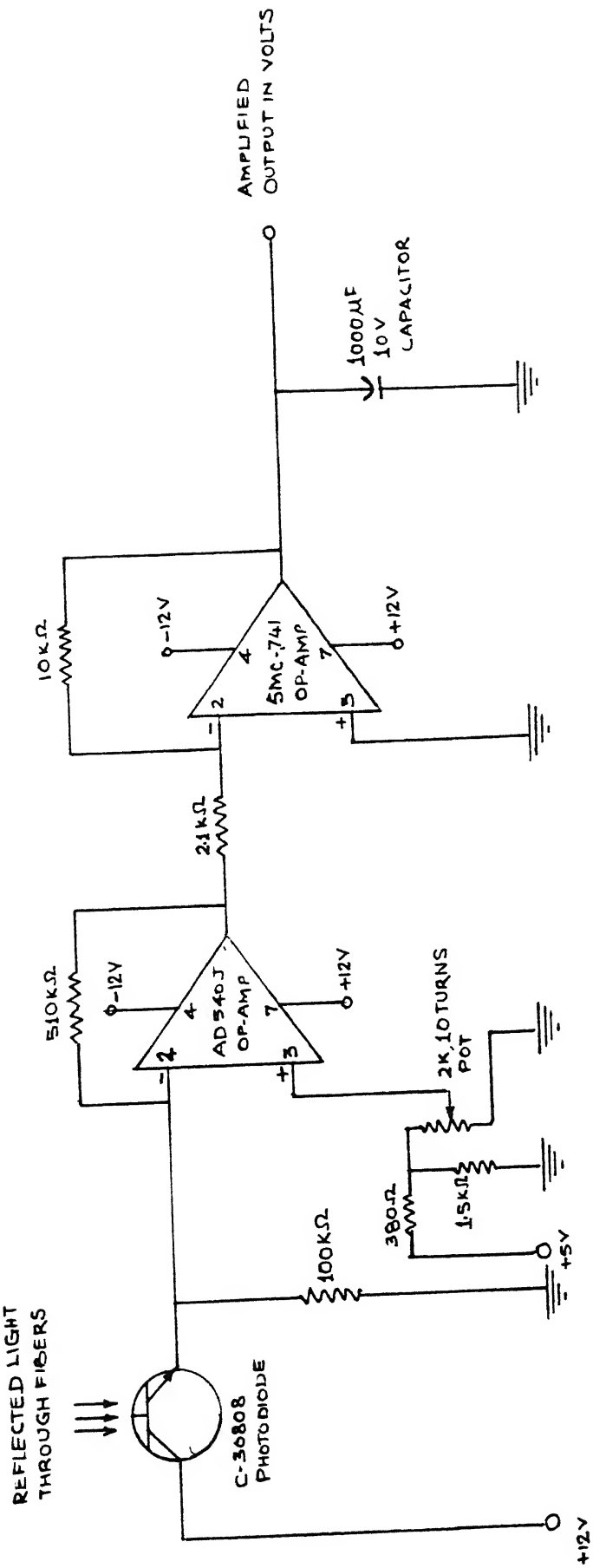

FIG. 3.8 SENSING AND AMPLIFICATION CIRCUIT

ıultimeter of 2.5V and 10 V scale, omini-scribe recorder, ,tabilizer for stabilized power supply to all the electrical :quipments and various specimens. The block diagram of the :xperimental set-up is shown in Fig. 3.7.

The He-Ne laser source is used for providing laser light source, through the bifurcated optical fibers, to illuminate the workpiece (specimen). The reflected light from the workpiece is falling on the receiving fibers is transmitted though fibers to photodiode. The photodiode detects the light falling on it and converts this optical signal to the electrical signal in terms of nanoamperes current. This weak current is sensed by op-amps in the sensing circuit and amplified to give the output in terms of voltage. This voltage is recorded by ominiscribe recorder and is cross checked by viewing the voltage on oscilloscope and multimeter which are connected in parallel (See Fig.3.7).

3.1.5.1 Experimental Set-up On Static Model

Experiments carried out on static model are to study the effects of surface roughness, type of material of workpiece, medium like air, water and Nacl solution between the probe and workpiece and varying gap between probe and workpiece, on the output voltage. For this the bifurcated optical-fibers are held perpendicular to the workpiece. This is achieved by press fitting the optical fibers end in the hollow brass tube and this tube is guided in the brass housing. The brass housing collar is screwed on the perspex stand like structure on the bottom of the perspex

ox which is joined by the chloroform.

The gap between the fiber (fitted in tool called as probe) ınd the workpiece is varied by the vertical up and down motion ›rovided by screw-gauge of 0.01 mm least count fitted on top of the brass tube through aluminium cap. The spring is provided to counter the force by screw-gauge around the brass-tube in the brass housing. The screw-gauge is press fitted in the brass bush which is screwed on the aluminium plate. The plate which in turn is screwed at the ends on the L-shape perspex sheets fixed at the side of box-like structure. The provision is made for placing the various specimens one by one and medium like air, water and Nacl solution in the small box-like structure of perspex sheets below the tool holder. This arrangement on the static model and its photograph are shown in Fig. 3.9 and 3.9(a).

3.1.5.2 Experimental Set-Up Utilising Feed Mechanism of EDM machine

These experiments are carried out to detect the profile of the given specimen, measure height of the artificially created burrs and to study the effect of angular inclination of workpiece (specimen) on output voltage.

Fig. 3.9

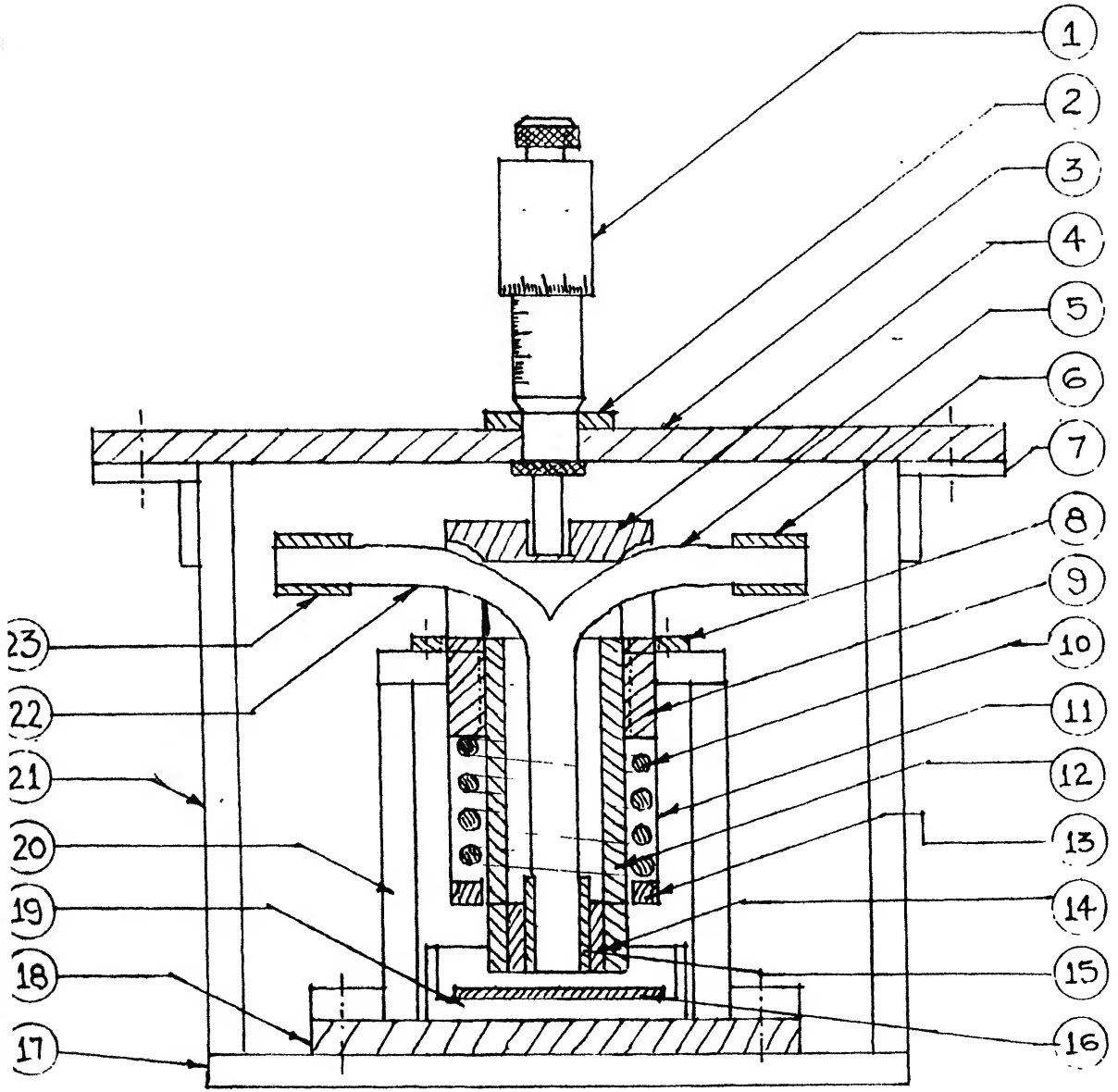

S.No	DESCRIPTION	MATERIAL
1	SCREW-GAUGE	-
2	BUSH	BRASS
3	TOP- PLATE	Al.
4	HOUSING FOR FIBERS	Al.
5	RECEIVING FIBERS	-
6	METAL SLEEVE	BRASS
7	ELBOW PLATE	PERSPEX
8	BUSH	BRASS
9	GUIDING- BUSH(PISTON)	BRASS
10	SPRING	-
11	HOUSING (CYLINDER)	BRASS
12	HOLLOW TUBE (TOOL)	BRASS
13	BUSH	BRASS
14	BUSH	PERSPEX
15	METAL SLEEVE	BRASS
16	WORK PIECE	ALLOY STEEL
17	BOTTOM PLATE	PERSPEX
18	SUPPORTING PLATE	M.S
19	WORKPIECE HOLDER	PERSPEX
20	HOUSING	PERSPEX
21	SIDE -PLATE	PERSPEX
22	TRANSMITTING FIBERS	-
23	METAL SLEEVE	BRASS

FIG. 3.9 EXPERIMENTAL SET-UP ON STATIC MODEL

FIG.3.9 (a) PHOTOGRAPHS OF EXPERIMENTAL SET-UP ON STATIC MODEL

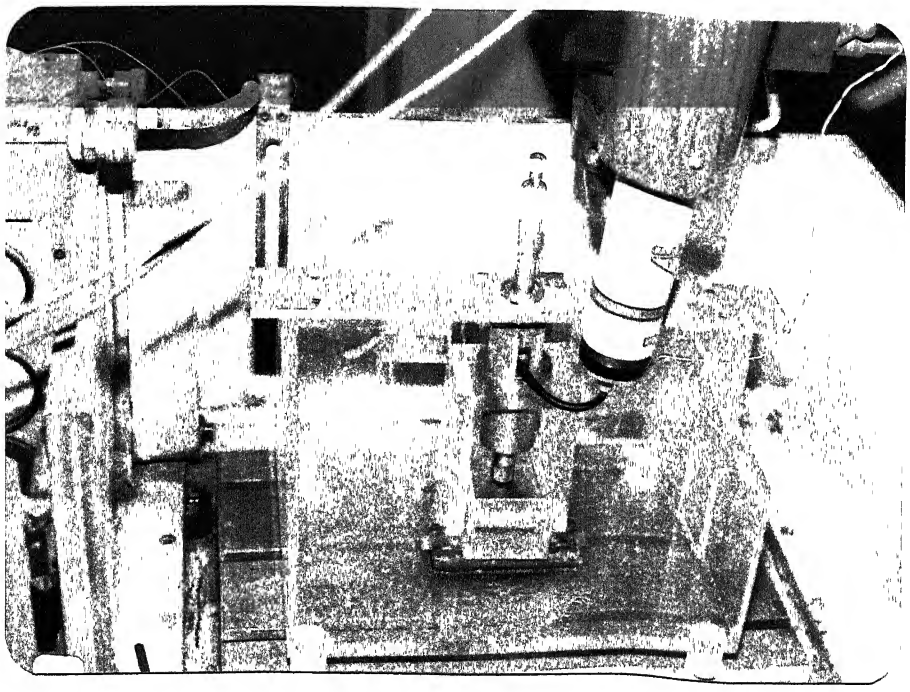

For the above experiments the tool holder (with fibers as sensor) is required to move vertically up and down and also in the longitudinal and traverse directions i.e. x,y and z directions.

Hence for all these movements the feed mechanism of the commercially available EDM machine is used. The tool holder is made of aluminium material and the optical-fibers end are press fitted in the tool with perspex bush. The tool holder is designed in such a way that it holds optical-fibers perpendicular to the specimen. The tool holder is fixed to the vertical spindle head by screw on the EDM machine. Vertical up and down motion is provided by servo motor to the spindle head and hence to the tool holder, which can be measured by the dial-gauge of 0.01 mm least count attached to the head. This dial gauge will give directly the gap between the probe and workpiece in mm. The longitudinal and traversing motion (X and Y direction respectively) of the workpiece fitted on the table is obtained by manually feeding the table which is having 0.005 mm least count on each side. The workpiece (specimen) is fixed on the three-jaw self aligning chuck which in turn is fixed on indexing fixture by screws and this fixture is fixed to table by nut and bolt in slots. The schematic diagram and the photograph of the experimental set-up is shown in Fig. 3.10 and 3.10(a) respectively.

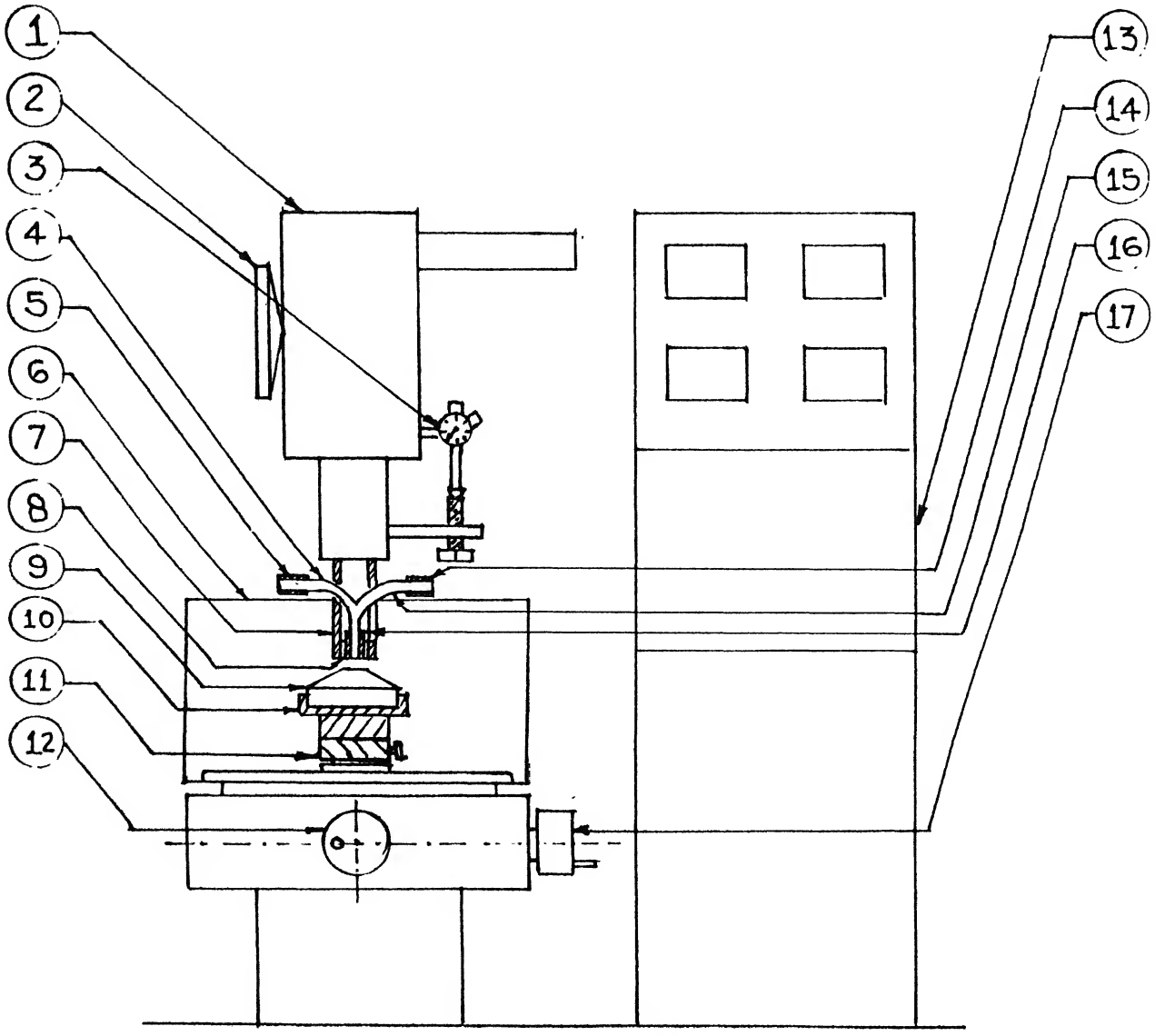

S.No	DESCRIPTION
1	SPINDLE HEAD WITH S.MOTOR
2	HANDLE FOR UP-DOWN MOTION
3	DIAL-GAUGE, .01 L.C, 10MM RAN.
4	TRANSMITTING FIBERS
5	METAL SLEEVE OF BRASS
6	TABLE WITH COVERS
7	TOOL HOLDER FOR FIBERS, AL.
8	BUSH OF PERSPEX
9	WORKPIECE, ALUMINIUM
10	3-JAW CHUCK FOR WP.
11	INDEXING FIXTURE
12	LATERAL MOTION TO TABLE
13	CONTROLLING PANEL
14	METAL SLEEVE OF BRASS
15	RECEIVING FIBERS
16	METAL SLEEVE OF BRASS
17	LONGITUDINAL MOTION TO TABLE

FIG. 3.10 EXPERIMENTAL SET-UP ON ELECTRO DISCHARGE MACHINE

FIG. 3.10(a) PHOTOGRAPH OF THE EXPERIMENTAL SET-UP ON EDM MACHINE

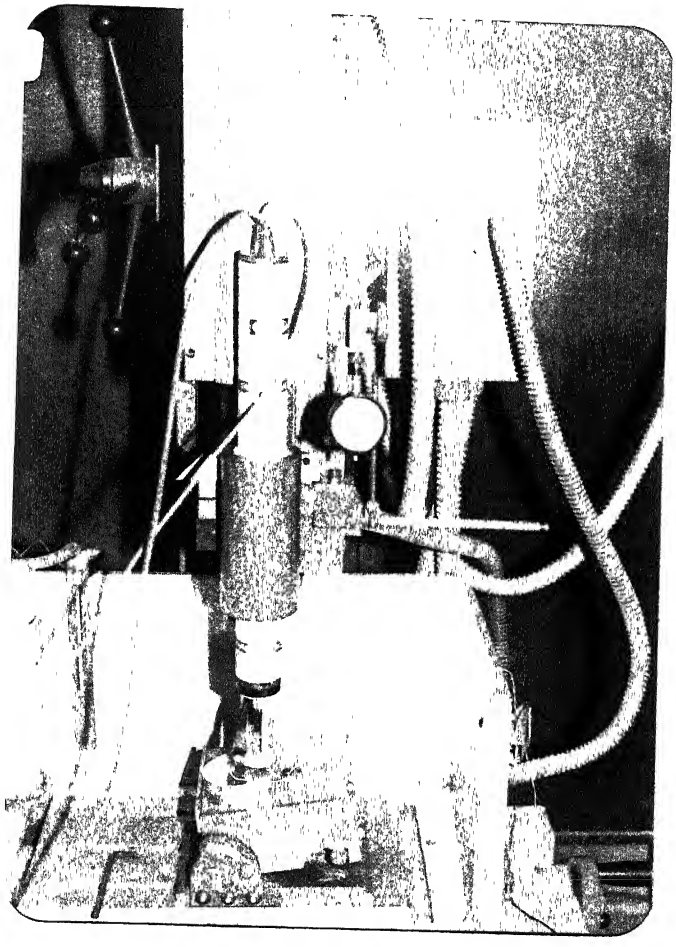

3.2 PROCEDURE

The workpiece (specimens) used in the experiments are as follows:

3.2.1 Affect of Various Parameters on Reflected Light Intensity

To study the effect of surface roughness, standard plates of alloy steel material of given surface roughness (Ra. values) are used in the experiments. They are 4 μ in, 32 μ in, 63 μ in, 125 μ in and 250 μ in, Ra. values. Apart from these to study the effect of type of material and surface roughness on output voltage, aluminium material is chosen and specimens are prepared by various machining operations on lathe. They are, specimens prepared by buffing operation, by turning operation with feed 0.05 mm per revolution and speed 800 rpm ("TURN-1") and turning operation with feed 0.1 mm per revolution and speed 640 rpm ("TURN-2").

Various specimens of alloy steel and aluminium material as discussed earlier are placed one by one below the probe on the static model. After the initial adjustment i.e. by zeroising the output DC voltage and GND, the gap between the probe and specimen is varied by the screw gauge in vertical direction in steps of 0.2 mm and the output voltage is recorded at different gaps. These experiments were carried out in air, water and Nacl solution. The output voltages for different gaps and in various mediums are recorded by omini-scribe recorder. The recorded output voltage for air medium is shown in Appendix-D as an example. The

experiments carried out in water and Nacl solution medium, it is ensured that the probe and the specimens are completely immersed in the liquid medium during the course of experiments. The results obtained by these experiments can be used as the calibration result and these are not the actual experimental result.

3.2.2 To Detect and Trace the Profile

For this, aluminium material is chosen and slope is cut on the NC lathe. The profile of this specimen is to be detected by fibers. The aluminium flat plate is also prepared of same surface finish on NC lathe with same speed and feed for the calibration purpose.

3.2.2.1 Calibration for profile measurement

(a) Determining Inclination Angle of the Profile

To determine the inclination of the profile and to study the effect of the inclination of specimen on the output voltages, for this the sine-plate which is hinged at one end and another end, has rollers below which slip-gauges of calculated value from known inclination angle, θ in degrees, are placed below rollers. The flat aluminium specimens of approximately same surface finish of the given specimen whose profile is to be traced is placed on the sine-plate. This arrangement is shown in the Fig 3.11. The sine-plate inclined at various angles and its calculation for values of slip-guage is shown in Table No. 3.1

Table 3.1: Calculation of Slip Gauge Values for Inclination θ.

θ	5 Sin θ	Combination of slip-guages of standard values in inches	Remarks
2	.1745	.050 + .124 = 174	.0005 inches slip gauge NA.
3	.2617	.1007 + .111 + .050 = .2617	
4	.3488	.1008 + .148 + .100 = .3488	
5	.4358	.1008 + .135 + .200 = .4358	
6	.5226	.1006 + .122 + .300 = .5226	
7	.6093	.1006 + .109 + .400 = .6093	
8	.6959	.1009 + .145 + .050 + .400 = .6959	
9	.7822	.1002 + .132 + .050 + .500 = .7822	
10	.8682	.1002 + .118 + .050 + .600 = .8682	
11	.9540	.1000 + .104 + .050 + .700 = .9540	

The specimen (flat) of Aluminium placed on sine plate is inclined at 4°, 6°, 8°, and 9° and the probe is moved horizontally along the slope in the steps of 1 mm and the output voltage is recorded for each step by the recorder. This arrangement is shown in Fig. 3.12. The recoroded output voltages for various inclinations are tabulated in Appendix-E.

Fig. 3.11 and 3.12

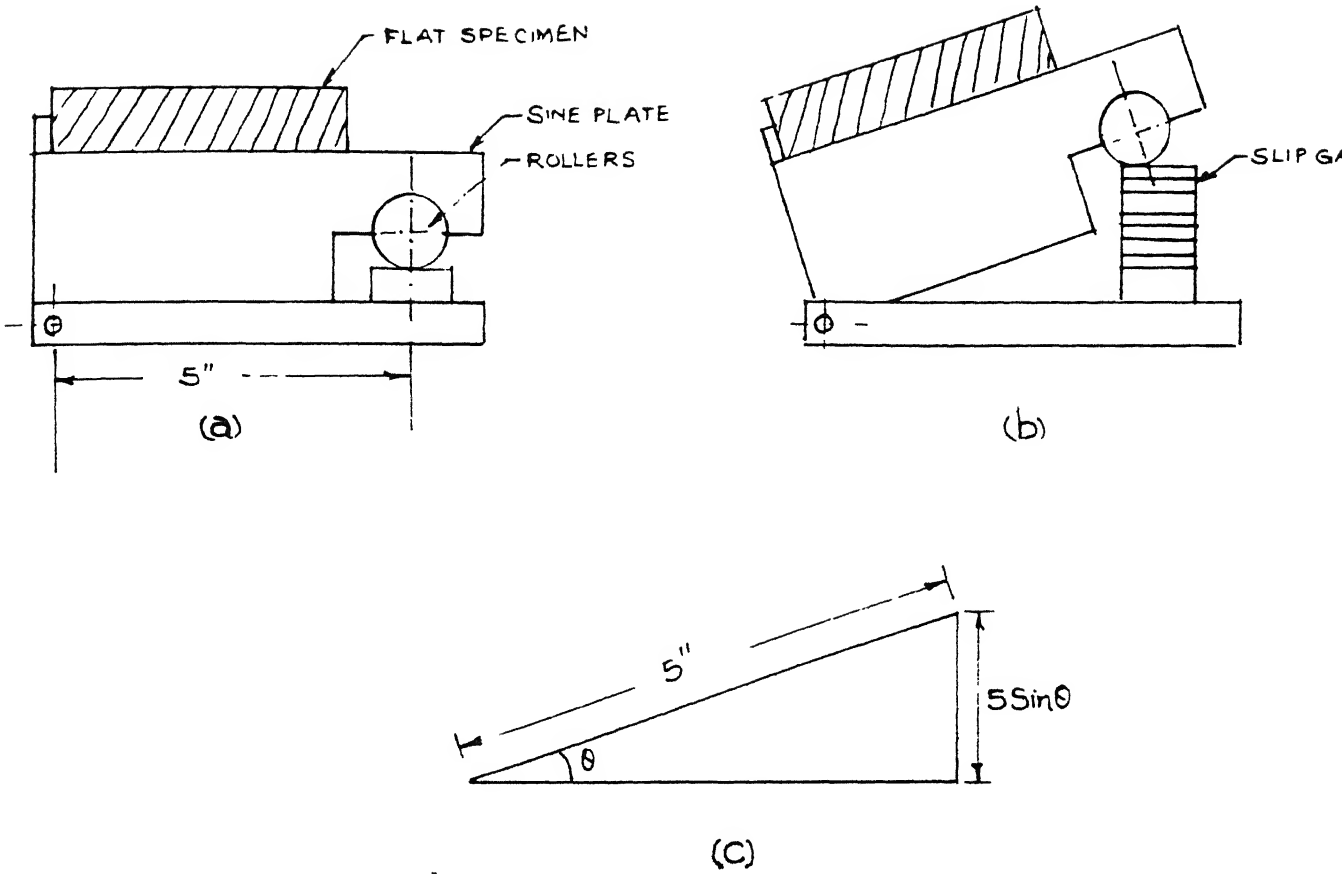

FIG.3.11 CALLIBRATION OF THE SPECIMEN WITH INCLINATION

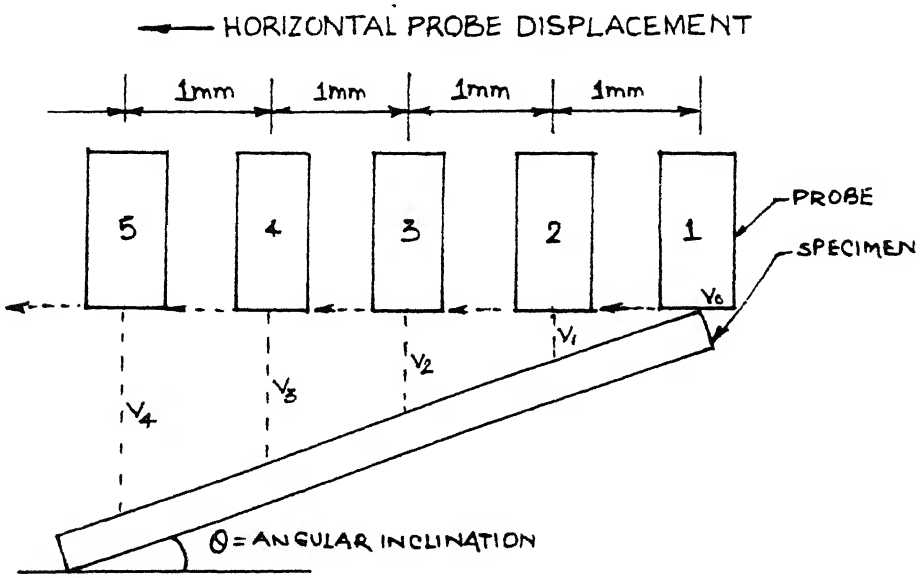

FIG.3.12 ARRANGEMENT OF PROBE FOR DETERMINING SLOPE ANGLE

From the above paragraph, the graph is plotted between the output voltage in volts against the angles of inclination in degrees for constant horizontal displacement of the probe for 1 mm, 2 mm, 3 mm, 4 mm, 5 mm and 6 mm, shown in Fig. 3.13. This graph is used as a basis for determining the slope of the profile to be traced. For this the probe is moved horizontally along the slope of the specimen whose profile is to be traced and it is kept at certain distance from the initial distance from where the profile or slope has commenced and the output voltage is recorded. This output voltage is marked on the same distance line of Fig. 3.13 on the Y-axis line and corresponding X-axis gives the inclination of the actual profile to be traced. The corresponding inclination obtained for the actual profile to be traced is 9.0°.

(b) Callibration graph for profile measurement

As the inclination of the actual slope determined is 9.0° as discussed in above section. The flat aluminium specimen is inclined at 9.0° angle and the probe is moved horizontally and the output voltage is recorded by the ominiscribe-recorder in steps of 1 mm. As the angle, $\theta = 9.0^{\circ}$ is known and the horizontal distance in steps of 1 mm is known, the corresponding vertical gap between the probe and the specimen can be calculated as follows with Fig. 3.14. From ΔAOB, we get $\tan\theta = Y/X$ or $Y = X \tan\theta$. But $\theta = 9.0^{\circ}$. Hence $Y = X \tan(9.0^{\circ}) = X.16 = .16\ X$. The calibration graph is

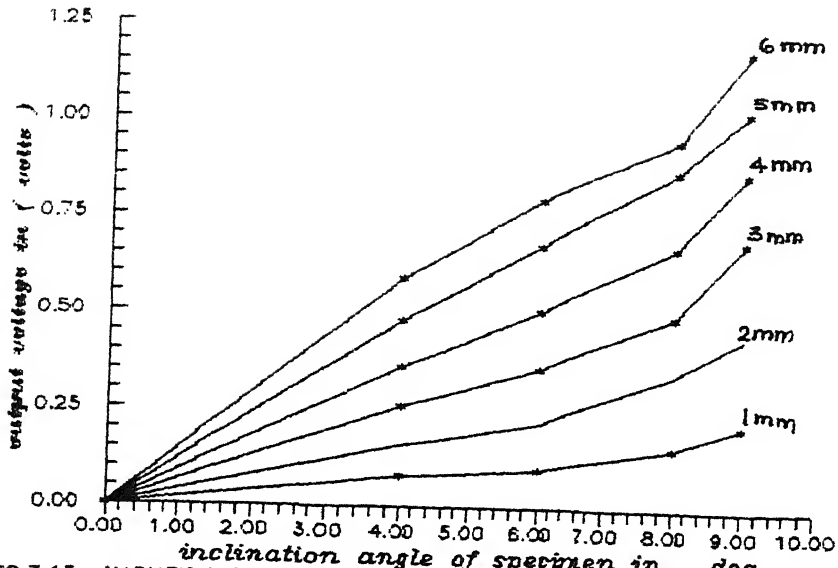

FG.3.13 VARIATION OF OUTPUT VOLTAGE BY VARYING INCLINATION FOR GAP = 1 mm, 2 mm,3 mm 4 mm 5 mm & 6 mm.

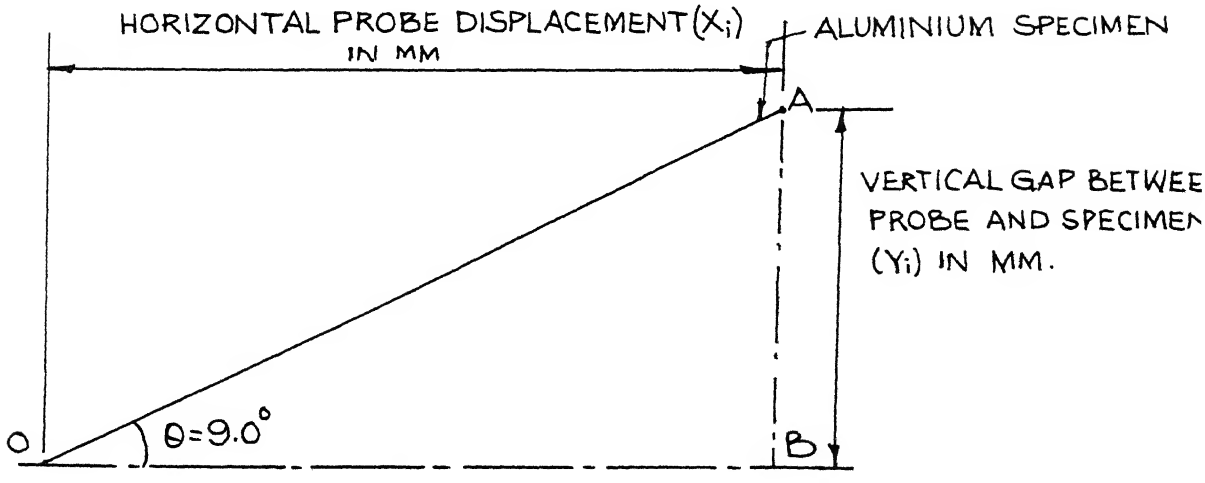

FIG.3.14. CALCULATION FOR VERTICAL GAP

FIG. 3.15 PHOTOGRAPHS OF SET-UP

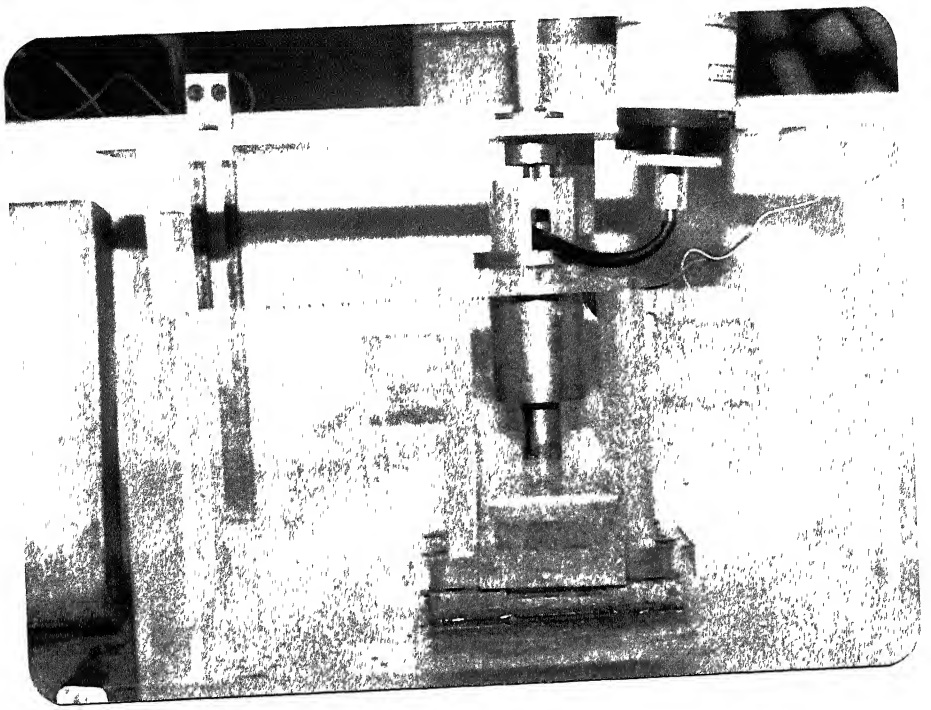

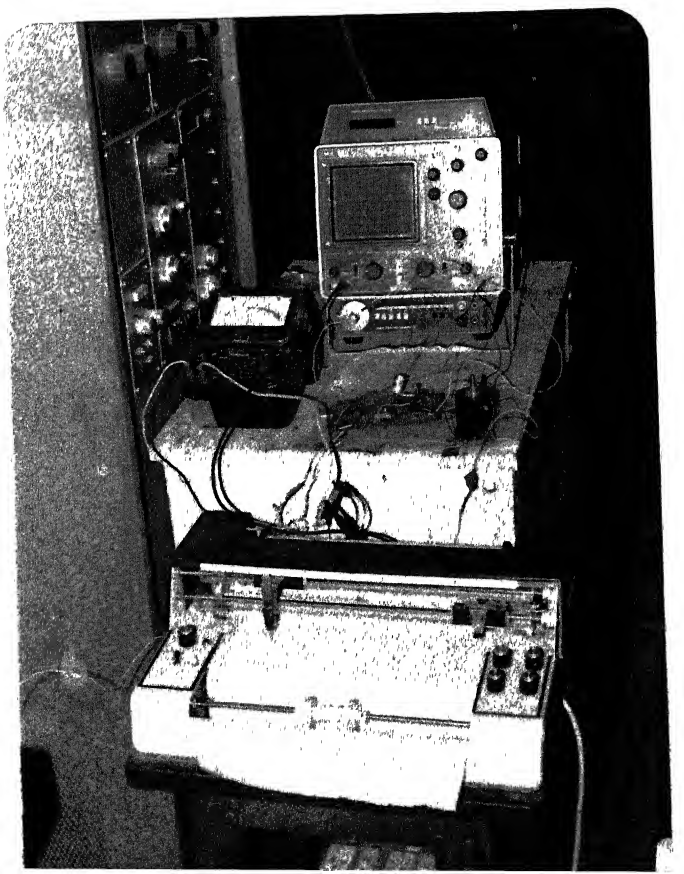

plotted with the output voltage (V_i) in volts and the corresponding horizontal probe displacement (Y_i and X_i) in mm as shown in Fig. 3.15 and 3.16.

3.2.2.2 Determining actual profile of the specimen

(a) by Optical-Fibres

For this the probe is moved horizontally along the slope in steps of 0.2 mm and the output voltages are recorded by the recorder as shown in Fig. 3.17. But as it is clear form the earlier graphs, the nature of variation of the output voltage with the gap between probe and specimen is in three phases. In the first phase it is linearly increasing, then in the second and third phase it is non-linear. Hence the first phase is highly sensitive. So to achieve the accurate results the effort is made so that the gap between the probe and the specimen lies in the linear region. For this the slope of the specimen is detected in segments i.e. the probe is moved in horizontal distance in steps for first segment of the slope and then the probe is moved downwards at particular distance and then again moved horizontally in steps and same way for third segment and so on. The results of all segments are combined to get the actual profile of the specimen. The arrangement of probe is shown in Fig. 3.18 and output voltages are recorded by recorder. The output voltages

Fig. 3.16

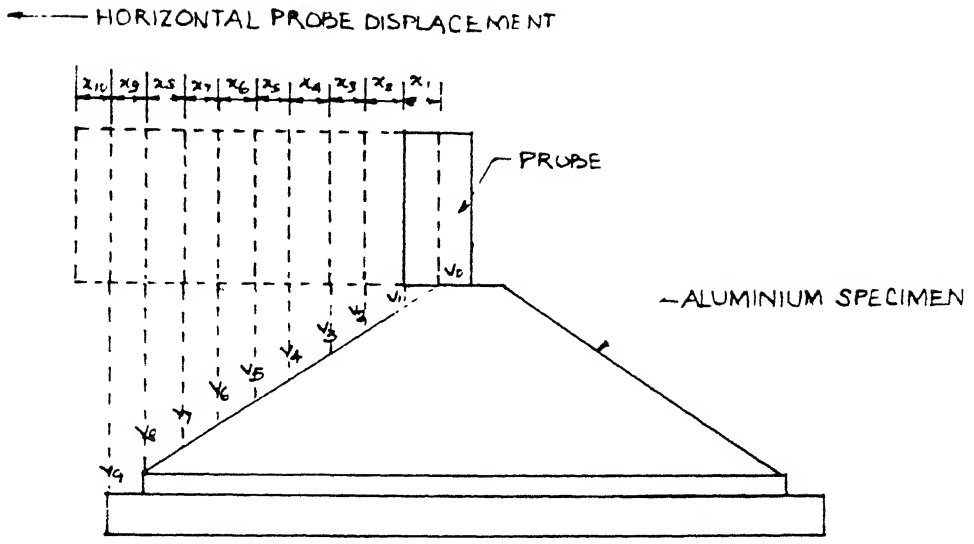

FIG. 3.17 ARRANGEMENT OF PROBE FOR PROFILE MEASUREMENT

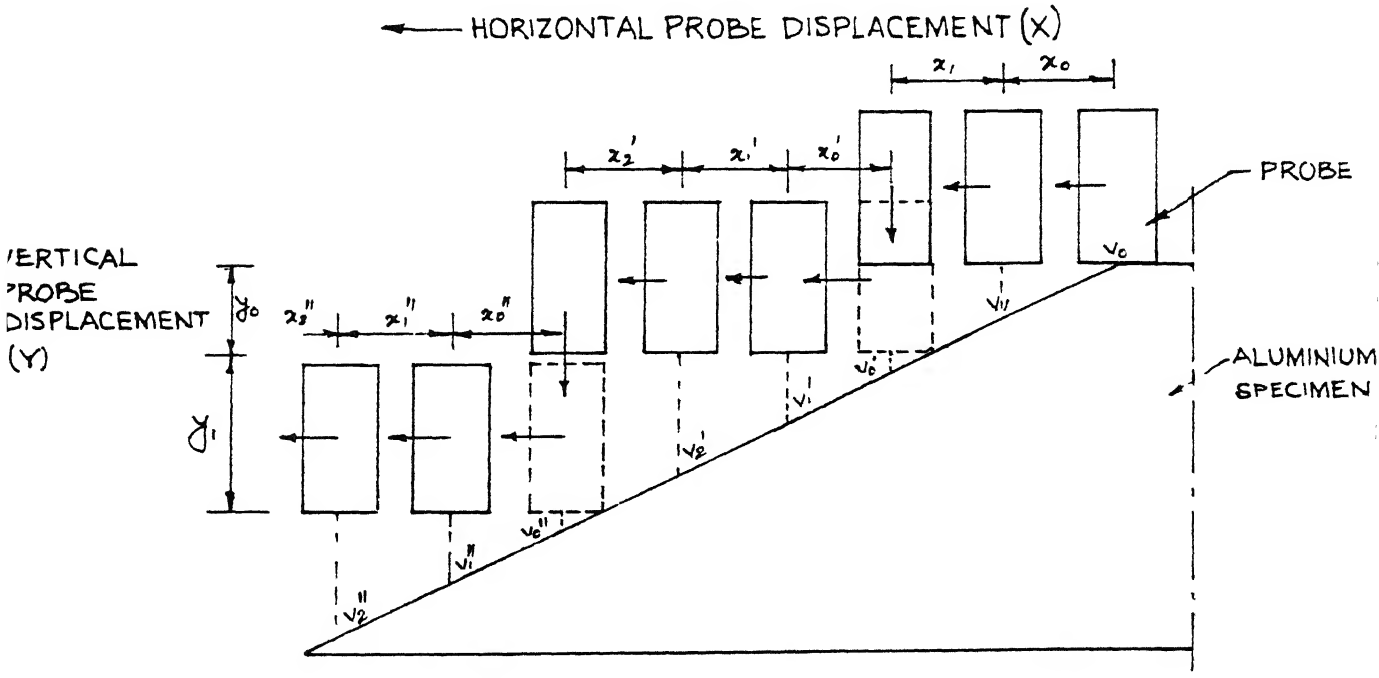

FIG. 3.18 RE-ARRANGEMENT OF PROBE FOR ACCURATE PROFIE MEASUREMENT

obtained here for the horizontal displacement of the probe are converted to the vertical gap between probe and specimen from the calibration graph of Fig. 3.16. The recorded output voltages along with the corresponding vertical gap in mm are tabulated in Appendix-G.

The graph is plotted between the horizontal displacement (X_i) in mm and vertical gap between probe and specimen (Y_i) in mm as shown in Fig. 3.19. This is the actual half profile of the specimen traced by the optical fibers. The other half profile can be traced in the similar manner as shown in dotted lines in Fig. 3.19 to get the full profile of the specimen.

(b) By Dial-Gauge

The dial-gauge of 0.01 mm least count and 10 mm range is used to measure and trace the profile of the specimen. The specimen is placed and secured on the table of the EDM machine as shown in Fig. 3.10. The dial gauge is fixed to the spindle head of the machine. The table feed is given manually in steps of 0.2 mm and the dial-gauge readings are noted down. This arrangement is shown in Fig. 3.20. The horizontal displacement (X_i) in mm, the corresponding reading of the dial-gauge minus initial readings gives the vertical gap (Y_i') in mm. The graph is plotted between X_i and Y_i' as shown in Fig. 3.21. This is the actual half profile of the specimen obtained by dial-gauge. The other half profile

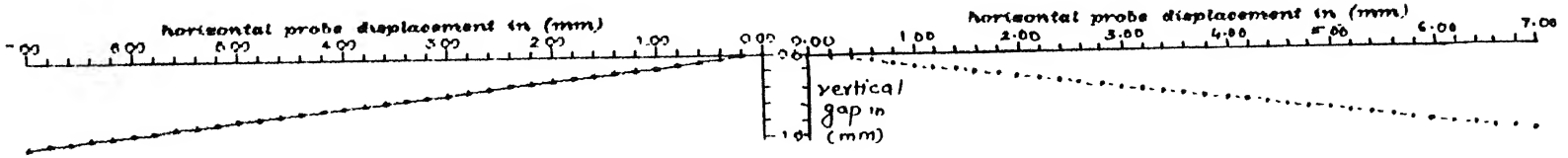

FIG. 3.19 HALF PROFILE OF ALUMINIUM SPECIMEN TRACED BY OPTICAL-FIBERS

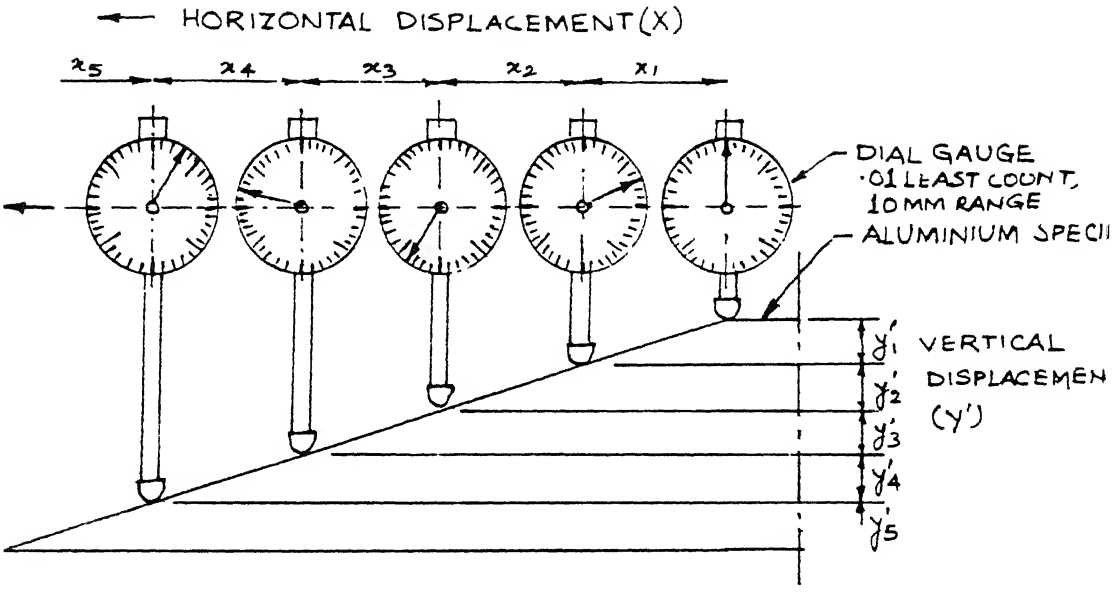

FIG. 3.20 ARRANGEMENT OF DIAL-GAUGE FOR MEASURING SLOPE OF THE SPECIMEN

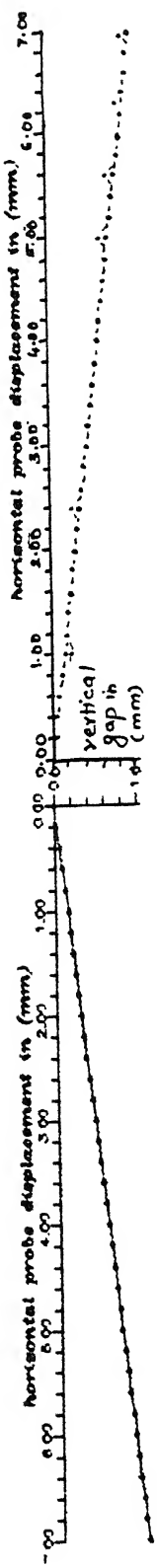

FIG. 321 HALF PROFILE OF ALUMINIUM SPECIMEN TRACED BY DIAL—GAUGE

can be traced in a similar manner, hence it is shown in dotted lines in Fig. 3.21.

3.2.3 Measuring Height of Artificial Burrs

For this, aluminium material is chosen and the burrs are artificially simulated on specimen in two ways:

(i) As the illuminating fiber diameter is 2.8 mm which is quite big to detect small burrs of hardly 0.1 or 0.2 mm thick obtained actually in various machining operations like drilling, boring, turing, milling and others. Therefore in the first case artificially the burrs were simulated on the aluminium specimen by keeping thickness of burrs 2 mm and different heights like 0.25 mm, 0.50 mm, 0.75 mm and 0.80 mm approximately on the lathe (specimen no. 1) shown in Fig. 3.22.

(ii) In the second case the burrs were simulated on the aluminium specimens during facing operations by sudden stopping of facing operations. The burrs produced are actually chips with different depths of cut, several burrs are produced on the surface whose heights are required to be measured by fiber-optics, (specimen no. 2) as shown in Fig. 3.23.

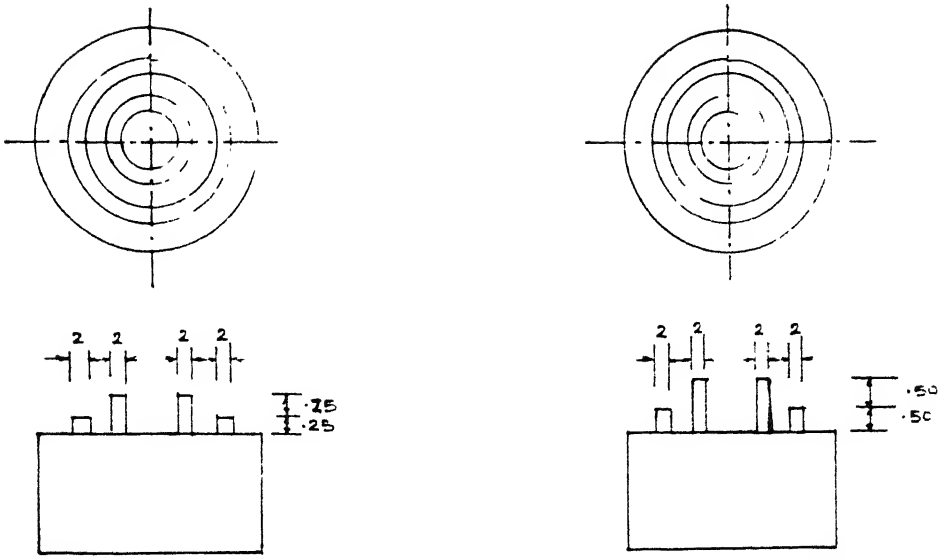

MATERIAL - ALUMINIUM
ALL DIMENSIONS IN MILLIMETRES

FIG.3.22 ARTIFICIALLY SIMULATED BURRS WITH THICKNESS - SPECIMEN NO.1

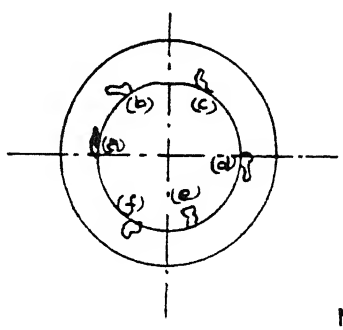

MATERIAL-ALUMINIUM

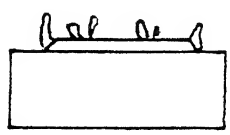

FIG.3.23 ARTIFICIALLY SIMULATED BURRS WITH IRREGULAR THICKNESS - SPECIMEN NO.2

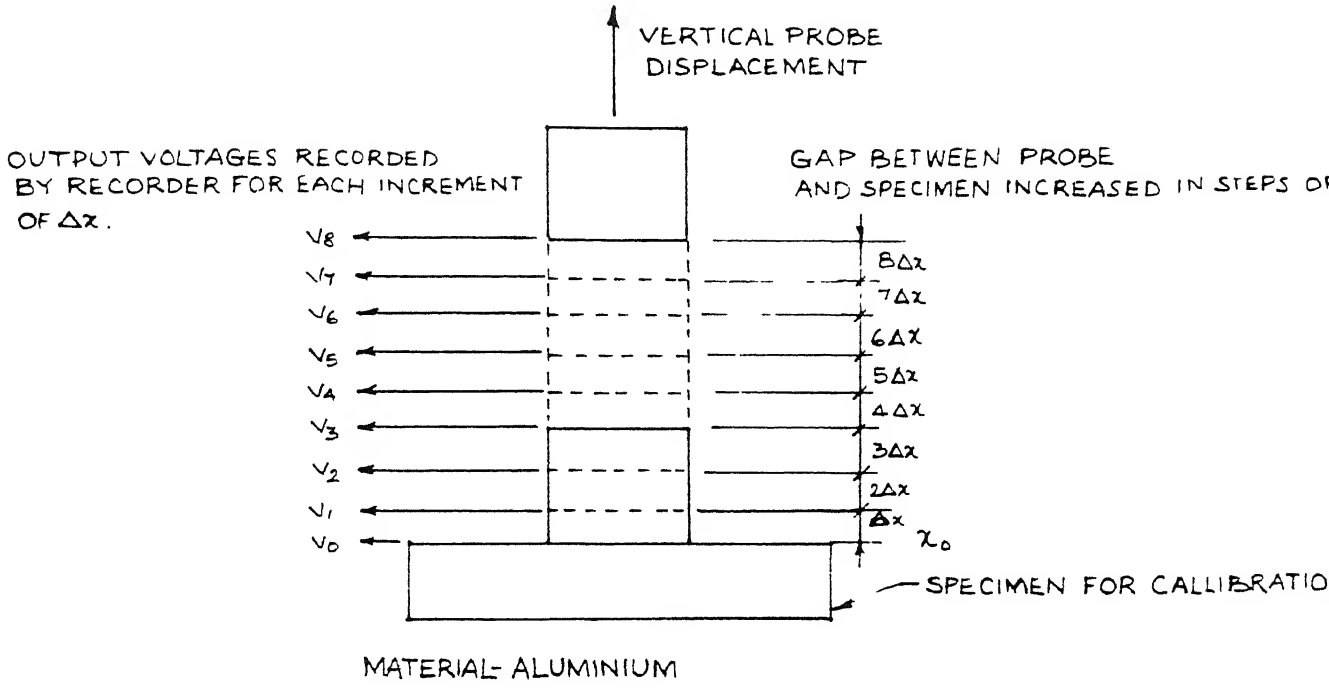

FIG. 3.24 ARRANGEMENT FOR CALLIBRATION OF BURR HEIGHT MEASUREMENT

3.2.3.1 Calibration for Burr Height Measurement

For calibration of specimen no. 1 and 2, the wavy surface of the artificial burrs (approx. same nature) is generated on the aluminum material by machining operations. These specimens are placed one by one below the probe (fibers) on the machines. The vertical gap between the probe and the specimen is varied in steps and the output voltages are recorded by the recorder at each step. This arrangement of calibration is shown in Fig. 3.24. The graph is plotted between the output voltage (V_i) in volts and vertical probe displacement (Y_i) in mm for specimen no. 1 and 2 as shown in Fig. 3.25(a) and (b) respectively. These are the calibration graphs used for artificial burr height measurement.

3.2.3.2 Measurement of Height of Artificial Burrs

(a) By Optical-Fibers

Specimen No. 1: For measuring height of artificial burr the probe is kept away from the base line, at a suitable distance, justified by the calibration curve (Fig. 3.25 (a)) and output voltages are recorded in steps as shown in Fig. 3.26 as the probe is moved horizontally. The voltages obtained at different heights of artificial burr are subtracted from the initial voltage at the base line, which from the calibration curve gives the height of artificial burr. This is tabulated in Table No. 3.2.

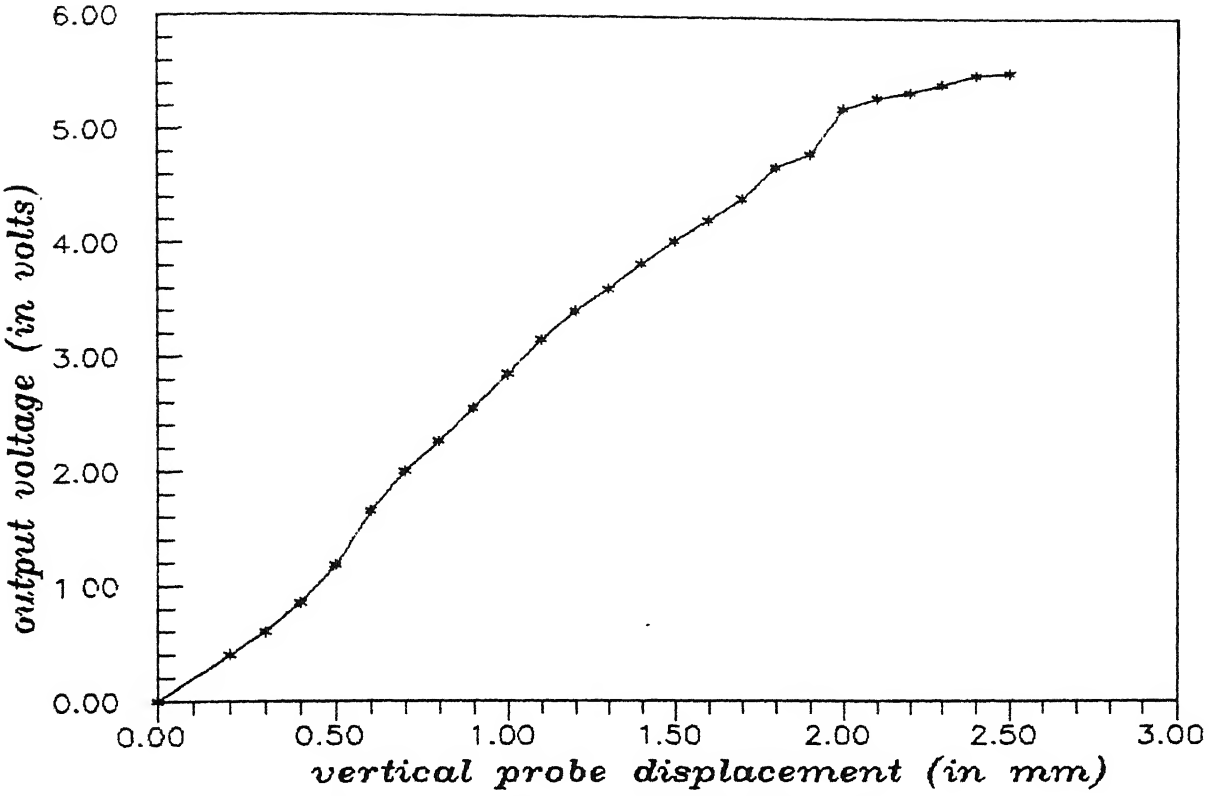

Fig.3.25(a) Callibration graph for specimen no.1.

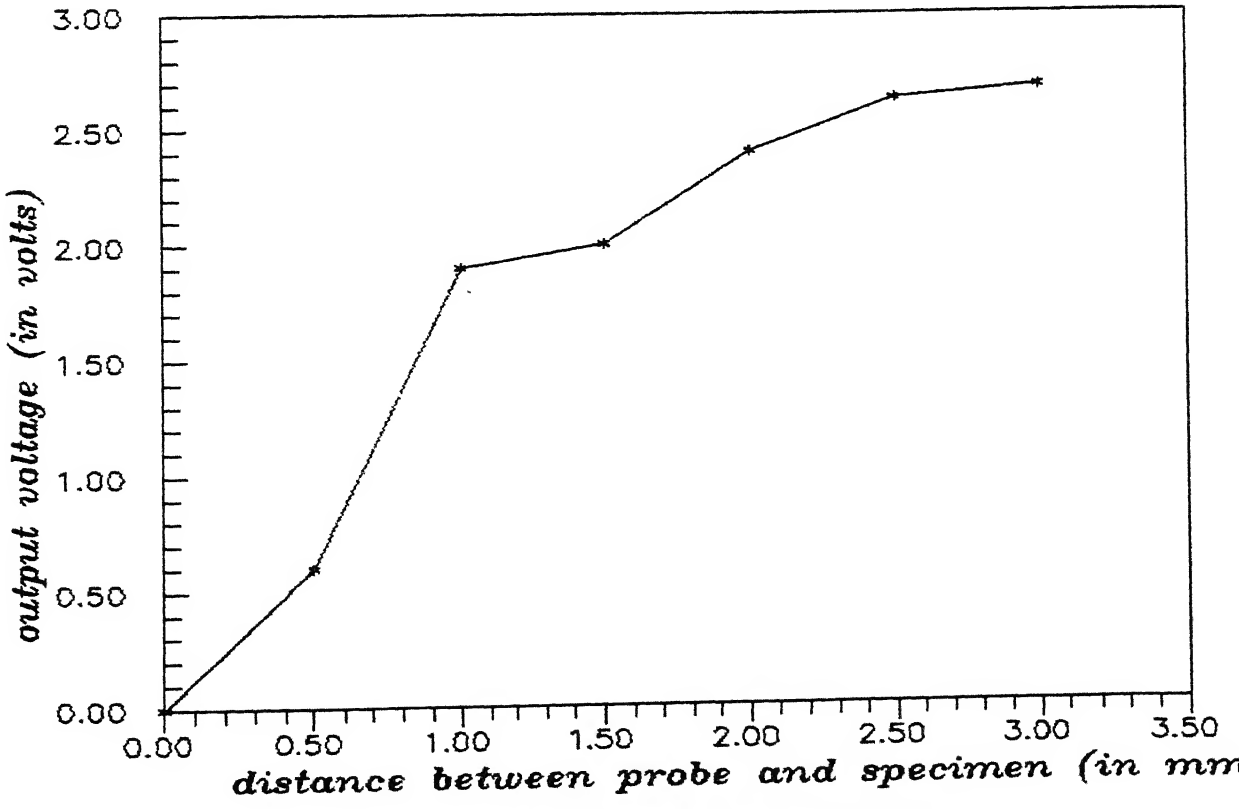

Fig.3.25(b) Callibration graph for specimen no.2.

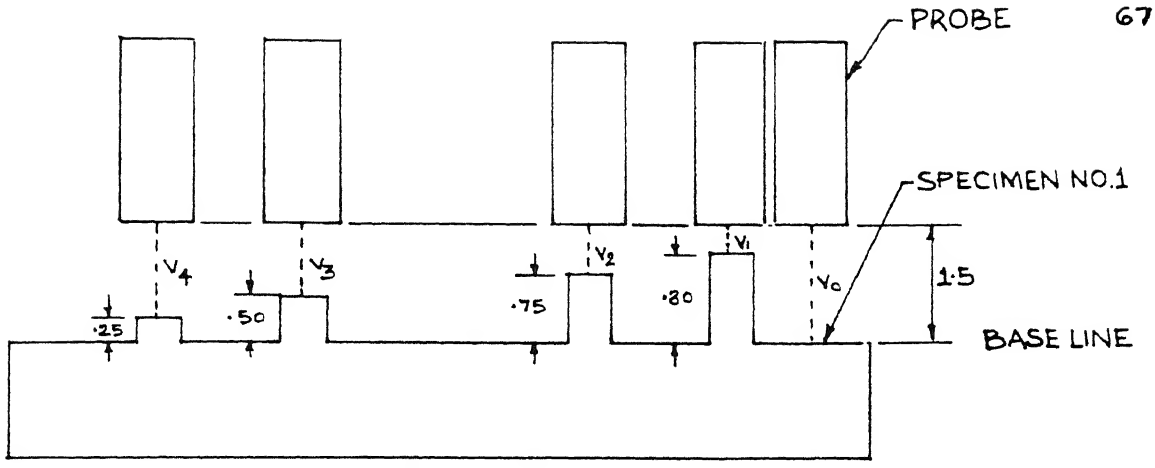

MATERIAL-ALUMINIUM
ALL DIMENSIONS IN MILLIMETRES

FIG 3.26 BURR HEIGHT MEASUREMENT BY OPTICAL-FIBERS FOR SPECIMEN NO. 1

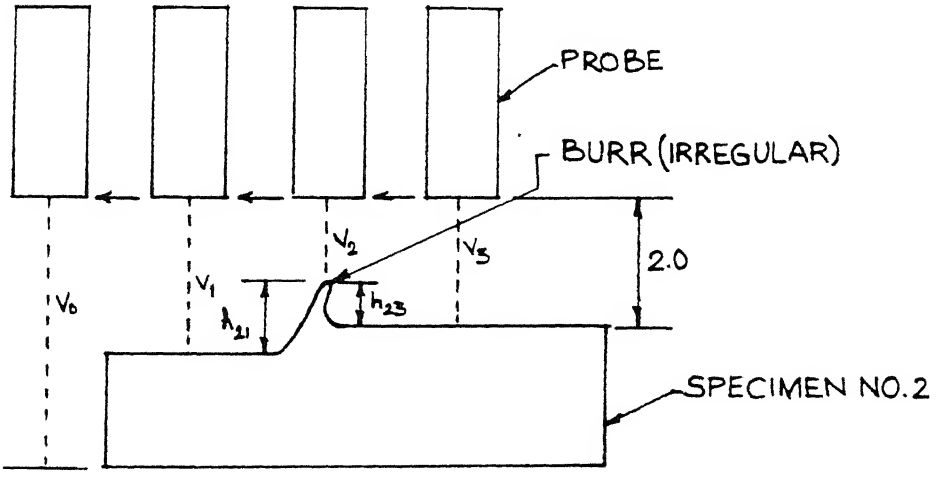

FIG. 3.27 BURR HEIGHT MEASUREMENT BY OPTICAL-FIBERS FOR SPECIMEN NO. 2

Table 3.2: Burr Height Measurement by Optical-Fibers.

Sl. No.	Approx.Burr height (mm)	Output Voltage (V_i) (volts)	V_0-V_i (V_0 = 4V) (volts)	Burr Height from Calibration Graph (mm)
1.	0.25	3.7	0.3	0.27
2.	0.50	3.2	0.8	0.49
3.	0.75	2.8	1.2	0.70
4.	0.80	2.6	1.4	0.78

Specimen No. 2: The artificial burrs produced on specimen are irregular in shape and sizes. The heights of these irregular burrs are measured by optical-fibers. The probe is kept away again at a suitable distance from the base line justified by the calibration curve (Fig. 3.25 (b)). The experiments were carried out on the EDM machine utilizing its feed mechanism. The probe is fixed to the spindle head and the specimen on the table is given feed manually across each artificial burr i.e. horizontally. The output voltages are recorded for each burr by the recorder. The arrangement of burr height measurement for Specimen No. 2 is shown in Fig. 3.27. The difference in voltages i.e. V_3-V_2 will give corresponding burr height (h_{23}) from the calibration curve 3.25(b). This is tabulated in Table 3.3.

Table:3.3: Burr Height Measurement by Dial-gauge

Sl. No.	Output Voltages in Volts				
	V_1	V_2	V_3	V_4	Burr Height from Calibration Graph (V_3-V_2) (mm)
1.	0	2.7	1.9	2.45	1.45
2.	0	2.8	1.5	2.20	1.10
3.	0	2.4	1.7	2.15	1.25
4.	0	2.2	0.7	2.10	0.58
5.	0	2.1	1.4	2.20	1.0
6.	0	3.1	1.7	2.20	1.25

(b) By MP-320 Shadowgraph

The Specimen No. 1 and 2 are placed one by one for each burr on the shadowgraph equipment and the heights of artificial burrs are obtained in mm by subtracting the readings of horizontall distance (in mm) and longitudinal distance (in mm). The heights obtained for Specimen No. 1 and 2 for various burrs are shown in Table 3.4 and 3.5 respectively.

Sl. No.	Approx. Burr Height (mm)	Horizontal Distance (A) (mm)	Longitudinal Distance (B) (mm)	Burr Height (A - B) (mm)
1.	0.25	18.182	17.911	0.271
2.	0.50	20.843	20.369	0.474
3.	0.75	18.182	17.460	0.722
4.	0.80	20.843	20.041	0.802

Table 3.5: Measurement of Burr Height by Shadowgraph.
For Specimen No. 2.

Sl. No.	Horizontal Distance (A) (mm)	Longitudinal Distance (B) (mm)	Burr Height (A - B) (mm)
1.	15.485	13.843	1.642
2.	13.188	12.025	1.113
3.	16.602	15.496	1.106
4.	18.262	16.940	1.322
5.	18.028	16.457	1.571
6.	17.889	16.292	1.597

Table 3.4: Measurement of Burr Height by Shadowgraph.
For Specimen No. 1

CHAPTER - IV

EXPERIMENTAL RESULTS AND DISCUSSION

4.1 AFFECT OF VARIOUS PARAMETERS ON THE INTENSITY OF THE REFLECTED LIGHT (OUTPUT VOLTAGE)

4.1.1 Affect of Surface Roughness

The results obtained from Sec. 3.2.1 (recorded outputs for various specimens) is represented in graphical form. The graphs are plotted between the output voltage (V_i) in volts and the vertical probe displacement (Y_i) in mm, for various medium like air, water and Nacl solution between probe and specimen as shown in Fig. 4.1, 4.2 and 4.3 respectively.

The inferences drawn from all the above graphs are as follows:

(i) *The output voltage increases with the increase in vertical gap between the probe and specimen initially, then it reaches at peak voltage and then it decreases with the increase in gap.*

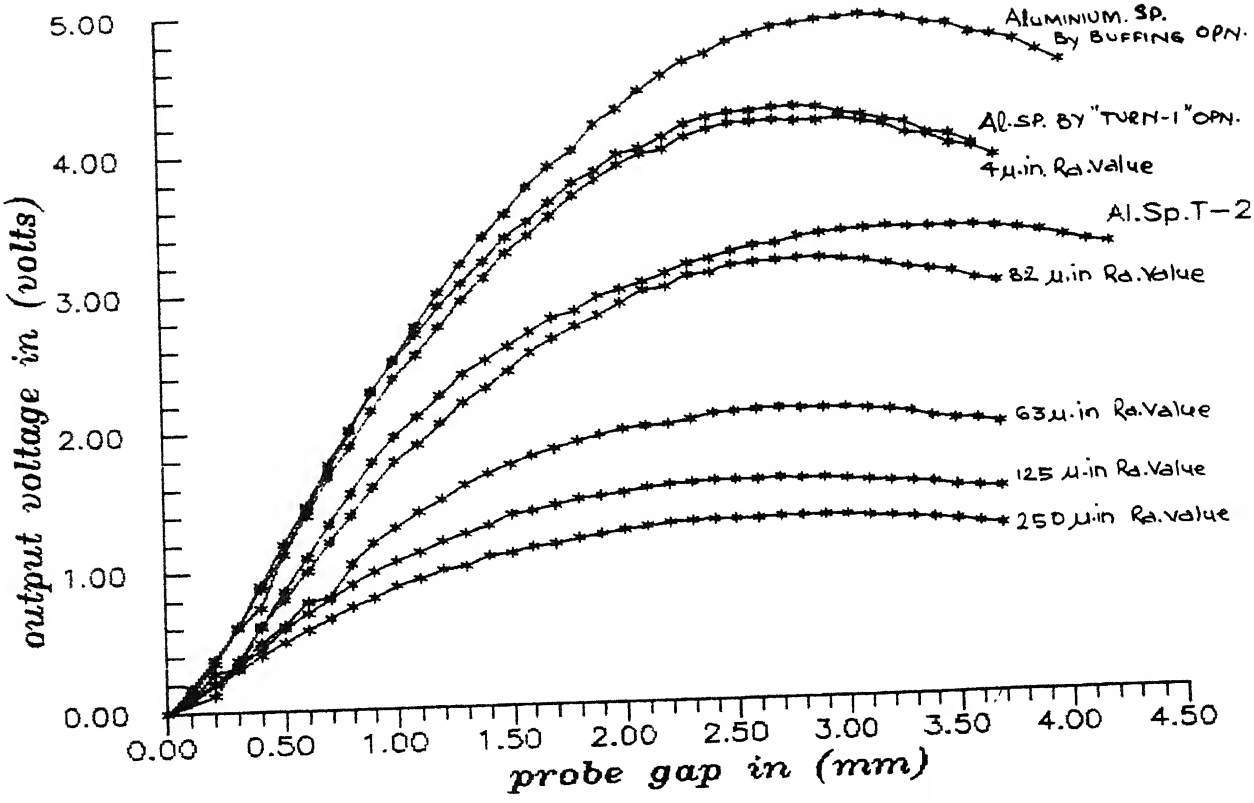

FIG.4.1 VARIATION OF OUTPUT VOLTAGE BY VARYING VERTICAL GAP BETWEEN PROBE AND SPECIMEN (Medium = Air)

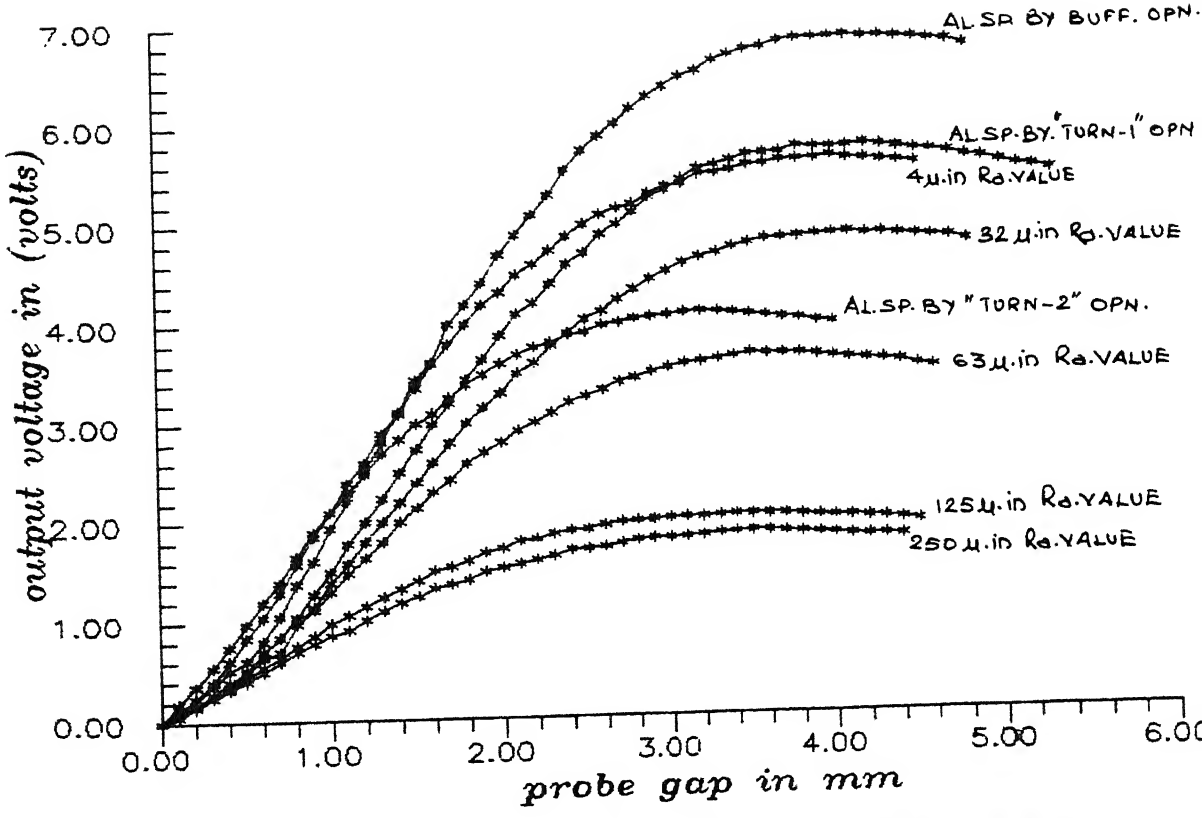

FIG.4.2 VARIATION OF OUTPUT VOLTAGE BY VARYING VERTICAL GAP (Medium = Water))

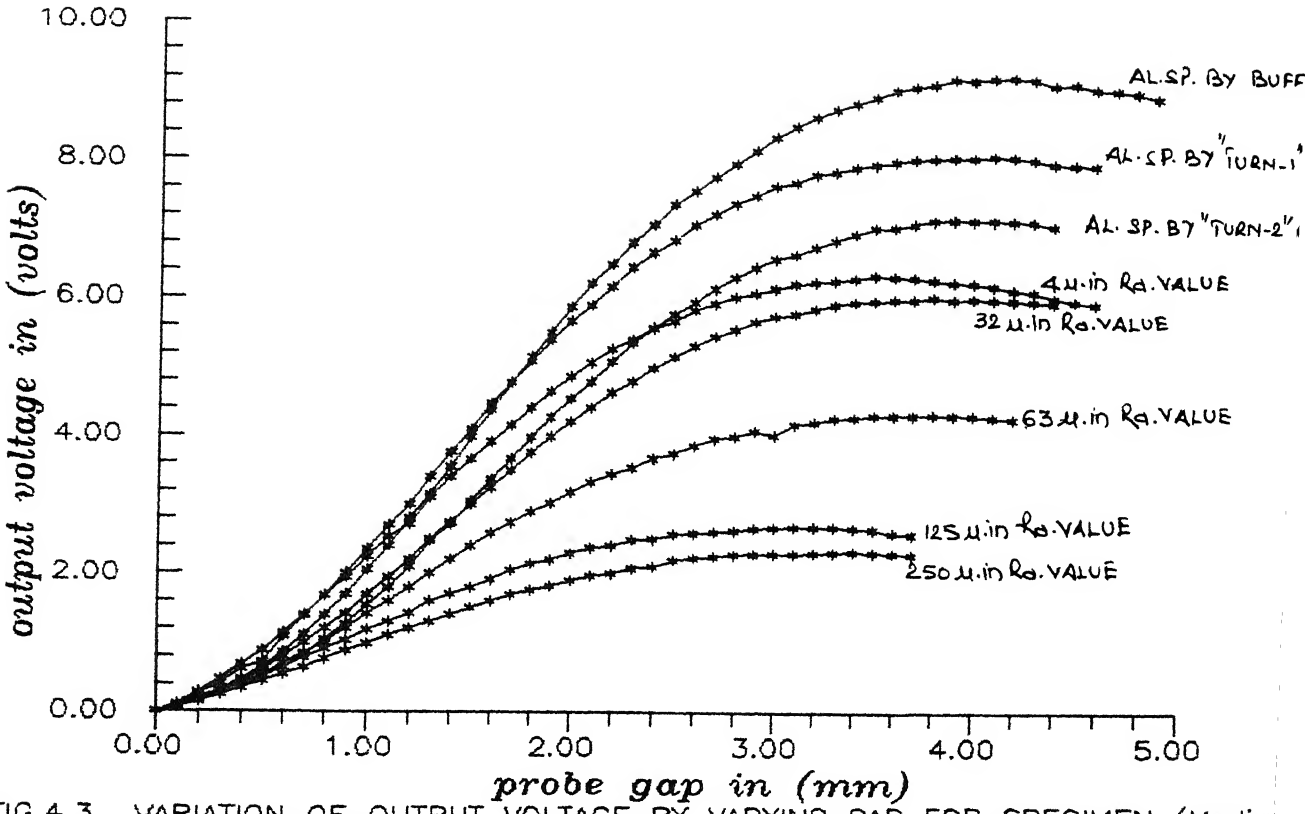

FIG.4.3 VARIATION OF OUTPUT VOLTAGE BY VARYING GAP FOR SPECIMEN (Mediu
Nacl SOLUTION

This can be well explained by the fact the the light reflected by the specimen is scattered all around, but the scattering is concentrated in particular angle around the incident beam. So initially when the gap is less, then less light goes in the receiving fibers covering less area, giving rise to less voltage. As the gap increases more reflected light is received by the fibers and hence more voltage. At the particular or critical gap between probe and workpiece, all the reflected light around the incident beam covers the whole area of the receiving fibers giving rise to maximum voltage. Still increase in gap gives rise to losses of scattered light outside the receiving fibers, thus voltage is decreased. This phenomenon is proved for all specimens of different surface roughness, for alloy-steel and aluminium material and for all three mediums like air, water an Nacl solution between probe and specimens.

(ii) *The peak output voltage decreases with the increase of surface roughness (Ra values).*

This can be well explained by the fact that the scattering of light around the incident beam by the specimen of least surface roughness (Ra value) or good surface finish is more concentrated and hence more reflected light enters the receiving fibers which gives rise to higher peak voltages. With the decrease in surface finish of the specimen or increase in Ra value the irregularities

on the surface of specimen is more which scatters more light all around and thus very less light is concentrated around the incident beam. Hence less light enters the receiving give area giving rise to less peak output voltage. This phenomenon is also observed in all the three medium.

Refer to Sec. 2.1.3, the output voltage theoretically obtained for aluminum (by buffing operation) material in air medium is 4.2 volts. Experimentally, the results obtained for the same conditions and at Z_{max} = 3.1 mm gap is 4.9 volts. The error between the theoretical and the experimental results are due to following reasons:

(a) Loses in the fibers due to bending and other losses are not considered.

(b) Light absorption by atmosphere and fibers is not considered.

(c) Scattering of light by specimen is assumed to be uniform in all directions whereas practically it is not so.

(d) Errors in equipments for recording and amplification circuits is not considered.

4.1.2 Effect of Medium

The results obtained in the Sec. 4.1.1 is utilized in studying the effect of medium like air, water and Nacl solution between probe and specimen, on the output voltage.

The graph is plotted between output voltage and the vertical probe displacement in various mediums for same surface finish of

specimen as shown in Fig. 4.4 and 4.5 for 32 and 125 μ in Ra. values standard plates. The inferences drawn from above graphs are as follows:

(i) *The peak output voltages increases in the order of air, water and Nacl solution, medium between probe and specimen for same surface finish.*

This can be well explained by the fact that the refractive indexes of air, water and Nacl solution are 1.003, 1.33 and 1.43 respectively. According to snell's law of refraction $n_1 \sin \theta_1 = n_2 \sin \theta_2$, where n_1 and n_2 are index of refraction of two mediums. θ_1 and θ_2 are the angles subtended by the incident and the reflected ray with the normal. This means that when the light travels from the lighter to denser medium then the light gets refracted away from the normal and vice versa. Hence the incident beam in the case of water and Nacl solution of higher index of refraction the light gets refracted away from normal thus covering more area on the surface of the specimen. Thus the light reflected by the surface is more compared to air giving rise to higher peak voltages in the case of water and Nacl medium. This is shown in Fig. 4.6.

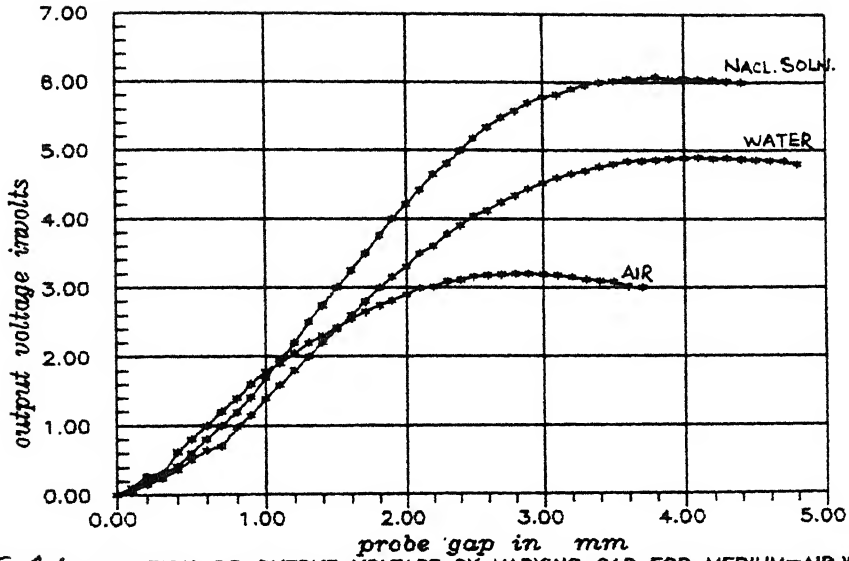

FIG.4.4 VARIATION OF OUTPUT VOLTAGE BY VARYING GAP FOR MEDIUM=AIR,WATER & NACL. SOLn (Ra.=8 μ.in)

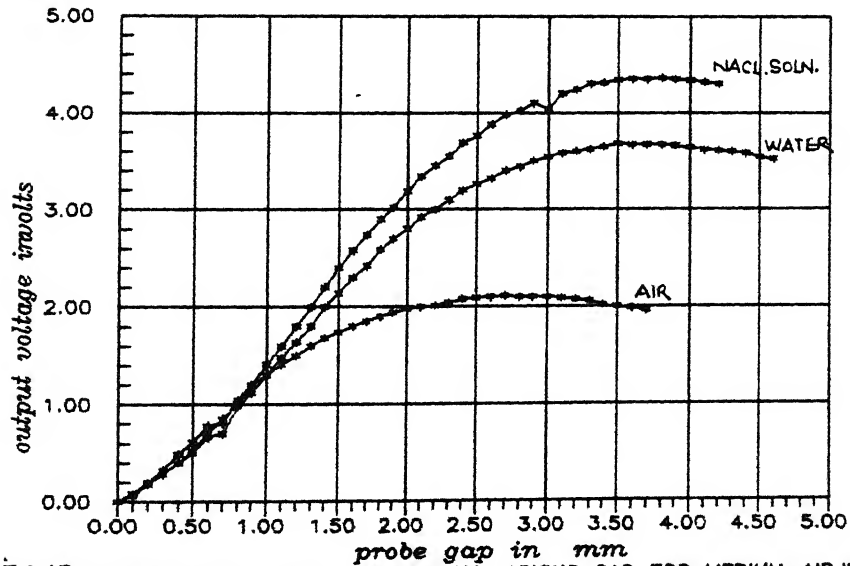

FIG.4.5 VARIATION OF OUTPUT VOLTAGE BY VARYING GAP FOR MEDIUM=AIR,WATER & NACL. SOLn.(Ra.=32 μ.in)

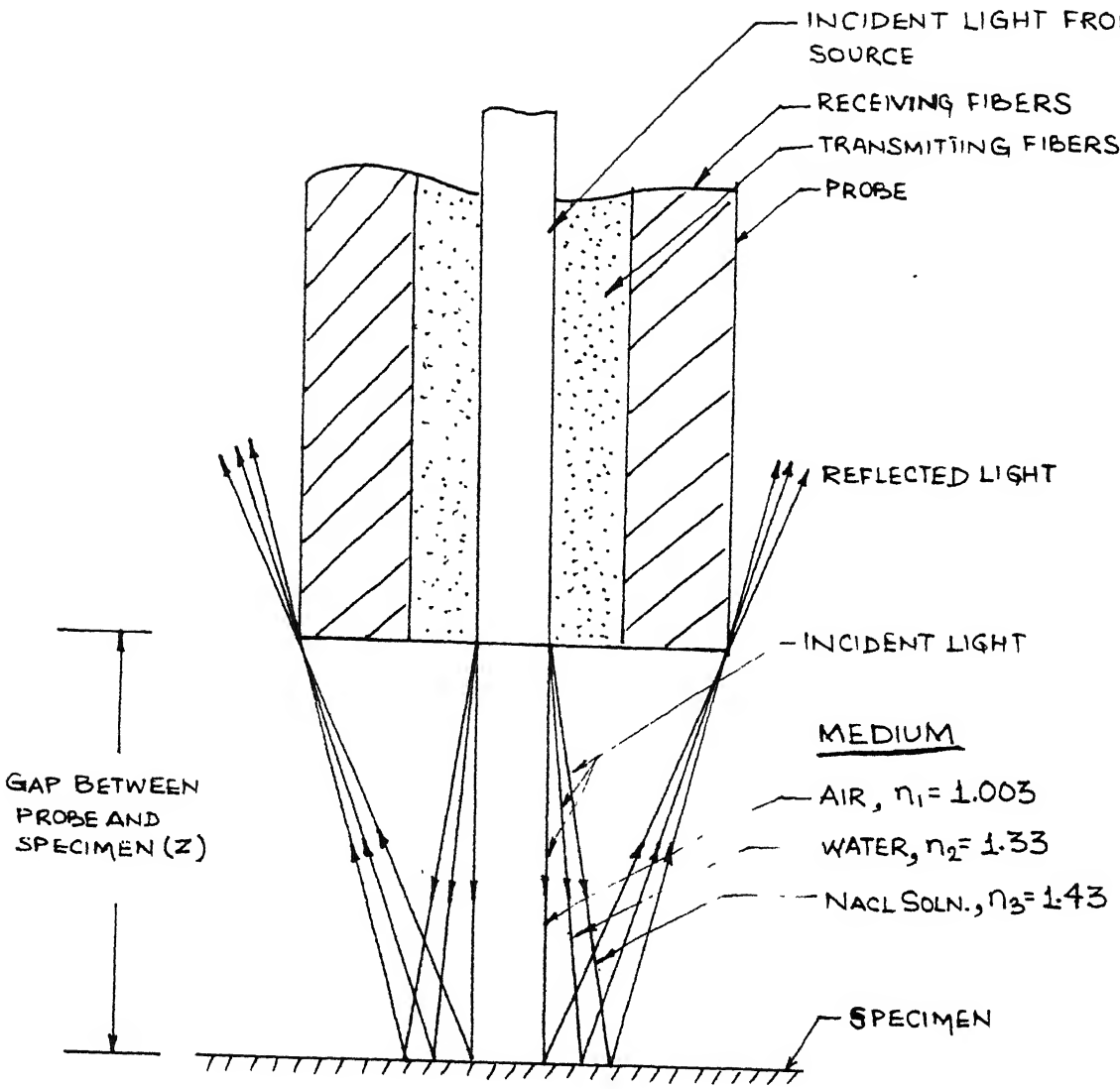

n_1, n_2, n_3 are refractive indexes of air, water and Nacl. solution

FIG.4.6. EFFECT OF MEDIUM ON INCIDENT LIGHT

4.1.3 Affect of Type of Material

The results obtained in Sec. 4.1.1 is utilized in studying the affect of type of material (Specimen) on the reflected light intensity (output voltage) for the water medium between probe and specimen.

The graph is plotted between the output voltage (in volts) and vertical probe displacement (in mm) for aluminum and alloy steel material for same surface finish (4 μ in. Ra. value) and water medium between probe and specimen. This is shown in Fig. 4.7. The inferences drawn from the above graphs are as follows:

The peak voltage is more in case of aluminum. This means that the reflectivity of aluminum is more in comparison to alloy steel.

4.2 AFFECT OF INCLINATION OF WORK PIECE ON THE OUTPUT VOLTAGE

4.2.1 Deviation between Experimental and Actual Profile for Various Inclination

As discussed earlier in Sec. 3.2.2.1 (a) the angle of inclination (θ) for calibration purpose is 9.0^{0}. The graph plotted between the output voltage (V_i) and vertical gap (Y_i) is shown in Fig. 4.8. The graphs are plotted for various inclinations (θ) = 4^{0}, 6^{0} and 8^{0} separately, between the output voltages (V_i) and horizontal displacement (X_i), shown in Fig. 4.9

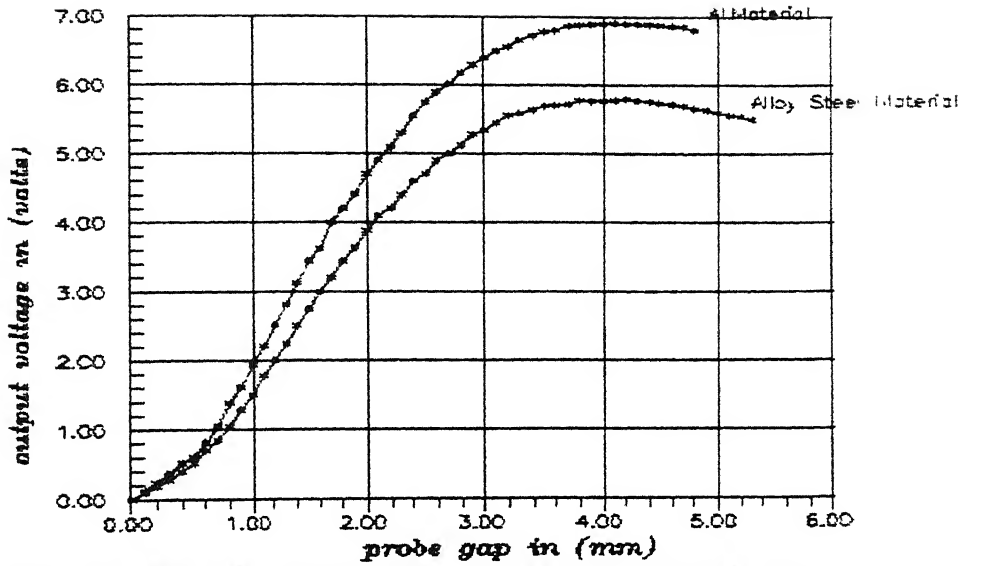

FIG. 4.7 VARIATION OF OUTPUT VOLTAGE BY VARYING VERTICAL GAP FOR ALUMINIUM AND ALLOY STEEL MATERIAL OF 4.0 u.in Ra. VALUE
(Medium = Water)

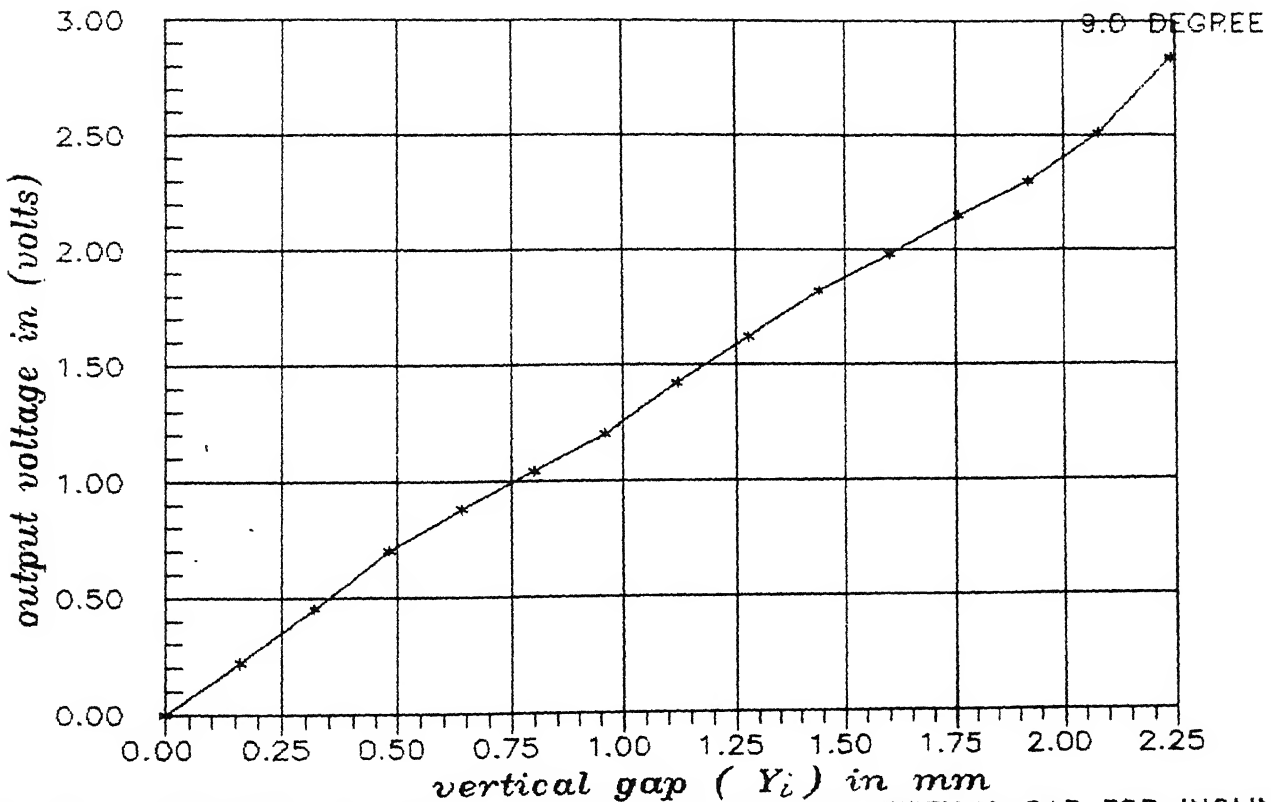

FIG. 4.8 VARIATION OF OUTPUT VOLTAGE BY VARYING VERTICAL GAP FOR INCLIN
(θ) = 9.0 DEGREES.

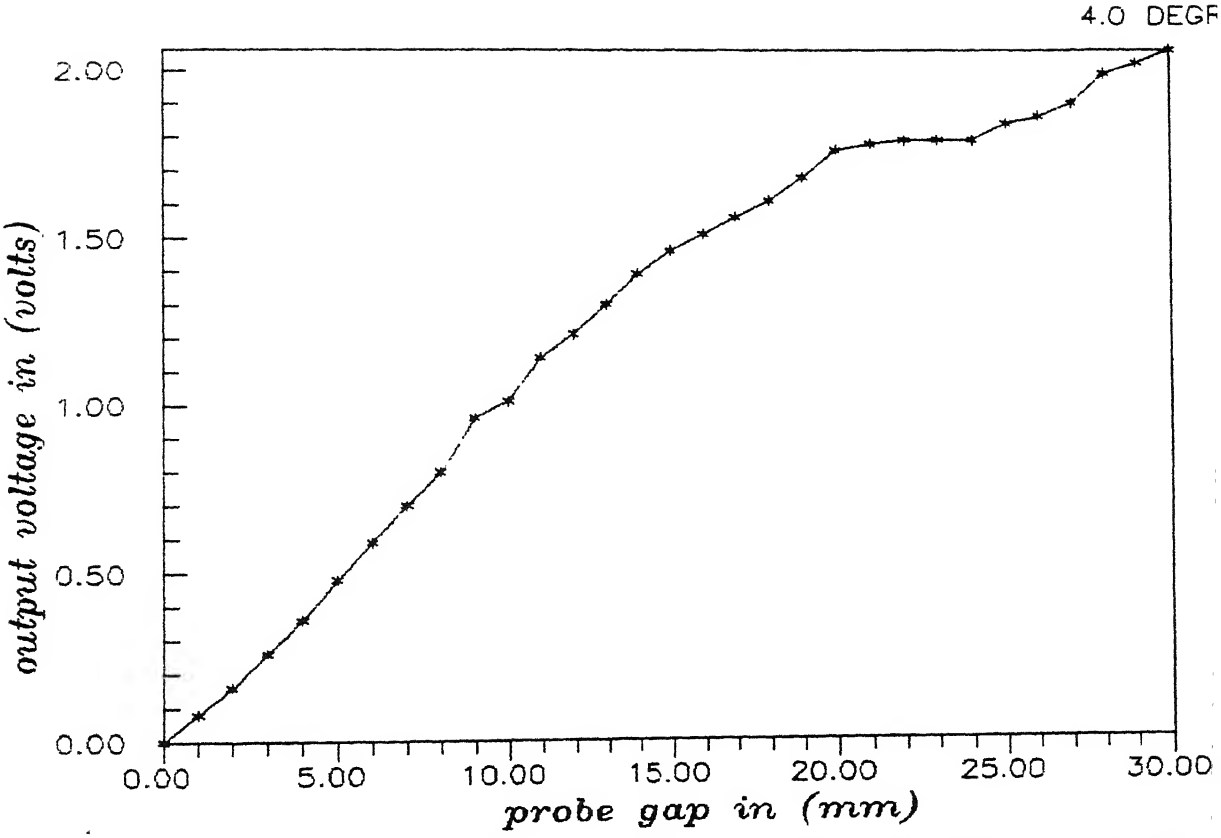

FIG. 4.9 (a) VARIATION OF OUTPUT VOLTAGE BY VARYING HORIZONTAL PROBE DISPLACEMENT FOR INCLINATION (θ) = 4.0 DEGREE.

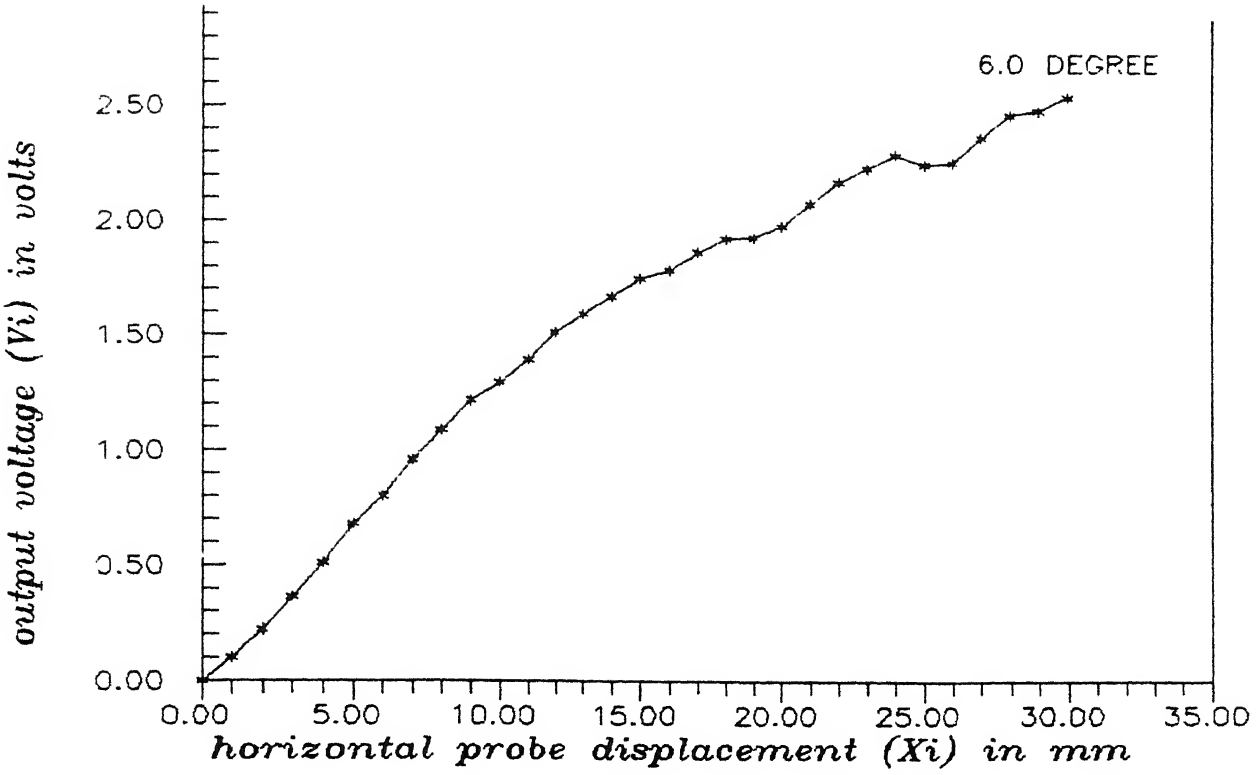

FIG. 4.9(b) VARIATION OF OUTPUT VOLTAGE BY HORIZONTAL PROBE DISPLACEM
FOR INCLINATION (θ) = 6.0 DEGREE.

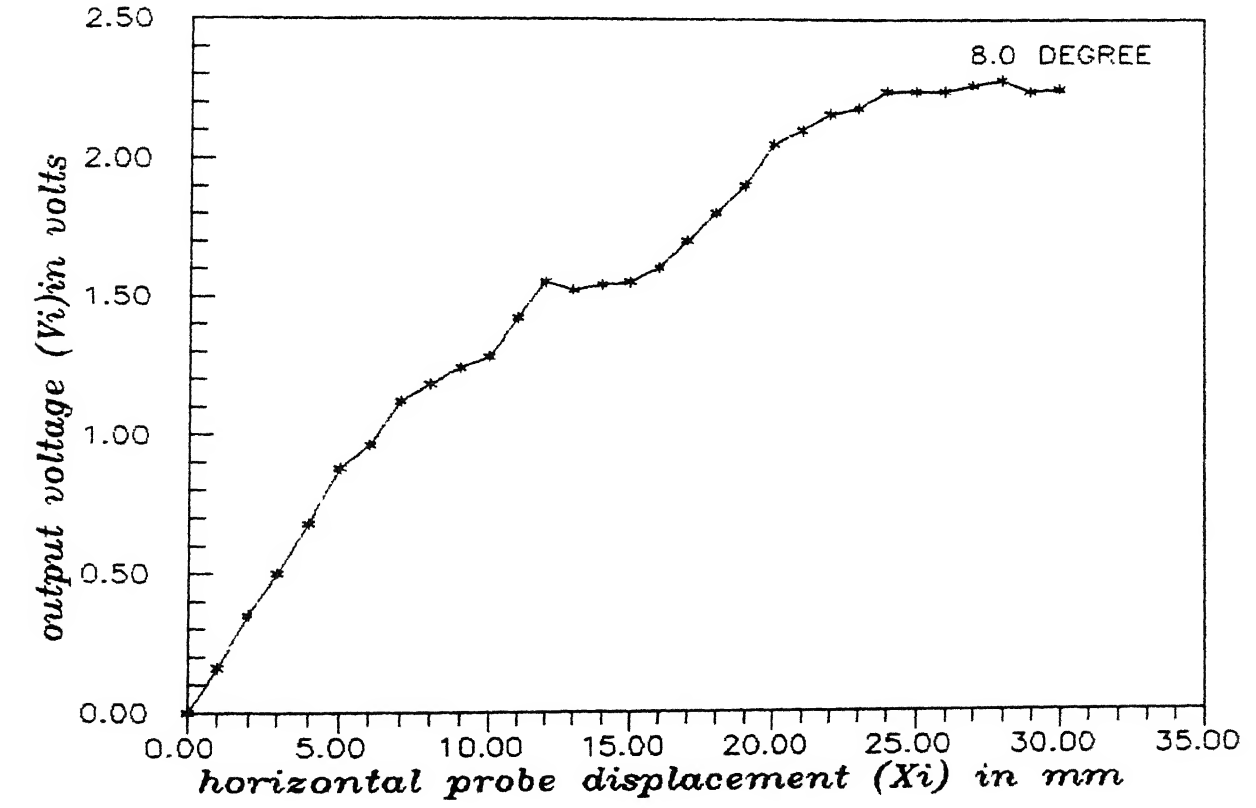

FIG. 4.9(c) VARIATION OF OUTPUT VOLTAGE BY HORIZONTAL PROBE DISPLACEM
FOR INCLINATION (θ) = 8.0 DEGREE.

(a), (b) and (c). Now the graph is plotted between the vertical gap (Y_i) and horizontal displacement (X_i) from Fig. 4.8 and 4.9 for 4^o, 6^o and 8^o inclination separately. These are the experimental profile obtained. The actual profile is obtained from Fig. 4.9 (a), (b) and (c) for 4^o, 6^o and 8^o inclinations by following relations: $Y_i = X_i \tan(\theta)$. Thus the graph is plotted between the Y_i and X_i. This comparison of profile obtained experimentally and theoretically is shown in Fig. 4.10 (a), (b) and (c) for 4^o, 6^o and 8^o inclinations.

The inferences drawn from above graphs are as follows. The results obtained theoretically and experimentally coincides only upto certain vertical gap Y_i. Moreover, as the inclination increases, the experimental results deviates from actual results earlier. This is because the losses i.e. scattering of reflected light not sensed by probe, increases with the inclination. Hence the method proposed here is not valid for higher inclinations. Hence the rearrangement of probe for slope measurement in steps is justified (Fig. 3.18) to achieve experimental and theoretical results close to each other.

4.2.2 Comparison of Output Voltage between Calculated and Experimental Results for Inclined Specimen

The value obtained experimentally for inclination (θ) = 8^o at Z_{max} = 3.9 mm is 2.28 volts (Fig. 4.9 (c)) and Appendix-(E). The

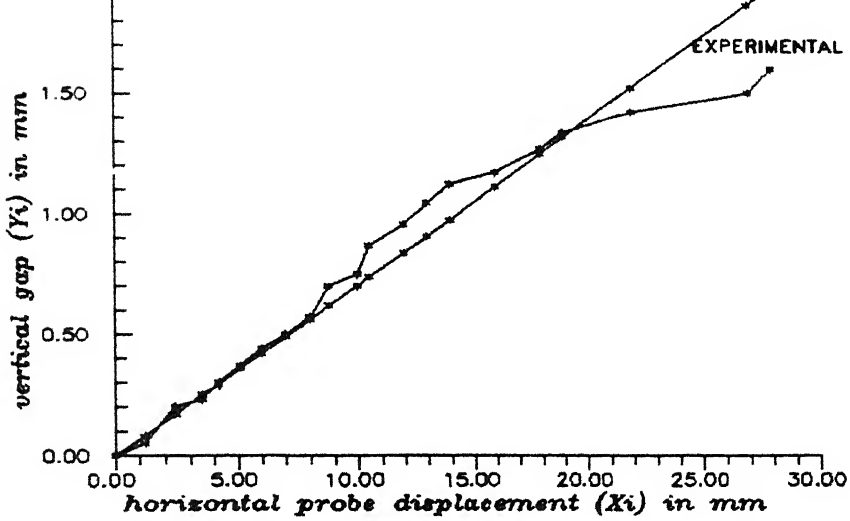

FIG. 4.10(a) COMPARISON OF PROFIE OBTAINED EPERIMENTALLY AND THEORETICALLY FOR 4.0 DEGREE INCLINATION

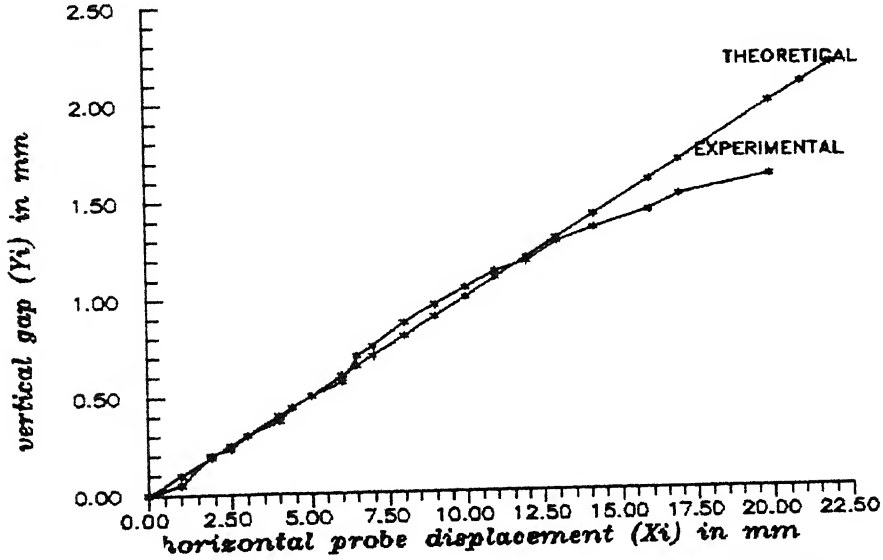

FIG. 4.10(b) COMPARISON OF PROFILE BY EXPERIMENTAL AND THEORETICAL RESULTS FOR 6.0 DEGREE INCLINATION

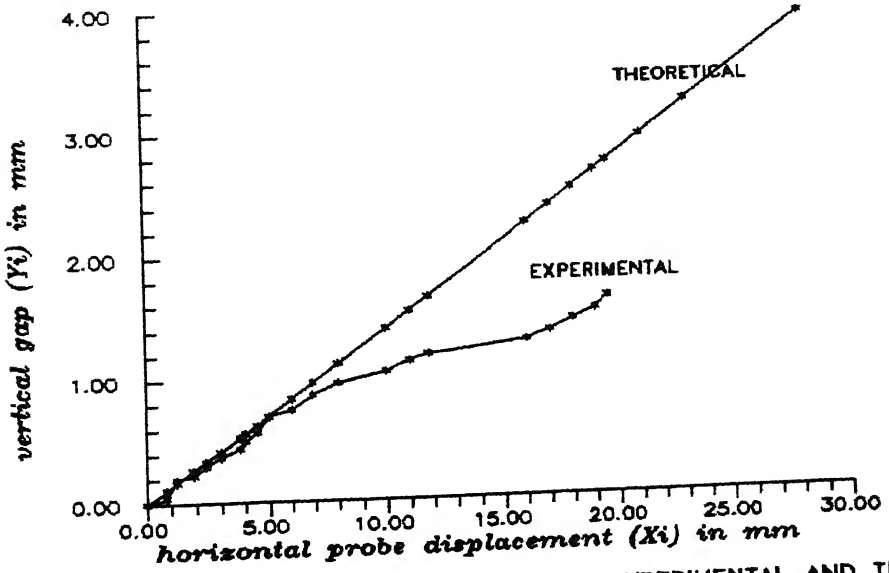

FIG. 4.10(c) COMPARISON OF PROFILE BY EXPERIMENTAL AND THEORETICAL RESULTS FOR 8.0 DEGREE INCLINATION

output voltage obtained theoretically for same inclination and same gap is 2.431 volts (Sec. 2.1.4). The error in the results are due to the same reasons as discussed earlier in Sec. 4.1.1 (for flat specimen).

4.3 COMPARISON OF PROFILE BY OPTICAL-FIBERS AND DIAL-GAUGE

The comparison is made for the measured half profile by optical-fibers and dial-gauge as shown in Fig. 4.11. This is obtained from Fig. 3.19 and 3.21. From the above figure, Fig. 4.11 it is found that the results obtained by the optical-fibers for detecting and tracing the profile of the specimen are in good agreement with the results by dial-gauge. Hence the profile traced the optical-fifbers, i.e. contactless method, is very accurate and reliable for precision measurement.

4.4 COMPARISON OF HEIGHTS OF THE ARTIFICIAL BURRS BY OPTICAL-FIBERS AND SHADOWGRAPH

The comparison is made for the results obtained by the optical-fibers and shadowgraphs for specimen no. 1 and 2 in Table No. 4.1 and 4.2 respectively (Refer Sec. 3.2.3.2 and 3.2.3.3).

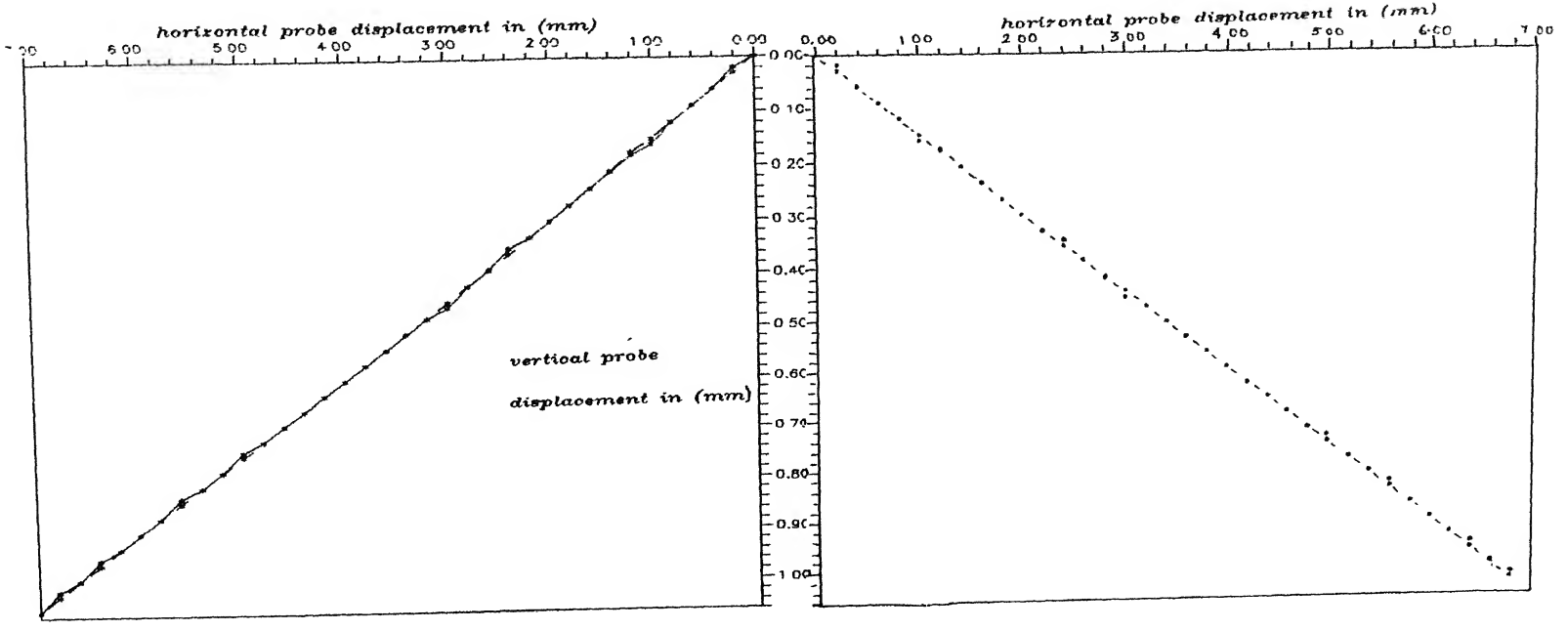

FIG.4.4 COMPARISON OF PROFILE'S TRACED BY OPTICAL-FIBERS AND DIAL-GAUGE (POINTS CONNECTED – OPTICAL FIBERS & DASH-LINES-DIAL GAUGE)

Table 4.1: Comparison of Height of Artificial Burr for Specimen No. 1.

Sl.No.	Height of Artificial Burr		Error %
	By Optical-Fibers (mm)	By Shadowgr-ph (mm)	
1.	0.27	0.271	- 0.1
2.	0.49	0.474	1.6
3.	0.70	0.722	- 2.2
4.	0.78	0.802	- 2.2

Table 4.2: Comparison of Height of Artificial Burr for Specimen No. 2.

Sl.No.	Height of Artificial Burr		Error %
	By Optical-Fibers (mm)	By Shadowgraph (mm)	
1.	1.45	1.642	-19.2
2.	1.10	1.113	- 1.3
3.	1.25	1.106	14.4
4.	0.58	1.322	-74.2
5.	1.00	1.571	-57.1
6.	1.25	1.597	-34.7

From the Tables 4.1 and 4.2, it is observed that the results obtained for specimen no. 1 are quite close with less error. But the results obtained for specimen no. 2 varies and with large error. This discrepancy in the results are due to two main reasons.

(i) The shape, size and cross-sections of the artificial burrs, are especially on specimen no. 2 are quite random in nature and it cannot be predicted.

(ii) Secondly, the commercially available optical-fibers end are very thick i.e. the diameter of receiving and transmitting fibers were large compared to the thickness of burrs (especially for specimen no. 2).

Hence, due to the above discrepancies, the results obtained for specimen no. 2 are not close and with large errors.

CHAPTER - V

CONCLUSION

The non-contact sensor utilizing fiber-optics is successfully employed to study the feasibility of this technique to measure surface roughness, work piece profile and to detect the presence of burrs. The proposed method is highly sensitive to the environment like medium between the probe and the work piece (air, water and Nacl solution) and also the type of work piece material.

It is concluded that there is a good correlation between experimentally measured (using contactless sensor) profile and actual (theoretical) profile if the gap between the probe and the work piece is made to remain in the linear region of the calibration curve. As the gap goes beyond the linear range, the deviation between the two goes on increasing. It has been explained on the basis of unpredictable high losses with the increase in the gap.

It is also concluded that with the help of this technique, orientation and location of the burrs even if it exists in the inaccessible areas can be detected.

SUGGESTIONS FOR FUTURE SCOPE OF WORK

The contactless precision measurement can be successfully employed in following areas:

(i) Measurement of workpiece profile in the case of blind cavities and through cavities using optical-fibers.

(ii) Measurement of burr shape and size actually formed by various machining operatios by optical-fibers.

(iii) In-process interelectrode-gap measurement during unconventional machining process like ECM, EDM, ECDrilling, ECBo etc. by optical-fiber.

This can be achieved by inserting very thin bifurcated optical-fibers in the tool and using the same principle of reflected light intensity variation with the gap (interelectrode gap).

(iv) Automatic setting of tools in ECM operations like deburring, boring and driling etc.

The tools can be positioned exactly with respect to the workpiece and particular gap by just knowing the output voltage. Thus this automatic setting will reduce the setting up time and will be more accurate.

(v) Inspection of deburred components by optical fibers.

In this the optical fibers can detect whether the component is free from burrs or not. Secondly it will give full details of burrs. Thirdly it can suggest as how much voltage is required to

make the component burr free. This will also lead us in knowing the time required to removes the burrs.

(vi) Detection of sparking in the surrounding area by optical-fibers.

The sparking during unconventional machining processes takes place when the tool touches the workpiece. This can be detected by optical-fibers as sparking will lead to the momentarily sudden increase in reflected light intensity giving a sharp kink on the recorder and oscilloscope.

(vii) To control the unconventional machining operations by optical fibers.

The output-voltage obtained from the optical-fiber sensing unit can be given as input or feed back to the voltages applied across the tool and workpiece. This will control the material removal rate (MRR) and hence the machining processes is controlled.

REFERENCES

[1.] Khare M.K., Vajpayee S., "Dimensional Metrology", Mohan Primiani, Oxford & IBH Publishing Co., New-Delhi.

[2.] Chai Yeh,"Handbook of Fiber Optics, Theory and Applications", Academic Press Inc., USA, 1990.

[3.] Dietrich Marcuse,"Principles of Optical Fiber Measurement, Academic Press (Inc.) London Ltd.

[4.] Thomas O. Mensah and Pundil. Narsimham, "Fiber Optics Engineering: PRcoessing and Applications", Americal Institute of Chemical Engineers, Symposium Series 258, Vol. 83, 1987.

[5.] Vorburger T.V., Teague E.C., "Optical Techniques for On-line measurement of Surface Topography", Precision Engineering Vol., 1981, 00.61-84.

[6.] Peters J., Vanherck P., Sastrodinolo M., "Assessment of Surface Topology Analysis Techniques", Annals of CIRP, Vol. 28/2/1979, pp. 539-554.

[7.] Tanner L.H., "A Comparison of Talysurf 10 and Optical Measurements of Roughness and Surface Slope Wear", Vol.57, 1979.

[8.] Takeyama, H., Sekiguchi H., Munta R., "In-Process Detection of Surface in Machinery; CIRP Annals, Vol.25, 1976, pp.467-475.

[9.] Spurgeon D., and Slater R.A.C., "In-process Indication of Surface Roughness using Fiber-opticstransducer", Proc. 15th International Machining Tool Design and Research, Vol.15, 1974, pp. 339.

[10.] Lin G.C., Shea T., and Hosing K., "Measurement of Surface Roughness with Laser Beam", Australian Confreence on Manufacturing Engineering, Aug. 1977, pp. 132-133.

[11.] K. Mitsui, "In-process Sensors for Surface Roughness and their Applications", Precision Engineering, Vol.8, No.4, October 1986, pp. 212-220.

[12.] W.P.f North and A.K. Agrawal,"Surface Roughness Measurement with Fiber Optics", Journal of Dynamic Systems, Measurement and Control, Vol.105, December, 1983, pp.295-297.

[13.] Noval. A, B. Colding, "Sensing of Workpiece Diameter, Vibrations and Out-off roundness by laser-way to automate quality control", Annals of CIRP, Vol.30, 1981.

[14.] Ikawa N., Shimada S., and Morroka H., "Photoelectronic Displacement Sensor with Nanometer Resolution", Precision Engineering, Vol.9, No.2, April, 1987.

[15.] Kiyoshi YAMAGI, Takashi MIYOSNI and Katumasa SAITO, "Developement of the displacement sensor by Fiber optics", Bulletin Japan Soc. of Prec. Engg., Vol. 14, No.3, September 1980, pp. 175-176.

[16.] Sigeru VENO, "New Method for Detecting Surface Texture on Turning by Using Fiber Optics", Bull Japan Soc. of Prec. Engg., Vol.7, No.3, September, 1973, pp.87-88.

[17.] Tanner, L.H. Fahovm, M., "A Study of the Surface Parameters of Ground and Lapped Metal Surfaces, Using Specular and Diffuse Reflection of Laser Light, "Wear, Vol.36, 1976, pp.299-316.

[18.] Fogiel M., "The Optics Problem Solver", Research and Education Association, 1980, New-York.

[19.] Masaji SAWABE, "Recent Development of Measurement Technique for Dimension and Profile in Japan", Bull Japan Soc. of Prec. Engg., Vol.18, No.2, June, 1984, pp.158-164.

[20.] Izumi SAKAI and Masaji SAWABE, "A MEthod for Surface Roughness Measurement by means of light Reflectence", Bull. Japan Soc. of Prec. Engg., Vol.16, No.2, June, 1982, pp.123-124.

[21.] E.G. Thwaite,"Advanced in Optical Methods of Measuring form and Roughness", 11th AIMTDR Conference, 20-22 Dec. 1984.

APPENDIX-A

DEFINITION OF TERMS

The following are the definitions of terms used for the study of contactless measurement by fiber optics. The *surface* of an object is the boundary which separates an object from another object. The *nominal surface* is the intended surface contour (excluding any surface roughness), the shape and extent of which is usually shown and dimensioned on a drawing or descriptive specification. The *surface texture* is the repetitive or random deviations from the nominal surface which forms the three dimensional topography of the surface. Surface texture includes roughness, waviness, lay and flows (Fig. A1). *Roughness* consists of finer irregularities of surface texture which are inherent in production processes. *Waviness* is the more widely spaced component of surface texture upon which roughness is superimposed. *Lay* is the direction of predominant surface pattern, ordinarily determined by the production method. *Flaws* are unintentional, unexpected and unwanted interruptions in the topography. The *profile* is the contour of the surface in a plane perpendicular to the surface, unless some other angle is specified. The *nominal profile* is a profile of the nominal surface. It is the intended profile exclusive of any roughness. The *measured profile* is a representation of the profile obtained by instrumental or other means (Fig. A2).

Precision is the degree which determines how well identically performed measurements agree with each other. It is the repeatability of a measuring process. *Accuracy* is the degree of agreement between the measured result and its true value and the difference between the two is known as the error of "measurement". In short, accuracy is the quality of conformity. *Sensitivity* gives an idea about the ability of the equipment to detect small variation in the "input signal", i.e. the quantity being measured. *Readability* is the susceptibility of a measuring device to having its indications converted to a meaningful number. Readability implies the ease with which observations can be made accurately [1].

Specular Reflection occurs on smooth mirror like surfaces where a reflected beam of light is not significantly scattered (Fig. A3(i)). If the average depth of the surface irregularities of the reflector is substantially less than the wavelength of the incident light, a reflected beam will be formed. *Diffuse Reflection* occurs on a rough surface such as a piece of paper, a ground piece of glass, or skin, where the depth of the irregularities on the surface is greater than the wavelength of the incident light (Fig. A3(ii)). When a reflected light is concentrated in the region around the specularly reflected beam, *spread reflection* occurs (Fig. A3(ii)) [18].

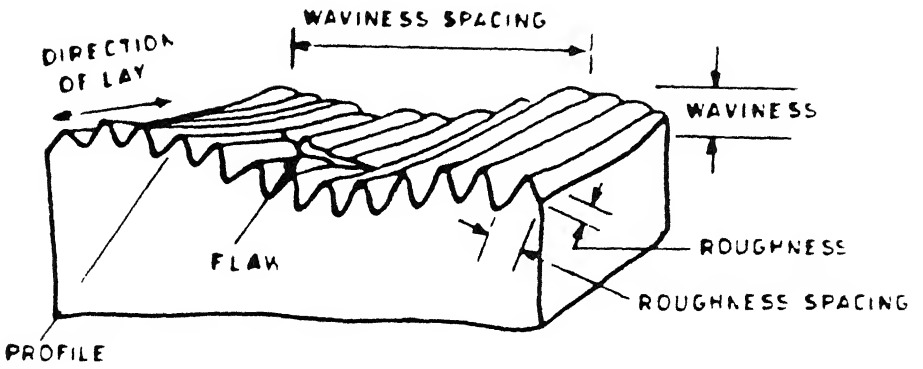

FIG. A1 SURFACE CHARACTERISTICS.

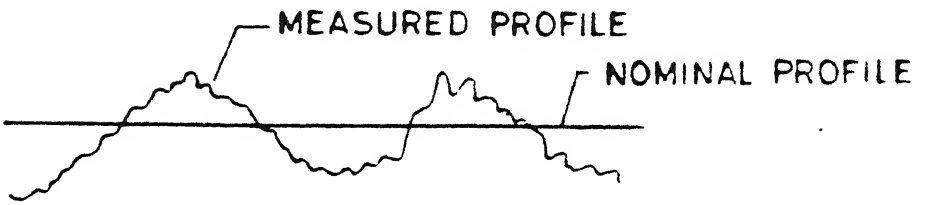

FIG. A2 NOMINAL AND MEASURED PROFILE.

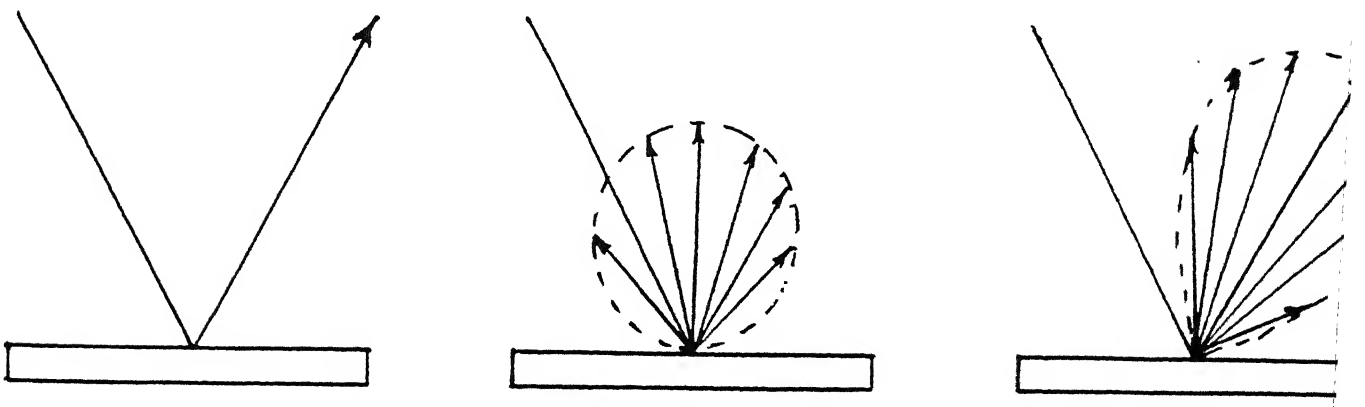

(a) SPECULAR (b) DIFFUSE (C) SPREAD

FIG. A3 TYPES OF REFLECTIONS

APPENDIX-B

PHOTODIODE SPECIFICATIONS

Photosensitive surface		Typical spectral response range	Maximum Ratings					Field of view
			DC reverse	Photocurrent density, I_p		Forward current, I_F		
Area (mm^2)	Dia. (mm)	10% point (nm)	voltage VRm (volt)	Average DC (mA/mm^2)	Peak value (mA/mm^2)	Average DC (mA)	Peak value (mA)	(deg.)
		400						
5	2.5	70	100	5	20	10	100	72
		100						

APPENDIX-C

AD 540J FET INPUT OP-AMP

a) Features: (i) Low cost

(ii) Low I_b; 25pA max (K)

(iii) Low V_{os}; 20 mV max (k)

(iv) Low V_{os} Drift; 25 $\mu V/^{\circ}C$ max. (k)

(v) High differential Input Voltage Capability; ± 20V

b) Specifications:

(i) Open Loop Gain

V_{OUT} = ± 10 V, $R_L \geq$ 2 k ohm	20,000 min
T_A = min. to max.	15,000 min

(ii) Output Characteristics

Voltage @ R_L = 2 K ohm, T_A = min. to max.	± 10 V min (± 13V Typical)
Voltage @ R_L = 10 K ohm, T_A = min. to max.	± 12 V min (± 14V Typical)
SC current	25 mA

(iii) Frequency Response

Unity gain, small signal	1.0 MHz
Full power, response	100 KHz
Slew Rate, unity gain	6.0 v/μs

(iv) Input Offset Voltage 50 mV max.

V_s Temp. 75 $\mu V/^{\circ}C$ max.

V_s Supply, T = min. to max.	400 μV/V max.
(v) Input Bias Current	50 pA max.
either Input	
(vi) Input Impedance	
Differential	10^{10} ohm // 2pF
Common Mode	10^{11} ohm // 2pF
(vii) Input Voltage Range	
Differential	± 20 V
Common Mode	± 10 V min
	(± 12 V Typical)
Common Mode Rejection	70 db min.
Vin = ± 10V	
(viii) Power Supply	
Rated Performance	± 15 V
Operating	± 10 V min
	(± 12 V Typical)
Quiescent Current	7 mA max.
	(3m A Typical)
(ix) Temp. Range	
Operating, Rated Performance	0 to + 70°C
Storage	-65°C to + 150°C

c) Pin Configuration

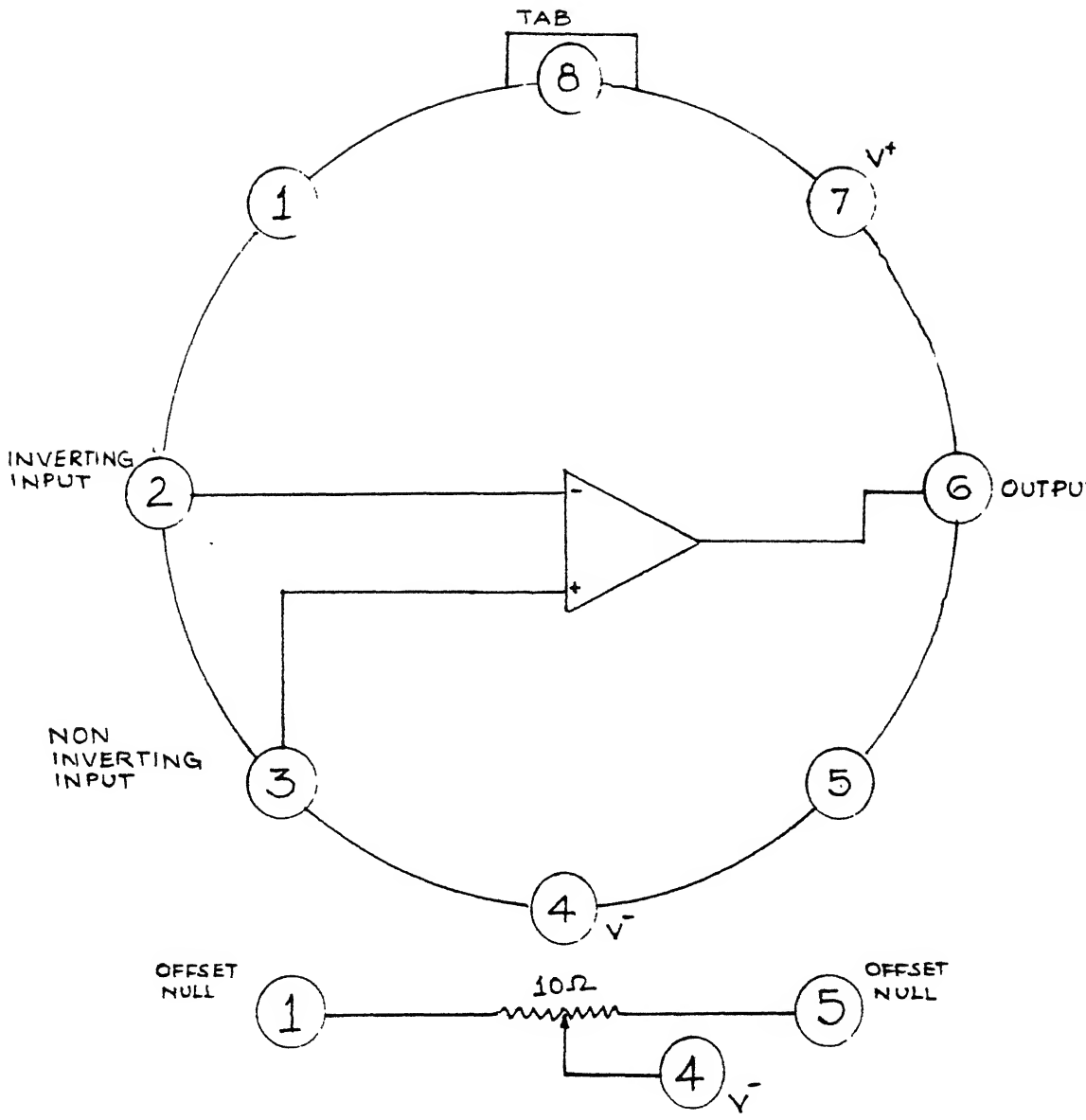

PIN CONFIGURATION

APPENDIX-D

Recorded Output Voltage by Varying Gap for Air Medium

AIR MEDIUM

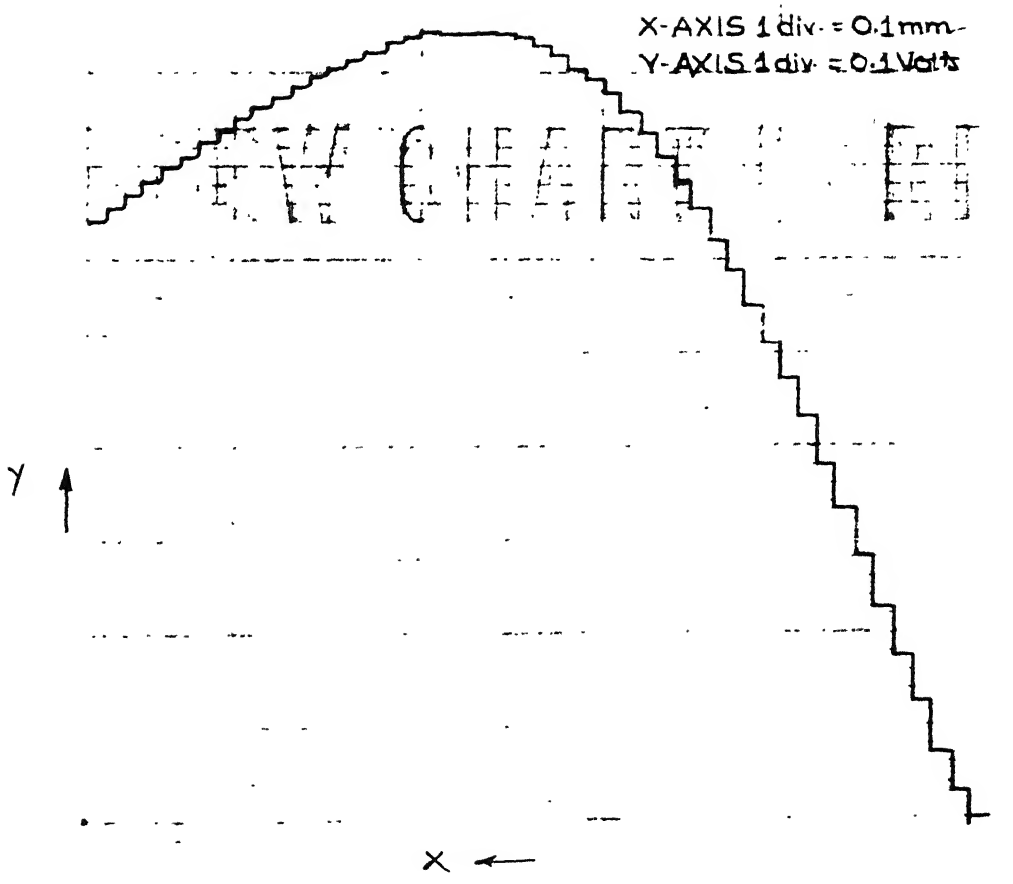

(a) ALLOY STEEL STANDARD PLATE OF Ra. VALUE = 4 μ.in

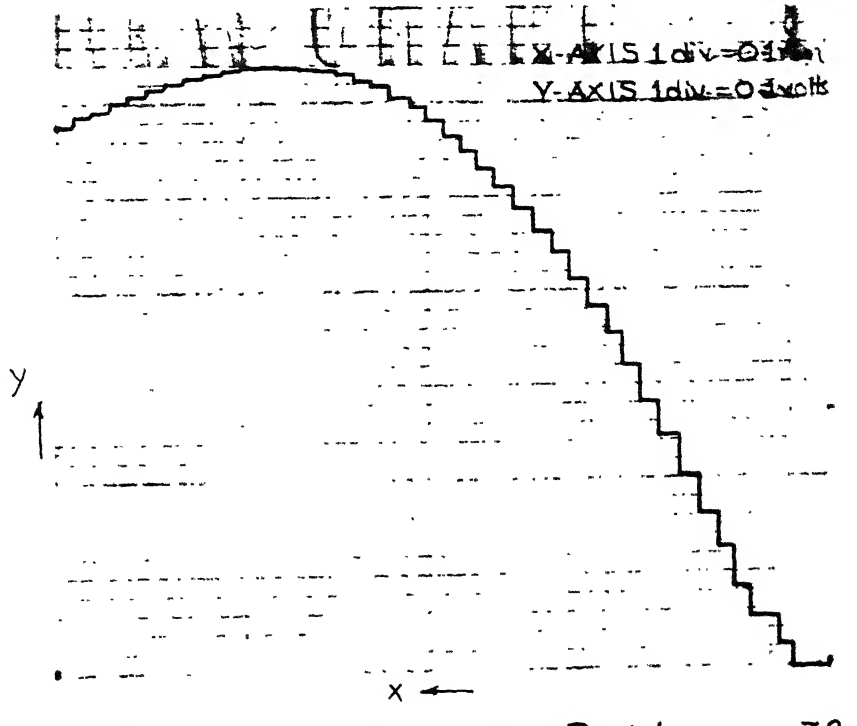

(b) ALLOY STEEL STANDARD PLATE OF Ra. VALUE = 32 μ.in

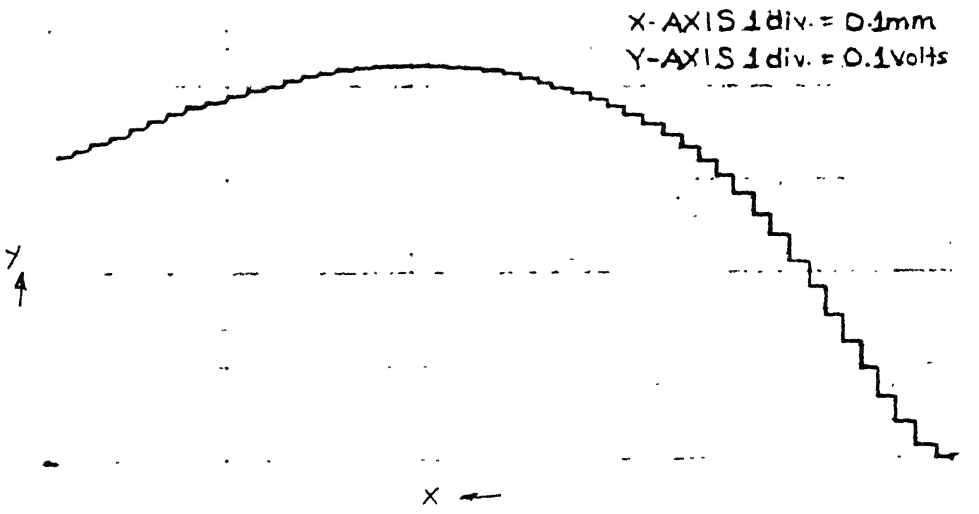

(C) ALLOY STEEL STANDARD PLATE OF Ra. VALUE = 63μ.in

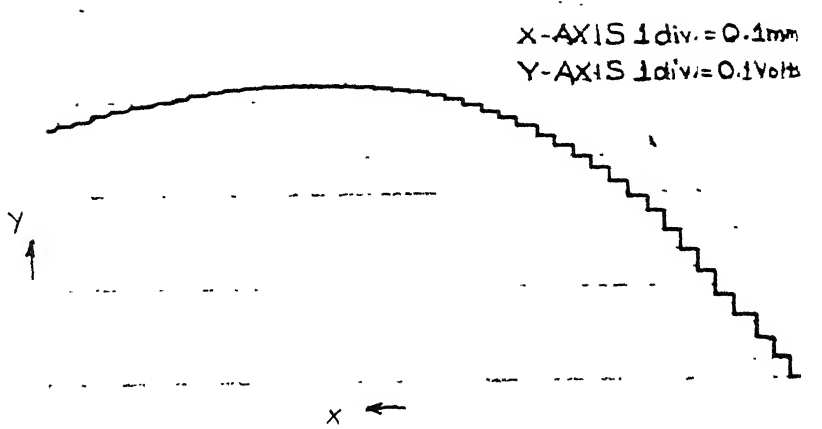

(d) ALLOY STEEL STANDARD PLATE OF Ra. VALUE = 125μ.in

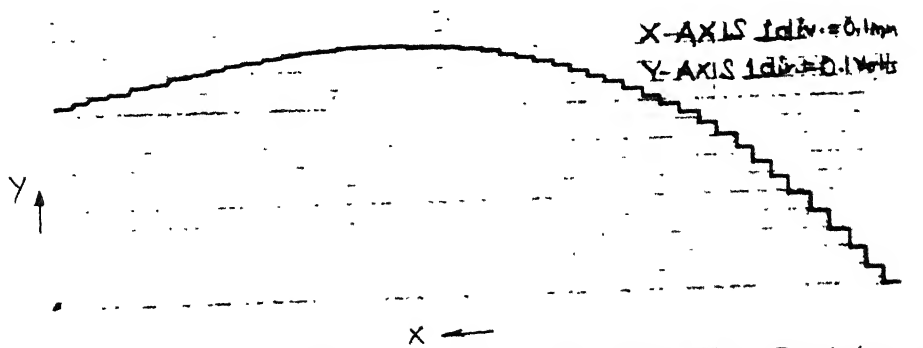

(e) ALLOY STEEL STANDARD PLATE OF Ra. VALUE = 250μ

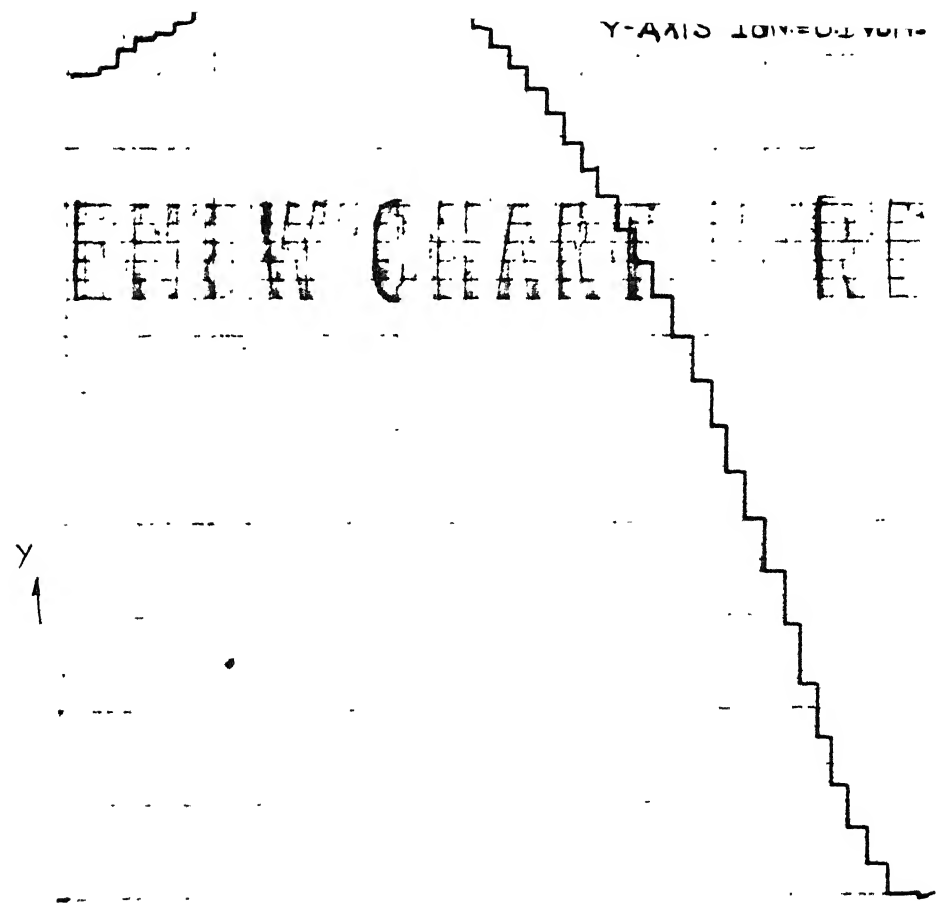

(f) ALUMINIUM SPECIMEN BY BUFFING OPERATION

"TURNING-1" OPERATION WITH

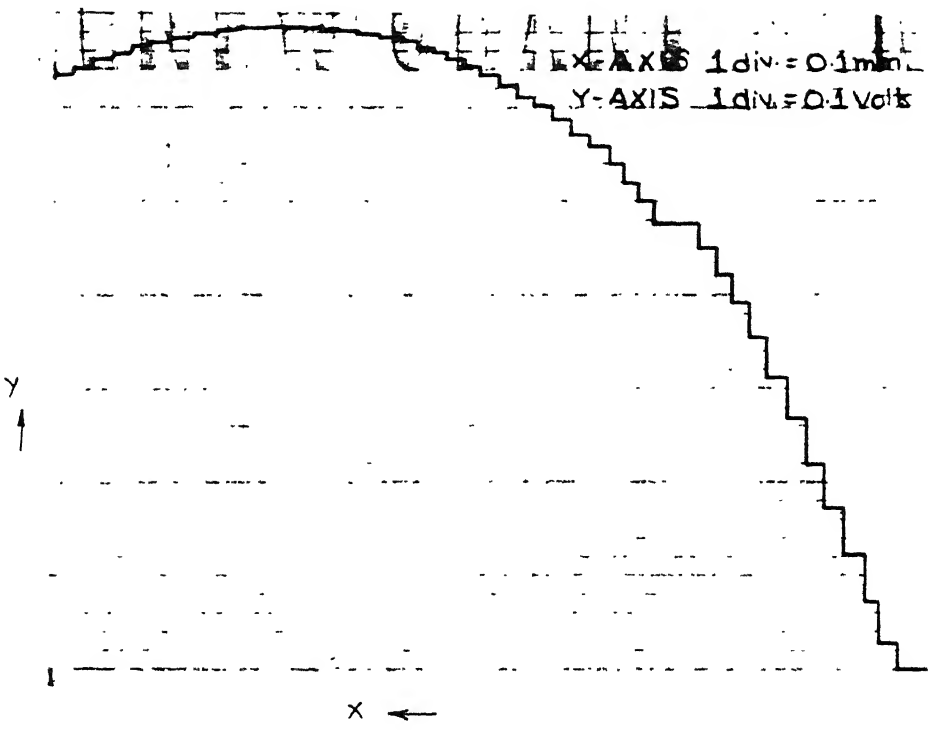

(h) ALUMINIUM SPECIMEN BY "TURNING-2" OPERATION WITH FEED = 0.10mm/rev. AND SPEED = 640 rpm.

APPENDIX-E

Results of the Effect of Horizontal Displacement of Probe on Output Voltages for Various Angular Inclination of Specimen

Horizontal distance x in mm	Output Voltage for angular Incl. in volts			
	4°	6°	8°	10°
0	0	0	0	0
1.0	.08	.10	.16	.22
2.0	.16	.22	.35	.45
3.0	.26	.36	.50	.70
4.0	.36	.51	.68	.88
5.0	.46	.68	.88	1.04
6.0	.56	.80	.96	1.20
7.0	.70	.96	1.12	1.4
8.0	.80	1.09	1.18	1.62
9.0	.96	1.2	1.25	1.6
10.0	1.01	1.30	1.28	1.96
11.0	1.14	1.40	1.42	2.15
12.0	1.21	1.52	1.55	2.30
13.0	1.30	1.60	1.52	2.51
14.0	1.39	1.68	1.54	2.84
15.0	1.46	1.76	1.55	
16.0	1.51	1.80	1.6	
17.0	1.56	1.88	1.7	
18.0	1.61	1.92	1.8	
19.0	1.66	1.94	1.9	
20.0	1.76	2.0	2.0	
21.0	1.78	2.1	2.1	
22.0	1.79	2.2	2.16	
23.0	1.79	2.26	2.18	
24.0	1.79	2.32	2.24	
25.0	1.84	2.28	2.24	
26.0	1.86	2.29	2.24	
27.0	1.90	2.40	2.26	
28.0	1.99	2.5	2.28	
29.0	2.0	2.52	2.24	
30.0	2.06	2.58	2.25	

APPENDIX-F

Calculation of Vertical Gap for Inclination θ = 9.0°

X in mm	Y = 0.16x in mm	Output Voltage in volts	X in mm	Y = .16x in mm	Output Voltage in volts
0	0	0	16.0	2.56	1.60
1.0	0.16	0.20	17.0	2.72	1.65
2.0	0.32	0.36	18.0	2.88	1.74
3.0	0.48	0.51	19.0	3.04	1.90
4.0	0.64	0.66	20.0	3.20	2.05
5.0	0.80	0.78	21.0	3.36	2.10
6.0	0.96	0.90	22.0	3.52	2.16
7.0	1.12	0.98	23.0	3.68	2.18
8.0	1.28	1.11	24.0	3.84	2.24
9.0	1.44	1.20	25.0	4.0	2.24
10.0	1.60	1.32	26.0	4.16	2.24
11.0	1.76	1.40	27.0	4.32	2.26
12.0	1.92	1.50	28.0	4.48	2.28
13.0	2.08	1.52	29.0	4.64	2.24
14.0	2.24	1.54	30.0	4.80	2.25
15.0	2.40	1.61			

APPENDIX-G

Conversion of Output Voltage to Vertical Gap from Calibration Curve for Profile Measurement by Optical-Fibers

Horizontal displacement (X) in mm	Output Voltage in volts	Corresponding vertical gap from call.graph (Y) in mm
0	0.0	0
0.2	0.04	0.03
0.4	0.10	0.06
0.6	0.14	0.09
0.8	0.20	0.12
1.0	0.23	0.15
1.2	0.29	0.18
1.4	0.31	0.21
1.6	0.36	0.24
1.8	0.40	0.27
2.0	0.46	0.30
2.2	0.50	0.33
2.4	0.54	0.36
2.6	0.59	0.39
2.8	0.64	0.42
3.0	0.68	0.45
3.2	0.73	0.48
3.4	0.80	0.51
3.6	0.82	0.54
3.8	0.86	0.57
4.0	0.88	0.60
4.2	0.92	0.63
4.4	0.96	0.66
4.6	0.98	0.69
4.8	1.00	0.72
5.0	1.04	0.75
5.2	1.08	0.78
5.4	1.14	0.81
5.6	1.21	0.84
5.8	1.29	0.87
6.0	1.36	0.90

ME-1992-M- DIX-FEA